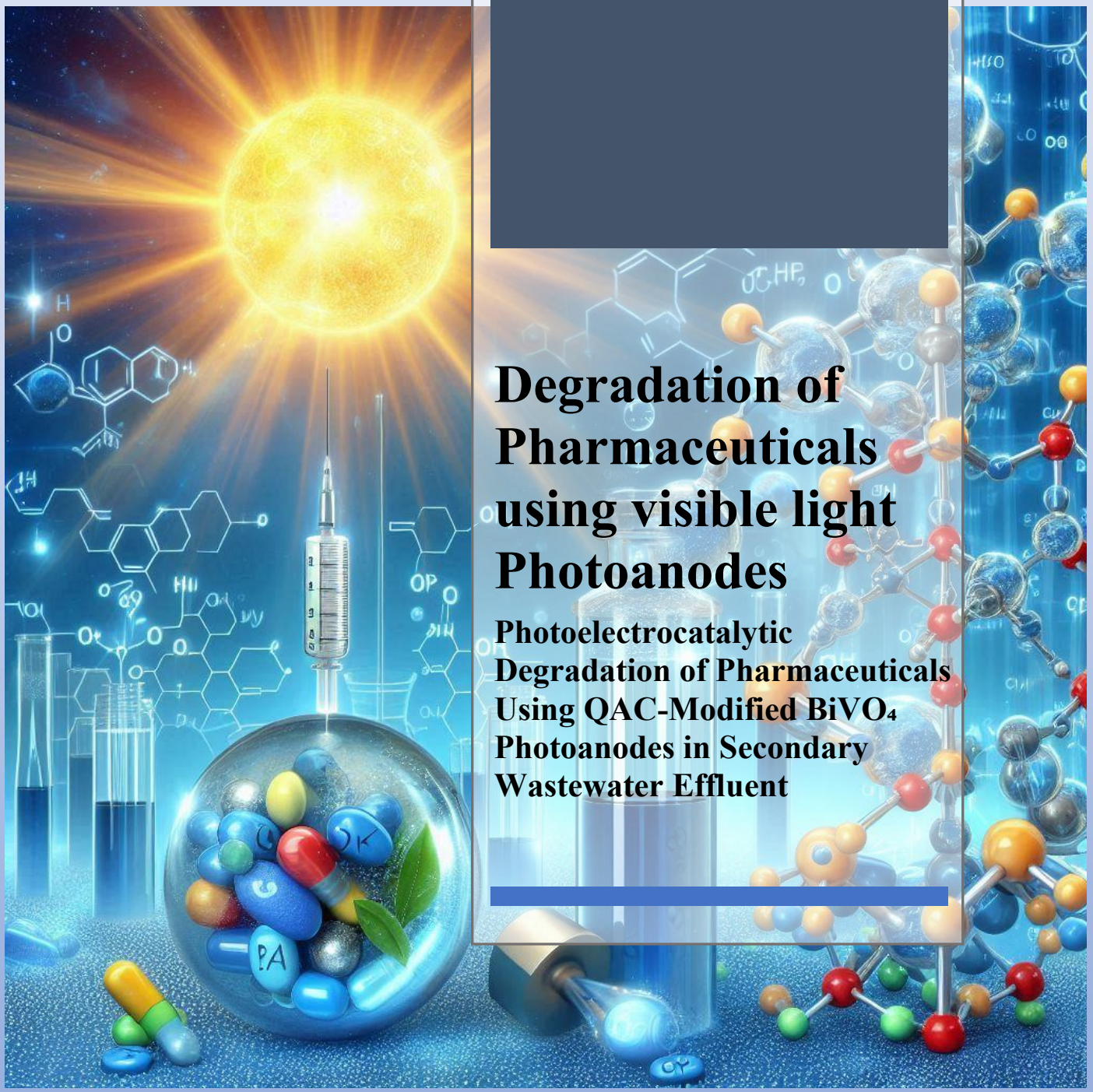

Degradation of Pharmaceuticals using visible light Photoanodes

Photoelectrocatalytic Degradation of Pharmaceuticals Using QAC-Modified $BiVO_4$ Photoanodes in Secondary Wastewater Effluent

Degradation of Pharmaceuticals using visible light Photoanode : Photoelectrocatalytic Degradation of Pharmaceuticals Using QAC-Modified $BiVO_4$ Photoanodes in Secondary wastewater Effluent

Master's Thesis submitted to Delft University of Technology

In partial fulfilment of the requirements for the degree of

Masters of Science

In Environmental Engineering

Faculty of Civil Engineering and Geosciences

By

Tejas Vasa

Student Number: 5847907

To be defended in public on 29th April, 2025

Prof Dr Ir Luuk C Rietveld	Committee Chair, TU Delft
Dr Sanjeeb Mohapatra	Daily Supervisor, TU Delft
Prof Dr Ir Henri Spanjers	External Supervisor, TU Delft

TU Delft

Acknowledgement

As I reach the end of this thesis journey, I want to sincerely thank everyone who has supported me along the way.

First, my deepest gratitude to Prof. Luuk Rietveld for stepping in at short notice and offering his full support, Helping, and guiding me throughout the course of this project and my study period in TU Delft. I also sincerely thank Prof. Henri Spanjers, who, despite being close to retirement, provided invaluable feedback and guidance.A special thanks to my supervisor, Dr. Sanjeeb Mohapatra, who introduced me to the world of organic micropollutants and electrochemistry. Special Thanks to Prof. Jan Peter van der Hoek**,** who could not be directly involved in this project but was the first to shape the initial idea with me

This project was highly multidisciplinary, and I am grateful to those from different labs who helped me along the way. Prasad and Prasanth from Materials Science supported me with characterization and troubleshooting, while Bart and Bahiya from Chemical Engineering assisted with analysis. A big thanks to Paul from Stevin Lab II, CiTG, for fixing countless technical issues and keeping things running smoothly. I am also grateful to the Water Lab team, Armand, Bryt, Boku, and Tania for assisting with lab procedures & Jane and Patricia for their help with analysis.

In the lab, I had the privilege of working with Akhilesh and Sumit, who spent endless hours troubleshooting and guiding me through tough phases—thank you for your patience and support. Beyond the research, my friends—Anshu, Daman, Deepesh, and Shrey—were my greatest support system, always there to encourage me through the highs and lows.

Lastly, my biggest thanks go to my parents Vaishali & Nilesh, brother Vinit and my extended family, whose emotional, financial, and unwavering support made this entire journey possible. I could not have done it without them.

To everyone who played a part in this journey—thank you!

Tejas Vasa
April 2025

Contents

List of Figures and Tables

List of Figures:

List of Table :

Executive Summary

Pharmaceutical pollutants in wastewater pose a significant environmental and public health risk, as conventional treatment plants fail to remove them completely. These contaminants contribute to antibiotic resistance and disrupt aquatic ecosystems. Advanced oxidation processes (AOPs) can effectively degrade pharmaceuticals, and among the AOPs, Photoelectrocatalytic (PEC) Treatment could offer an environmentally friendly solution. Among the semiconductors used for PEC, Bismuth Vanadate ($BiVO_4$) provides a good option as it utilises maximum solar visible light. However, there are some challenges with $BiVO_4$ regarding the rapid recombination of electrons which reduces photoelectrocatalytic performance. Researchers have modified $BiVO_4$ with various methods to enhance photoelectrocatalytic properties. Among these methods, the use of good surfactants for surface modification of $BiVO_4$ has been explored. Among the surfactants, there has been some initial research regarding the use of quaternary ammonium compounds (QAC) on $BiVO_4$ as a modification method to increase the photocatalytic performance of the photoanode.

This study further looks upon the use of six commonly found QACs' effects on $BiVO_4$ photoanodes, how it changes the surface properties and if it can enhance the photoelectrocatalytic performance. Based on the studied literature , key research questions were formulated on how QAC modification affects the physiochemical properties of $BiVO_4$ and how the modified $BiVO_4$ impact PEC performance and pharmaceutical degradation efficacy. Further studies were done to understand the implication of full-scale studies of using PEC with the $BiVO_4$ photoanode. To help answer these, $BiVO_4$ photoanodes were synthesized and modified with different QACs. Their structural, morphological, and electrochemical properties were analysed using XRD (X-ray diffraction), SEM (Scanning electron microscope), EDX (Energy dispersive Xray Photo spectroscopy), XPS (X-ray Photon spectrophotometer), UV-Vi's spectroscopy and LSV (Linear Sweep Voltammetry). The PEC degradation experiments were conducted in secondary treated effluent collected from wastewater treatment plant (WWTP) Horstermeer; the water was spiked with 20 selected pharmaceutical compounds. The removal efficacy of the modified $BiVO_4$ under simulated solar light was tested.

The results of these studies show that the QACs did not alter $BiVO_4$'s monoclinic phase but introduced minor shifts, SEM revealed the QAC have been incorporated and the integral structure of $BiVO_4$ has been maintained. EDX and XPS showed there was slightly more oxygen vacancies in the modified Photoanode, affecting charge transport. LSV demonstrated that the QAC-modified photoanode showed a current response within the range and performed only under light conditions. After this degradation experiments were conducted over a period of 120 minutes under solar stimulation and among all the QAC variants and an unmodified pristine $BiVO_4$ photoanode, DADMAC C18 performed the best overall, this was followed by the pristine $BiVO_4$ itself, while BAC C18 did not perform well. The ATMAC C18 variant and achieved a fast degradation, and compounds degraded in the first 15 minutes. Kinetic studies were evaluated for the best-performing DADMAC C18 variant and it was concluded that sulfamethoxazole was the critical compound as it had the least half-life time. A full–scale analysis was done where different full-scale models of PEC reactors were studied and a circular model with annular electrodes was selected to be the best suited. It provides a balance of good photo electrocatalytic efficacy, light penetration and less operational complexities when compared to other models. A rough full-scale model was also developed in the sense of replacing the existing UV oxidation system in WWTP Horstermeer. The full scale was

deployed for 25000 m^3/d of secondary treated effluent and rough design estimates were made. Based on this a techno-economic analysis of the whole system was done and it was calculated, that the cost of treatment would be € 0.24 /m^3 .

List of Commonly used Abbreviations

1. **AOP** – Advanced Oxidation Process
2. **ATMAC** – Alkyltrimethylammonium Chloride
3. **BAC** – Benzalkonium Chloride
4. **BET** – Brunauer-Emmett-Teller (Surface Area Analysis)
5. **CAPEX** – Capital Expenditure
6. **CPC** – Compound Parabolic Collector
7. **CTAB** – Cetyltrimethylammonium Bromide
8. **CTAC** – Cetyltrimethylammonium Chloride
9. **DADMAC** – Diallyldimethylammonium Chloride
10. **EDX** – Energy Dispersive X-ray Spectroscopy
11. **FOV** – Field of View
12. **FTO** – Fluorine-Doped Tin Oxide
13. **HRT** – Hydraulic Retention Time
14. **KMC** – Kinetic Monte Carlo
15. **KPI** – Key Performance Indicator
16. **LSV** – Linear Sweep Voltammetry
17. **MLD** – Million Liters per Day
18. **NSAID** – Non-Steroidal Anti-Inflammatory Drug
19. **OEC** – Oxygen Evolution Catalyst
20. **OMP** – Organic Micropollutant
21. **OPEX** – Operational Expenditure
22. **PEC** – Photoelectrochemical Process
23. **PMS** – Peroxymonosulfate
24. **QAC** – Quaternary Ammonium Compound
25. **ROS** – Reactive Oxygen Species
26. **RWZI** – Rijkswaterstaat Waterzuiveringsinstallatie (Dutch for Sewage Treatment Plant)
27. **SEM** – Scanning Electron Microscopy
28. **UV** – Ultraviolet
29. **WWTP** – Wastewater Treatment Plant
30. **XPS** – X-ray Photoelectron Spectroscopy
31. **XRD** – X-ray Diffraction

Chapter 1. Introduction

Pharmaceutical compounds are frequently detected in wastewater, posing environmental and public health risks. These include antibiotics, beta-blockers, NSAIDs, and anticonvulsants, which often persist in aquatic environments due to incomplete removal during conventional treatment. Common pharmaceuticals such as carbamazepine, diclofenac, and sulfamethoxazole are found in concentrations ranging from ng/L to µg/L, posing ecological risks such as endocrine disruption, bioaccumulation, and antimicrobial resistance (Jelic et al., 2011; Mulla et al., 2021; Ulvi et al., 2022). Given these threats, the effective removal of pharmaceutical contaminants from wastewater is a pressing challenge (Kanaujiya et al., 2019; Kulistakova , 2023)

Extensive research is being conducted to develop effective methods for addressing the challenge of pharmaceutical contamination in wastewater. Some well-established methods are categorized into biological and physicochemical methods such as advanced oxidation proces (AOP) , membrane separation, and activated carbon adsorption processes (Loganathan et al., 2023). Among these methods, AOP have emerged as an effective means of removing organic micropollutants (OMPs) from wastewater. This is due to their ability to degrade OMPs into harmless byproducts such as CO_2, H_2O, and other reaction products, using highly reactive hydroxyl radicals (•OH). However. Despite their efficacy, conventional AOP faces challenges such as high capital and operational costs, limited scalability, and the potential to generate undesirable byproducts (Ma et al., 2021).

Among the various AOPs, photocatalysis offers a relatively low-cost and environmentally friendly technology for OMP treatment (Goodarzi et al., 2023). It operates on the principle of the redox capacity of photocatalysts when exposed to light, essentially converting solar energy into chemical energy to destroy the OMPs. Semiconductors typically serve as catalysts in photocatalytic reactions, breaking organic pollutants into harmless by-products. Materials such as titanium dioxide (TiO_2), and zinc oxide (ZnO) serve as catalysts, facilitating the breakdown of OMPs into harmless byproducts such as CO_2 and H_2O. Despite its potential, conventional photocatalysis faces limitations such as rapid recombination of electron-hole pairs and limited light utilization efficacy, which can hinder its effectiveness in treating wastewater contaminated with OMPs (Long et al., 2020). To combat these drawbacks of photocatalysis, Photoelectrocatalysis (PEC) was introduced.

1.1 Background Studies

1.1.1 What is PEC?

PEC has emerged as an advanced technique that integrates photocatalysis with electrochemistry to enhance pollutant degradation. The key mechanism involves the application of an external potential bias, which promotes charge separation and suppresses electron-hole recombination, thereby boosting the overall photocatalytic activity. There are several advantages to doing this. The external potential bias ensures effective separation of charge carriers, reducing the likelihood of electron-hole recombination. Additionally, applying an external potential accelerates the reaction rates, leading to faster degradation of OMPs. Further, PEC can achieve high degradation efficiencies with lower energy inputs compared to traditional photocatalytic methods (Alulema-Pullupaxi et al., 2021).

Working principle of PEC : The wide band gap semiconductor photocatalyst has two distinct energy bands – the valence band (VB) and the Conductivity band (CB). The energy gap between them is called the forbidden band. When light with energy (*hv*) equal to or higher than

the semiconductor band-gap energy hits the semiconductor, it provides energy to the electron(e^-) in VB, exciting it and allowing it to move to the CB, creating a hole (h^+) in the VB (Zarei & Ojani, 2017).

$$semiconductor + hv \rightarrow e^- + h^+$$

Some of these excited e^- and h^+ react with oxygen and water molecules to form reactive oxygen species (ROS) – O^- and OH^-,

$$semiconductor(h^+) + H_2O \rightarrow semiconductor + {}^\circ OH + H^+$$

$$semiconductor(e^-) + O_2 \rightarrow semiconductor + O^\circ{}_2$$

$$ROS(O^\circ{}_2\ , H_2O) + species\ (OMPs) \rightarrow\ \ oxidation\ products\ (CO_2\ and\ H_2O)$$

Under light irradiation, the semiconductor photocatalyst generates photoinduced electrons and holes, which migrate to the photoanode and counter electrode, respectively. The applied external potential bias suppresses electron-hole recombination and promotes charge separation, facilitating the oxidation of the OMPs adsorbed on the surface of the semiconductor photocatalyst as shown in Figure (1). Additionally, PEC systems can generate additional oxidants, such as hydroxyl radicals (•OH), which further enhance the degradation of OMPs (Bessegato et al., 2015)

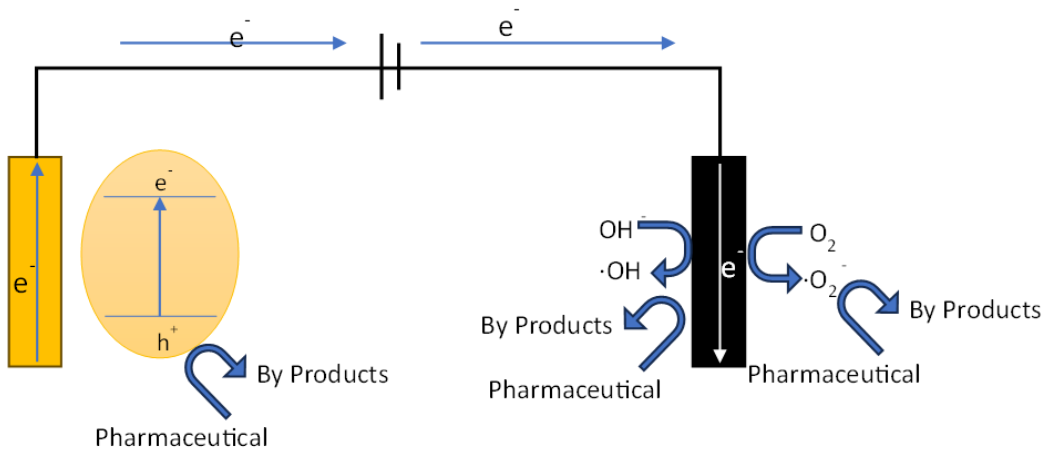

Figure 1. Principle of a PEC system for pharmaceuticals degradation in water. Adapted from (Wu & Hu, 2021)

While working with PEC, the semiconductor's bandgap energy, CB and VB are the most important properties to be considered. Bandgap energies in semiconductors range from 0.1 to 4 eV. Semiconductors with larger bandgap energy are preferred for PEC. In Table 1, some commonly used semiconductors for PEC are listed.

Table 1. Characteristics of some commonly used PEC semiconductor materials (Alulema-Pullupaxi et al., 2021)

PEC semiconductor	**Crystalline phase**	**Band gap (eV)**	Absorption **wavelength (nm)**
TiO_2	Rutile	3.05	405
	Anatase	3.25	385
WO_3	Tungstite	2.5−2.7	500
ZnO	Wurtzite	3.2−3.4	~400
SnO_2	Cassiterite	3.6	~345
α-Fe_2O_3	Hematite	2.2	Visible light (450 – 500)
Bismuth vanadate metal oxides	Monoclinic scheelite	2.4 – 2.5	Visible light (450 – 500)

TiO_2 and ZnO are widely used due to their large bandwidth, photocatalytic activity, non-toxicity, and high photostability. However, they only function under a specific light bandwidth and utilize only 4% of the total solar energy (Malathi et al., 2018). Accounting for this, more research is going toward synthesising "visible-light" driven semiconductors for wastewater treatment processes that can maximise the solar potential. In this regard, Bismuth-based metal oxide semiconductors such as $BiVO_4$, Bi_2WO_6, Bi_2MoO_6, $Bi_4Ti_3O_{12}$, and $BiFeO_3$, have shown good photocatalytic properties such as the right band gap and non-toxicity (Malathi et al., 2018).

1.1.2 Bismuth Vanadate ($BiVO_4$): Semiconductor Photoanode

Bismuth vanadate ($BiVO_4$) has been known to stand out due to its features such as low band gap, good dispersibility, non-toxicity, and corrosion resistance, all of which contribute to its good performance in degrading organic pollutants under visible-light illumination. It is an n-type direct bandgap semiconductor with a stable presence in neutral solutions and a bandgap of 2.4 eV, which theoretically allows for a photocurrent density of 7.5 mA/cm^2 under standard AM1.5 G solar irradiation (Y. Li et al., 2024a). $BiVO_4$ has three crystalline forms, with the monoclinic scheelite phase (m-s) showing the best photocatalytic performance under visible light. This is due to the unique overlap of O 2p and Bi 6s orbitals, which improves charge carrier mobility and enhances photocatalytic activity (Malathi et al., 2018).

Despite being a good semiconductor, $BiVO_4$ exhibits a photoelectric conversion efficacy of only around 10% (Zhong et al., 2023). The key challenges limiting the use of $BiVO_4$ include poor charge transport, slow water oxidation kinetics, and rapid recombination of photogenerated electron-hole pairs. The primary challenge with $BiVO_4$ in terms of charge transfer efficacy lies in the structure of its conduction band, which is predominantly composed of V 3d orbitals. In $BiVO_4$, the VO_4 tetrahedra are not interconnected, restricting the movement of free electrons within the material. As a result, electrons are forced to hop between isolated

VO_4 tetrahedra rather than flowing freely through an interconnected network. This structural limitation leads to low electron mobility, thereby reducing the overall efficacy of $BiVO_4$ in photocatalytic applications (Yu et al., 2023). Many modification methods have been introduced to combat this, including ion doping, crystal plane engineering, morphology control, and the creation of macroporous/mesoporous structures and heterojunctions. Currently, more than pure $BiVO_4$ is needed to achieve the theoretical photoelectric conversion efficacy. Different strategies have been combined to reach high photocatalytic efficacy (Zhong et al., 2023)

1.1.3 Modification of $BiVO_4$ Photoanodes

Surface modification is a widely used strategy to enhance the PEC performance of anodic materials by tuning their surface properties and structural features. The modifications improve catalytic activity, stability, and overall efficacy by addressing charge transfer limitations and recombination issues. In $BiVO_4$-based photoanodes, surface states play a pivotal role in determining both activity and durability during the photoelectrochemical process. Since the active sites for the redox half-reaction are located on the electrode surface, surface engineering techniques such as elemental doping, heterojunction construction, and cocatalyst loading as shown in Figure (2) help facilitate charge separation, improving water oxidation kinetics, and mitigating photo corrosion effects (Fu et al., 2024)

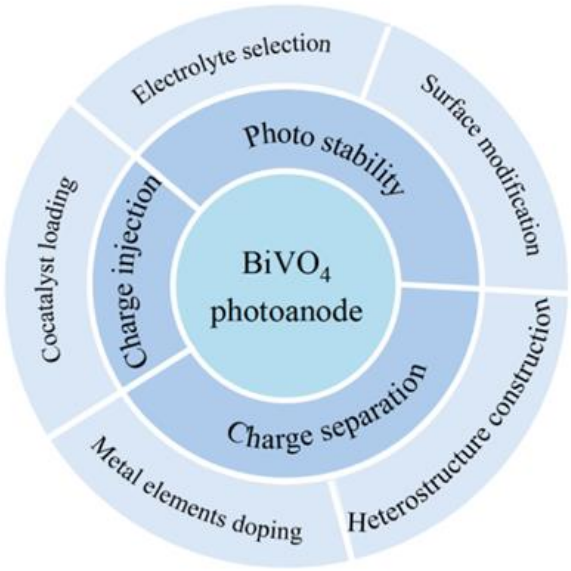

Figure 2 The modification strategies for the improvement of photo electrocatalytic properties of $BiVO_4$ adapted from (Fu et al., 2024)

1.1.4 Quaternary ammonium compounds

Quaternary ammonium compounds (QACs) are the primary cationic surfactants in fabric softeners, antistatic, disinfectants, biocides, detergents, phase transfer agents, and personal care products such as hair care items. They feature a hydrophobic hydrocarbon chain connected to a positively charged nitrogen atom, along with short-chain alkyl groups such as methyl or benzyl groups The most found QACs in natural environments are dialkyldimethyl ammonium compounds (DADMACs) with C8 to C18, alkyl trimethyl ammonium compounds (ATMACs) C12 to C18, and benzylalkyldimethyl ammonium compounds (BACs) C12 to C18 (Mohapatra et al., 2023).

QACs are highly effective surfactants due to their distinctive molecular structure and properties. Unlike other ammonium cations and organic amine groups, which are smaller and less complex, QACs are significantly bulkier. The four alkyl or aryl substituents attached to the central nitrogen atom in QACs cause a substantial separation between the positively charged quaternary nitrogen (R_4N^+) and its counter anion, especially in solution. This large separation is facilitated by the fully dissociated nature of R_4N^+ ions in water, often compared to synthetic alkali metals in terms of their behaviour. The solubility of QACs is another important factor contributing to their effectiveness as surfactants. They are highly soluble in polar and protic solvents such as water and alcohol. However, this solubility decreases with increasing chain length; QACs with chains longer than C14 are nearly insoluble in water but show improved solubility in nonpolar solvents. QAC solutions exhibit excellent ionic conductivity, which enhances their performance as electrolytes. Their structure, with polar (N+) and nonpolar (R) ends, allows them to absorb on surfaces or interfaces, reducing surface tension in aqueous environments. QACs maintain their cationic nature across a broad pH range, ensuring consistent surfactant activity in diverse environments. QACs also enhance surface conductivity and reduce resistivity. Their ability to reduce interfacial tension and improve surface conductivity makes them valuable as surfactants and reduces the accumulation of dust and dirt on surfaces (Bureš, 2019). These unique properties of QACs make them a promising choice as surfactants for enhancing the performance of $BiVO_4$ in PEC applications. However, limited studies have investigated the degradation efficacy of $BiVO_4$ modified with QAC compounds. Existing research indicates that QAC-modified $BiVO_4$ exhibits superior performance compared to its unmodified counterpart, demonstrating higher degradation efficacy and increased surface reactivity, which contribute to improved photo electrocatalytic activity (Z. Chen et al., 2022)

1.2 Research Objective and Research Questions

The objective of this study was to evaluate the degradation efficacy of a mixture of pharmaceutical compounds under controlled conditions using PEC oxidation. By studying the interactions between modified $BiVO_4$ photoanodes and pharmaceutical contaminants, the potential of this approach for enhancing pharmaceutical removal from wastewater was demonstrated.
This study specifically focused on $BiVO_4$ photoanodes, modified with various QACs, aiming to improve their performance in photoelectrochemical oxidation. The modifications were intended to enhance charge transfer efficacy, surface reactivity, and overall degradation effectiveness.

Furthermore, this study presents a novel approach, marking the first study to explore the simultaneous photoelectrochemical degradation of 20 pharmaceutical compounds using $BiVO_4$-PEC systems. Conducted in real wastewater conditions, it provides valuable insights into the challenges associated with complex wastewater matrices, competitive degradation effects, and the feasibility of scaling up this technology for wastewater treatment applications.

For the study the following research question was formulated:

1. Fabrication and Characterization

   What are the structural, optical, and electrochemical properties of $BiVO_4$ photoanodes modified with various QACs?

2. Performance Evaluation

What is the removal efficacy of the individual pharmaceuticals in the mixture of the target pharmaceuticals using QAC-modified $BiVO_4$ *photoanodes?*

3. Scaling UP PEC for Real-World Applications

   What are the key challenges and potential solutions for scaling up the PEC process for the removal of pharmaceuticals in wastewater treatment?

1.3 Thesis Structure

This report consists of six chapters.

Chapter 1: Introduction gives the background knowledge to the studies. It gives some insights into the PEC system and the importance of $BiVO_4$ and surface modification by QAC. Based on this the research objectives for this study are addressed.

Chapter 2: Literature review Dwells deep into the existing studies of the use of $BiVO_4$ in PEC for pharmaceutical removal; It addresses some research gaps as well which were found after the literature review

Chapter 3: Materials and Methods Concerns the materials and methodology used for this study. It tells about the method of synthesis of the photoanode and the characterization to be performed: XRD, SEM, XPS, UV-vis and LSV.

Chapter 4: Results and Analysis Evaluate the results and observations from the characterization studies and degradation experiments.

Chapter 5: Full-Scale Studies Implementation of the PEC system on a full-scale basis and economic analysis of a full-scale system is studied

Chapter 6: Conclusion The conclusion to the research question addressed in chapter 1 and the limitations and suggestions of this study

Chapter 2. Literature review: Use of $BiVO_4$ Photoanodes to treat Pharmaceutical in Water

2.1 Literature Review

2.1.1 Review of Review Papers

The review started with examining existing review papers on $BiVO_4$ and its use in PEC to understand the existing t knowledge, which are listed in Table 2.

Table 2. Summary of the review papers on the use of $BiVO_4$ in PEC and PC systems to degrade OMPs

Paper title	**Summary**
Bismuth vanadate in photo electrocatalytic water treatment systems for the degradation of organics: A review on recent trends (Orimolade & Arotiba, 2020a)	• Use of Bismuth vanadate in various photocatalytic and photo-electrocatalytic processes as an electrode • Structure and electronic properties of bismuth vanadate • Preparation and modification to improve its photo electrocatalytic efficacy • photo electrocatalytic degradation of different organic compounds
Bismuth vanadate-based semiconductor photocatalysts: a short critical review on the efficacy and the mechanism of photodegradation of organic pollutants (Monfort & Plesch, 2018)	• background of semiconductor catalysis: efficacy and mechanism – identification of oxidative species and by-products • structure and synthesis of Bismuth Vanadate • $BiVO_4$-based catalysts • Doped $BiVO_4$ and $BiVO_4$ composites
$BiVO_4$ photocatalysis design and applications to oxygen production and degradation of organic compounds: a review (T. D. Nguyen et al., 2020)	• Synthesis of monoclinic $BiVO_4$ catalyst by different methods • $BiVO_4$ crystal structure and optical characteristics and photocatalytic principles
Review on Synthesis, Modification, Morphology, and Combination of $BiVO_4$-based Catalysts for Photochemistry: Status, Advances, and Perspectives (Guan et al., 2024)	• Preparation methods of $BiVO_4$ • Modification by metal doping • The special structure of $BiVO_4$; special morphology oxygen and vandalism defects • Modification mechanism • Applications

Recent progress in $BiVO_4$-based heterojunction nanomaterials for photocatalytic applications (Zhong et al., 2023)	• Mainly about heterojunctions in $BiVO_4$ and types • Explanation of all heterojunctions • Application of $BiVO_4$-based heterojunctions in photocatalysis

The reviewed papers collectively provide a comprehensive overview of $BiVO_4$ in photocatalytic and PEC applications. From the analysis, information was obtained on various strategies used to enhance photocatalytic efficacy, the structure of the semiconductor's various applications, and degradation rates for various OMPs. Limited research exists on the long-term stability of $BiVO_4$ photoanodes in real-world applications and their scalability for practical water treatment. Financial feasibility and industrial-scale implementation remain underexplored. Additionally, a comprehensive review comparing $BiVO_4$ performance in PEC systems versus traditional photocatalysis is lacking. Addressing these gaps is crucial for advancing the practical adoption and optimization of $BiVO_4$-based water treatment technologies.

2.1.2 Review of Experimental Work

Based on the identified gaps, the next the literature review focussed on understanding the performance of $BiVO_4$-based photoanodes under PEC conditions. This involves reviewing studies that examine various types of $BiVO_4$ photoanodes, experimental conditions, degradation efficacy, and mechanisms involved in the degradation of different pharmaceuticals which are listed in Table 4. An extensive search of research articles was conducted using Scopus and Google Scholar databases to develop a comprehensive understanding based on the keywords listed in Table 3.

Table 3. Key words combinations used for Research search in Scopus

KEY WORDS USED	NO. OF ARTICLES
Photo AND electrocatalysis AND $BiVO_4$ AND Pharmaceuticals	7
Photo AND Electrocatalytic AND $BiVO_4$	45
Photo AND Electrochemical AND oxidation AND $BiVO_4$	142
Photo AND Electrochemical AND oxidation AND $BiVO_4$ AND Pharmaceutical	2

These papers were scanned and papers containing data related to only pharmaceuticals were intensively reviewed. The papers with data related to other indicators and OMPS were not considered.

Table 4 Overview of $BiVO_4$ – Based PEC System for Degradation of Pharmaceutical

Name of OMP	Initial concentration (mg/L)	Photoanode used	Removal %	Duration (min)	Photocurrent density (mA/cm^2)	Source
Caffeine (CAF)	10 mg/L	$BiVO_4$				(Łęcki et al., 2022)
		$BiVO_4$/ Co - Pi				
		$BiVO_4$/Co-pi with external potential				
Tetracycline Hydrochloride (TCH)	20 mg/L	$BiVO_4$	30	60		(Y. Li et al., 2024)
		$FeOOH/BiVO_4$	41.61			
		$FeOOH/BiVO_4$ 0.1 mM PMS	65			
		$FeOOH/BiVO_4$ 0.3 mM PMS	88			
Tetracycline Hydrochloride (TCH)	2(Arunachalam, Shaddad, Amer, & AL-Qadi, 2024)Shaddad, Amer, & AL-Qadi, 2024)					
		Zr:$BiVO_4$/NiFeOOH	96			
Ciprofloxacin (CIP)			74.6			
Riboflavin (RF)			57.8			
Chloramphenicol (CAP)	5 mg/L	Mo-doped $BiVO_4$	96			(Su et al., 2024)
Tetracycline Hydrochloride (TCH)	80 mg/L	Zr: $BiVO_4$	35	60	3.07	(Arunachalam, Shaddad, Amer, Alsalman, et al., 2024)
		Zr:$BiVO_4$ Bi_2S_3–CoS	99		0.89	
Ciprofloxacin (CIP)	10 mg/L	FTO/$BiVO_4$	43	180		(Yusuf et al., 2023)
		FTO/$NiSe_2$/$BiVO_4$	76			
Tetracyline		$BiVO_4$	36.8	60	0.19	(Pan et al., 2023)
		$BiVO_4$/ Co - Pi	52.8		1.99	
		$BiVO_4$/Co-Pi 0.2 mM PMS	97.4			
Benzyl alkyl dimethylammonium compounds (BAC – C 12)		WO_3/$BiVO_4$	99	90		(Davies et al., 2023)
Tetracycline	20 mg/L	$BiVO_4$/PMS	64	60		(W. Wang et al., 2023)
		$CoFe_2O_4$-$BiVO_4$ /PMS	89.1			
		$CoFe_2O_4$-$BiVO_4$	80.9			
Chlortetracycline (CTC)			88.2			

oxytetracycline (OTC)			88			
Ciprofloxacin (CIP)			35.6			
Ofloxacin (OFX)			49.2			
Acetaminophen (ACT)	40 µg/L	$BiVO_4$	88	180		(Ali, Wu, et al., 2023)
		$BiVO_4$/BiOI	97			
Ofloxacin	8 mg/L	$BiVO_4$-CF	48.1	120		(K. Wang et al., 2020)
		$BiVO_4$-PDA/CF	55.2			
		$BiVO_4$-CF-PMS 2.0Mm	100			
Caffeine (CAF)	10 µmol/L	$BiVO_4$	81.7			(Prado et al., 2022)
		$BiVO_4$ rGO	100	360		
Tetracycline Hydrochloride (TCH)	10 mg/L	$BiVO_4$	22.1		0.30	(Zeng et al., 2017)
		WO_3/$BiVO_4$	76.1		2.83	
		WO_3/Mo-$BiVO_4$	85.6		3.78	
Ciprofloxacin (CIP)	10 mg/L	$BiVO_4$ CTAB 0.2	98.5	70		(Z. Chen et al., 2022)
Tetracycline	20 mg/L	$BiVO_4$	59	60	0.18	(Y. Li et al., 2021)
		ZnO/$BiVO_4$	84.5		0.29	
Sulfamethoxazole (SMX)		$BiVO_4$	50	120	0.25	(Fuentes-Camargo et al., 2020)
Acetaminophen	10 mg/L	$BiVO_4$/BiOI	68	120	0.352	(Orimolade et al., 2019)
Ciprofloxacin			62			
Diclofenac sodium	10 mg/L	$BiVO_4$	68	120	0.0072	(Orimolade & Arotiba, 2022)
		$BiVO_4$/BiOI	59		0.18	
		Ag-$BiVO_4$/BiOI	56		0.58	
		Ag-$BiVO_4$/BiOI—Ag-BiOI	92			
Ciprofloxacin	10 mg/L	$BiVO_4$	53	120	0.362	(Orimolade et al., 2020)
		$BiVO_4$/MnO_2	73		0.589	
Ciprofloxacin	10 mg/L	$BiVO_4$/Ag_2S	80	120	1.194	(Orimolade & Arotiba, 2020b)
Sulfamethoxazole			86			
Tetracycline	20 mg/L	$BiVO_4$ + PMS (0.5 mM)	63.5	30		(Kang et al., 2021)
		CN/$BiVO_4$ + PMS	75.6			
		Na-$BiVO_4$ + PMS	69.9			
		CN/Na-$BiVO_4$ + PMS	98.2			
Tetracycline hydrochloride (TCH)	20 mg/L	$BiVO_4$	47	120	0.45	(J. Liu et al., 2020)
		F - $BiVO_4$	56		1.41	
		F-$BiVO_4$-NiFe-LDH	86		2.67	
Tetracycline	10 mg/L	$BiVO_4$	58.4	140	0.0015	(Singla et al., 2023)
		$BiVO_4$ BiOBr	73.5		0.0139	
		$BiVO_4$ BiOBr (1:3)	90.4		0.2198	
Acetaminophen (ACT)	45 ug/L	$BiVO_4$	99	120	0.16	

Benzotriazole (BTA)			70			(Ali, Jagannathan, et al., 2023)
Propranolol (PRO)			70			
Tetracycline	10 mg/L	R-BVO rod $BiVO_4$	96.4			(Y. Liu et al., 2024)
		P-BVO particle $BiVO_4$	66.5			
		SR-BVO short rod $BiVO_4$	74.8			
Tetracycline	30 mg/L	$BiVO_4$		30	3.9	(Xing et al., 2024)
		$Co_9S_8/BiVO_4$			3.2	
		Zn-$Co_9S_8/BiVO_4$	82		1.6	
Enrofloxacin (ENR)		$BiVO_4$/BiOBr	95	90		(C. Liu et al., 2024)
Tetracycline (TC)		$BiVO_4$/BiOBr	94	20		
Oxytetracycline (OTC)		$BiVO_4$/BiOBr /PMS	98			
Chlortetracycline (CTC)			90			
Norfloxacin (NRF)			86			
Ofloxacin (OFL)			89			

This review provided valuable insights into experimental methodologies, modification strategies, degradation mechanisms, and the specific pharmaceutical compounds targeted. Each study examined varied experimental parameters, setups, and conditions, offering a comprehensive understanding of the factors influencing PEC performance.

Various modification methods

As discussed, there are various methods and materials used to modify semiconductor material. Co – catalysts act as an effective method. This enhancement is primarily achieved by modifying the cocatalyst layer, isolating the electrode from the electrolyte, and providing physical protection against corrosion and metal doping (Fu et al., 2024; Guan et al., 2024). Łęcki et al., (2022) enhanced $BiVO_4$ for caffeine degradation by incorporating a cobalt-phosphate (Co-Pi) co-catalyst in a PEC system. Co-Pi extended electron lifetime, reduced recombination, and increased the degradation rate by up to 26 times. Similarly, research work has been done to enhance the $BiVO_4$ performance by loading it with other oxygen catalysts such as FeOOH, NiOOH and NiFeOOH (Arunachalam, Shaddad, Amer, & AL-Qadi, 2024). Li et al., 2021 studied a different aspect of co-catalyst on $BiVO_4$. The photoanode $BiVO_4$ was constructed on ZnO nanorod to understand the photo electrocatalytic process on 3-dimensional coral structure ZnO/$BiVO_4$ nanocomposite. This crystal facet engineering of semiconductor nanomaterials increases the efficacy of light absorption and mass transfer as it increases the contact area between the catalyst and the pollutant succeeding in degrading over 84% of TC in just 60 minutes. Metal doping is a method, where foreign metal ions are introduced into the semiconductor lattice to modify and enhance the semiconductor. Metal doping with appropriate elements has demonstrated improvements in degradation efficacy. Arunachalam et al. 2024

studied the combined effect of metal doping Zr along with the oxygen evolution catalyst (OEC) where the metal-doped Zr helped in charge separation and reduced further recombination. The cocatalyst helped increase the kinetics and reduce further recombination. Similar work has been done on the combination of cocatalysts and metal doping Zr: $BiVO_4$ Photoanodes with bismuth sulphide (Bi_2S_3) and cobalt sulphide (CoS) nanoparticles as cocatalysts (Arunachalam, Shaddad, Amer, Alsalman, et al., 2024). Su et al., 2024 performed surface modification by metal doping $BiVO_4$ with Molybdenum (Mo) doping in $BiVO_4$ (Mo-$BiVO_4$). (Zeng et al., 2017) studied Chloramphenicol (CAP) degradation, where Mo doping enhanced photoelectron trapping and oxygen vacancy formation, increasing degradation to 96%. This study notched up a level further and used Mo-doped WO_3/$BiVO_4$ and optimized Co–Pi/WO_3/Mo-$BiVO_4$ to degrade TCH.

Heterojunction formation between two or more semiconductors is another method of modification. This helps with the degradation as it allows for spatial separation of photogenerated e and holes, enhanced light absorption, and reduced recombination. Based on the semiconductor bandgap, electronic energy levels, and separation of photogenerated charge carriers, heterojunctions are classified into four types: Type I, Type II, p-n heterojunction, and Z-scheme system. Due to differences in band edge alignment, Type I offers the least efficient performance. In contrast, Type II enables efficient charge separation. When exposed to light, p-n heterojunctions facilitate the accumulation of electrons in the n-type semiconductor and holes in the p-type semiconductor, promoting more effective charge separation. The Z-scheme relies on energy level matching between the conduction band (CB) of semiconductor 1 and the valence band (VB) of semiconductor 2, enabling efficient recombination of charges across the heterojunction (Qiao et al., 2022). Various research work has also been established to study heterojunction mechanisms for PEC enhancement of $BiVO_4$ photoanodes. Yusuf et al., 2023 constructed an S scheme FTO/$NiSe_2$/$BiVO_4$. The S scheme heterojunction is such as the Z scheme restraining charge recombination. It overcomes the limitations of type II and Z schemes by carefully selecting semiconductors that can operate independently as reduction or oxidation photocatalysts. $NiSe_2$ (1.6 – 2.0 eV) and $BiVO_4$ (2.5 – 2.85 eV) were appropriate catalysts for the formation of S scheme heterojunction or n – n heterojunction. W. Wang et al., 2023worked on the junction of the $CoFe_2O_4$ layer on $BiVO_4$ which was an adoption of the heterojunction II mechanism which led to a 4 times improvement in the photocurrent density and enhanced degradation efficacy. Other heterojunction-based modifications include $BiVO_4$/MnO_2 which follows the n-n heterojunction mechanism (Orimolade et al., 2020), $BiVO_4$/BiOI (Ali, Wu, et al., 2023; Orimolade et al., 2019), $BiVO_4$/Ag_2S (Orimolade & Arotiba, 2020b) follows p – n heterojunction mechanism. Heterojunctions-photoanodes are also coupled with a few more modifications to increase their performanceClick or tap here to enter text. degradation of TC was studied under visible light over $BiVO_4$, g-C_3N_4 coupling and Na^+ doping was used to co-modify $BiVO_4$ to obtain g-C_3N_4/Na-$BiVO_4$ (CN/Na-$BiVO_4$) heterojunction catalyst which followed Z scheme formation, (Kang et al., 2021b). Liu et al., 2024 studied the crystal facet engineering of the $BiVO_4$ photoanode and prepared rod-like morphology $BiVO_4$ with monoclinic and tetragonal phase structure (R-BVO). This benefitted from the one-dimensional conduction of rod-like morphology and the p-n junction formed by the two-phase structure.

The use of surfactant to modify $BiVO_4$ Photoanode is an upcoming cheaper method to modify semiconductors. Chen et al., 2022 explored an alternative approach to enhancing PEC performance by using surfactants, and amphiphilic chemicals, as morphology-directing agents and stabilizers during semiconductor synthesis, rather than relying on traditional metal doping or co-catalysts. In this study, cetyl trimethyl ammonium bromide (CTAB), a long-chain carbon compound, was employed to assist in the synthesis of $BiVO_4$ for the photodegradation of ciprofloxacin (CIP). The use of CTAB generated a significant number of oxygen vacancies in

$BiVO_4$, improving the separation efficacy of photo-generated carriers. This method is relatively simple, and the degree of oxygen vacancy formation can be controlled by adjusting the amount of surfactant. The photodegradation efficacy of CIP using this approach was found to be 60 times higher than that of unmodified $BiVO_4$. This research presents a novel strategy for modifying $BiVO_4$ for PEC applications. Due to its easy application, this method will be further explored as a key focus of this research.

Pharmaceutical compounds studied

This review focused on the degradation of pharmaceutical compounds using BiVO4. Most studies focus on a single pharmaceutical compound. The most studied pharmaceuticals include tetracycline (Fiaz et al., 2021), ciprofloxacin(Ghosh et al., 2023), and chloramphenicol (Nguyen et al., 2022). All these are among the widely used antibiotics in our daily lives and have been known to have large effects as they enter water streams. Using PEC with surface-modified $BiVO_4$ has helped achieve 85 – 99% degradation of these OMPs in most cases. However, in these studies, these pharmaceuticals are examined individually. Research on the combined effects of these pharmaceuticals, as they would occur in wastewater, remains largely unexplored. Ali, Jagannathan, et al., (2023) explored the simultaneous removal of 3 OMPs acetaminophen (ACT), benzotriazole (BTA) and propranolol (PRO) using $BiVO_4$ photoanode resulting in 99% removal of ACT and BTA and 70% removal of PRO. The researchers worked on varying experimental conditions and backgrounds to understand the optimization of PEC. The experiments were carried out in various types of water including deionized water, simulated wastewater, and tap water. There were some studies conducted to understand the working of PEC in synthetic pharmaceutical wastewater (Orimolade et al., 2019; Yusuf et al., 2023b) and Wastewater (K. Wang et al., 2020a). The initial concentration of the Pharmaceuticals largely varied from experiments, major research work was done from values ranging between 5 – 80 mg/L which is much higher than what is present in the actual wastewater which ranged from 108 – 266 μg/L from 45 – 128 various OMPs in the influent of secondary treatment and 10.8 – 49.5 distributed between 42 – 95 in the secondary effluent from a wastewater treatment plant (J. Wang et al., 2018).

Experimental setup

Most experiments utilized a similar three-electrode PEC setup, consisting of a $BiVO_4$ photoanode, an Ag/AgCl reference electrode, and a platinum counter electrode. In these systems, an n-type semiconductor in the photoanode facilitates the oxidation reaction, while a p-type semiconductor in the photocathode drives the reduction reaction. A typical configuration for an n-type $BiVO_4$ photoanode includes a Pt counter electrode and an electrolyte solution, ensuring efficient charge transport and reaction kinetics. Light sources were predominantly xenon lamps with intensities around 100 mW/cm^2, simulating sunlight conditions. The applied potential voltages (external bias) ranged from 0.6 V to 1.23 V, ensuring effective photoelectrocatalytic performance. Most studies preferred using 0.1M Na_2SO_4 as the electrolyte due to its high ionic conductivity, chemical stability, and ability to support charge transport without interfering with the PEC reactions.

Experimental conditions and results

While the removal efficacy of the pharmaceutical when only $BiVO_4$ was used ranged from 35 – 55% in major cases, when modified by different techniques, they showed high removal efficacy ranging from 85 – 99%. Using the photoanodes Zr:$BiVO_4$ $Bi2S_3$–CoS in 60 min (Arunachalam, Shaddad, Amer, Alsalman, et al., 2024), WO_3/$BiVO_4$ in 90 min (Davies et al., 2023), $BiVO_4$ – CF/PMS in 120 min (K. Wang et al., 2020a) were few works which could reach 99% degradation of the pollutant. Although the experiments were conducted over 180

minutes, most of the degradation was achieved within the first 120 minutes. The goal is to maximize degradation efficacy within the shortest possible time frame. Photocurrent density is a critical parameter in PEC systems as it directly reflects the efficacy of charge carrier generation, separation, and transport under light irradiation. Most work uses the photocurrent density of just $BiVO_4$ as the benchmark which is around 0.85 – 0.89 mA/cm^2. Compared to this most modified photoanodes have much higher photocurrent density ranging from 2 – 3.7 mA/cm^2 indicating better performance. The stability and reusability of modified $BiVO_4$ photoanodes were also assessed, with several studies showing promising results. Good stability and up to 5 cycles uses were tested

Mechanisms involved

Reactive oxygen species (ROS) formation is the main component of the degradation process. Most photoanodes used hydroxyl radical (OH°) and superoxide anion radical (O_2°-) to attack the pollutants. Some research also relied on PMS which generated sulfate radicals (SO_4°-) improving the degradation efficacy by folds in the same duration as discussed previously (Wang et al., 2020). (K. Wang et al., 2020b) The generation of these ROS is done through efficient charge separation, the electrons and the holes migrate to the catalyst's surface to participate in the redox reaction leading to ROS generation.

While extensive research has been conducted on various $BiVO_4$ modification strategies, such as co-catalyst loading, metal doping, and heterojunction formation, studies specifically investigating the effects of surface modification with QACs on $BiVO_4$ remain limited. QAC modification represents an emerging and cost-effective alternative**,** offering potential advantages such as surface charge modulation, enhanced charge carrier separation, and improved oxygen vacancy formation. Despite these benefits, its application in $BiVO_4$-based PEC systems has not been widely explored. This section of the review aims to address this gap by analyzing the influence of QACs, such as CTAB and CTAC, on the structural, morphological, and electronic properties of $BiVO_4$, assessing their potential for improving photocatalytic degradation of pharmaceutical contaminants through some already existing research listed in table 5.

Table 5. Research work done on the modification of $BiVO_4$ Photoanodes with QAC used to degrade pollutants

Surfactant Type & Concentration	Solution Preparation & Mixing	Heating/Calcination Process	Performance	Mechanistic Insights	Source
0.05 M CTAB	2 mmol NH_4VO_3 in 20 mL water (96°C), cooled to room temp; 40 mL CTAB (0.05 M) + $Bi(NO_3)_3 \cdot 5H_2$	Heated at 80°C in an oil bath for 12 h; centrifuged, washed with water and ethanol, dried	RhB degraded in 20 min; 12× higher efficacy than aqueous $BiVO_4$	High efficacy due to crystal phase; impurity level narrows band gap; BET surface area, not	(Yin et al., 2010)

	O in 20 mL water, stirred for 10 min, added dropwise			primary factor	
2.0 g/L CTAB (with PVP, SDBS)	1 mmol $Bi(NO_3)_3 \cdot 5H_2O$ + 1 mmol NH_4VO_3 in 20 mL ultrapure water; surfactant added, stirred for 20 min; ultrasound for 10 min	Heated in a Teflon-lined autoclave at 180°C for 6 h; washed with ethanol and water, freeze-dried for 12 h	$BiVO_4$-CTAB shows 94.9% RhB degradation; BET surface area improved	CTAB enhances the surface area and stability of nanostructures; and improves the photocatalytic rate	(J. Liu et al., 2023)
0.053 – 0.212 mmol CTAB	0.096 g $NaVO_3$ + CTAB in 50 mL water, heated to 40°C with sonication; $Bi(NO_3)_3 \cdot 5H_2O$ dissolved in 30 mL HNO_3, added dropwise; pH adjusted to 6.0	Heated in a water bath at 60°C for 1 h; hydrothermal at 100°C for 24 h; centrifuged, washed with ethanol and water, dried in vacuum	~60× higher CIP photodegradation efficacy than neat $BiVO_4$	CTAB concentration affects $BiVO_4$ morphology and oxygen defects; enhances electron-hole separation	(Z. Chen et al., 2022a)
10 – 40 g/L CTAC	$Bi(NO_3)_3 \cdot 5H_2O$ + HNO_3 (ultrasound) mixed with NH_4VO_3 + NaOH; CTAC added, stirred for 4 h; pH adjusted to 9.0	Heated at 90°C for 4 h; calcined at 450°C for 5 h	99% dye degradation with 25 g/L CTAC in 100 min	Optimal CTAC concentration enhances photocatalytic efficacy; oxygen vacancies critical for increased activity	(Zhu et al., 2024)

Zhu et al. (2024) used Hexadecyltrimethylammonium chloride (CTAC), a QAC, to regulate the surface morphology of monoclinic $BiVO_4$. The oxygen defects caused by introducing 25 mg/L CTAC increased its photocatalytic performance to 99% compared to the CTAC-free $BiVO_4$ (73%). CTAC, being a cationic surfactant, can form micelles in aqueous solutions. The hydrophilic terminal groups of CTAC reabsorbed to Bi^+ ions through electrostatic attraction,

effectively controlling the growth and nucleation rate of $BiVO_4$ particles. The ability of CTAC to regulate the surface morphology of monoclinic $BiVO_4$ results in the formation of a porous structure that significantly enhances photocatalytic performance. The Density Functional Theory (DFT) calculations further proved the impact of CTAC modification, revealing an increase in electron density and carrier mobility near the top of the valence band. This enhancement improves charge separation and photovoltaic efficacy in the $BiVO_4$ system. Liu et al. (2023) studied the photocatalytic performance of $BiVO_4$ after assisting it with cetyltrimethylammonium bromide (CTAB). $BiVO_4$ – CTAB demonstrated irregular polyhedron structures and increased the specific surface area of the photoanode, enhancing its photocatalytic degradation. $BiVO_4$ modified with CTAB exhibited lower electron densities than pure $BiVO_4$. This characteristic is favourable for separating electron-hole pairs, which significantly improves photocatalytic activity and charge transfer.

Chen et al., (2022) investigated the photocatalytic performance of $BiVO_4$ by adding PMS, which improved photocatalytic efficacy and reduced degradation time. $BiVO_4$ was synthesized with CTAB, which served as a template for creating $BiVO_4$ nanosheets. CTAB facilitated surface modification, introducing a carbon-containing functional group on the catalyst, which enhanced the adsorption and activation of PMS. This carbon-containing group acted as a Lewis base site, inducing PMS hydrolysis under acidic conditions without requiring a metal active site. This process generated singlet oxygen, a highly reactive form of oxygen capable of breaking down organic pollutants. The use of singlet oxygen for pollutant degradation is an environmentally friendly method characterized by low chemical input and fast reaction kinetics. Additionally, the presence of carbon species improved the separation of photogenerated electrons and holes, boosting the overall efficacy of the photocatalytic reaction. This study provides new insights into the generation of singlet oxygen over $BiVO_4$ through PMS hydrolysis and supports the expansion of $BiVO_4$-based persulfate activation technology for pollutant degradation.

2.2 Research Gaps

Through the literature review, several key research gaps were identified

- **Experimental Comparison of $BiVO_4$ Photoanode Modifications**: While various studies have explored different methods to enhance the photoelectrochemical (PEC) performance of $BiVO_4$ photoanodes, there is a lack of comprehensive experimental comparisons between these modification techniques.
- **Surface Modification of $BiVO_4$ with Quaternary Ammonium Compounds (QACs)**: The potential of QACs to modify the surface of $BiVO_4$ for PEC applications remains largely unexplored. Given QACs' known benefits in enhancing surface properties and charge dynamics.
- **Competition Between Multiple Target Species**: Most existing research focuses on the degradation of one or two pharmaceutical compounds in isolation, without considering the competitive interactions that may occur when multiple contaminants are present and what impact different water matrices can have on degradation
- **Scaling PEC Systems to Real-World Applications**: There is a significant gap in translating lab-scale PEC systems to real-world applications. This research will explore the practical challenges and potential solutions for scaling up PEC technology, focusing on maintaining efficacy and reliability in large-scale or continuous operation settings.

Chapter 3. Materials and Methodology

3.1 Reagents and Pharmaceuticals

The $BiVO_4$ photoanodes were fabricated on fluorine-doped tin oxide (FTO) glass substrates (7 Ω/sq., 40 × 40 mm, Luoyang Guluo Glass Co., Ltd., China). The precursor solution was prepared by dissolving bismuth nitrate pentahydrate ($Bi(NO_3)_3 \cdot 5H_2O$, 98%, Sigma-Aldrich) and vanadyl acetylacetonate ($VO(AcAc)_2$, 98%, Sigma-Aldrich) in a mixture of acetic acid (99%, Sigma-Aldrich) and ethanol (100%, Sigma-Aldrich). This solution was used to fabricate $BiVO_4$ thin films via the ultrasonic spray pyrolysis process.

As part of the surface modification, additives were introduced into the fabrication process. These included alkyl trimethyl ammonium chloride (ATMAC, C16–C18), benzalkonium chloride (BAC, C16–C18), and dialkyl dimethyl ammonium chloride (DADMAC, C16–C18). These quaternary ammonium compounds were selected to enhance the photoelectrochemical performance of the electrodes. The electrode connections were prepared using carbon paste (Dycotec DM-CAP-4701S) for electrical conductivity and insulated with polyurethane resin (Electro lube) to ensure stability during experiments.

Secondary-treated wastewater was collected from the wastewater treatment plant at Waternet - RWZI Horstermeer for subsequent degradation experiments, ensuring the study's relevance to real-world wastewater conditions.

Figure 3. Collection of Secondary Treated wastewater effluent from RWZI Horstermeer

20 pharmaceutical compounds were selected as listed in table 6. and were spiked in the collected secondary wastewater sample. It was spiked such that all the pharmaceutical compounds reached ~ 10 ug/L concentration in the water.

Table 6. List of the pharmaceuticals in the mixture; all the data were obtained from (https://pubchem.ncbi.nlm.nih.gov/compound)

s/no	Pharmaceutical Name	Molecular Formula	Molecular Weight (g/mol)	Common Usage
1	Benzotriazole	$C_6H_5N_3$	119.12	Corrosion inhibitors, antifreeze
2	4-5-methyl-benzotriazole	$C_7H_7N_3$	133.15	Corrosion inhibitor
3	Carbamazepine	$C_{15}H_{12}N_2O$	236.27	Anticonvulsant
4	Diclofenac	$C_{14}H_{11}C_{l2}NO_2$	296.15	NSAID
5	Hydrochlorothiazide	$C_7H_8C_lN_3O_4S_2$	297.73	Diuretic
6	Metoprolol	$C_{15}H_{25}NO_3$	267.37	Beta-blocker
7	Sulfamethoxazole	$C_{10}H_{11}N_3O_3S$	253.28	Antibiotic
8	Propranolol	$C_{16}H_{21}NO_2$	259.34	Beta-blocker
9	Sotalol	$C_{12}H_{20}N_2O_3S$	272.36	Beta-blocker
10	Trimethoprim	$C_{14}H_{18}N_4O_3$	290.32	Antibiotic
11	Clarithromycin	$C_{38}H_{69}NO_{13}$	747.96	Antibiotic
12	Ketoprofen	$C_{16}H_{14}O_3$	254.28	NSAID
13	Metformin	$C_4H_{11}N_5$	129.16	Antidiabetic medication
14	Clofibric acid	$C_{10}H_{11}ClO_3$	214.65	Lipid-lowering agent
15	Sulfadimethoxine	$C_{12}H_{14}N_4O_4S$	310.33	Antibiotic
16	Caffeine	$C_8H_{10}N_4O_2$	194.19	Stimulant
17	Theophylline	$C_7H_8N_4O_2$	180.16	Bronchodilator
18	Acetaminophen	$C_8H_9NO_2$	151.16	Analgesic and antipyretic
19	Gabapentin	$C_9H_{17}NO_2$	171.24	Anticonvulsant and analgesic

3.2 Fabrication of $BiVO_4$ Photoanodes

The fabrication of $BiVO_4$ photoanodes was carried out in several distinct steps: preparation of the precursor solution, spray pyrolysis deposition using a spray nozzle, annealing, and finally, wire attachment for electrode connections. In this study, we followed the method followed by Ali et al., 2025.The precursor solution was prepared by first dissolving 0.106 g of $VO(AcAc)_2$ in a 20 mL solvent mixture comprising 15 mL of Milli-Q water and 5 mL of ethanol. This mixture was subjected to ultrasonication for 10 minutes, although complete dissolution was not achieved. Separately, 0.097 g of bismuth nitrate pentahydrate ($Bi(NO_3)_3 \cdot 5H_2O$) was dissolved in 10 mL of acetic acid and ultrasonicated for 10 minutes until fully dissolved. The bismuth

nitrate solution was then gradually poured into the vanadyl acetylacetonate solution while stirring, resulting in a light blue, transparent solution. The combined solution was ultrasonicated for an additional 10–15 minutes to ensure homogeneity and was used immediately to prevent precipitation.

$BiVO_4$ thin films were fabricated on FTO glass substrates using an ultrasonic spray pyrolysis system. The FTO substrates were cleaned by sonication in ethanol or acetic acid for 5 minutes, followed by demineralised water for another 5 minutes, and finally rinsed with Milli-Q water. The conductive side of the substrate was identified using a multimeter (17–21 Ω) and placed facing upwards for deposition. The precursor solution was loaded into a 60 mL syringe and installed in a dual syringe pump (NE-1010, ProSense B.V.). The spray nozzle, connected to a 0.05 W ultrasonic generator (MSK-SP-01A, MTI Corporation), was operated using compressed air at a fixed pressure of 0.25 bar. The nozzle was positioned 10 cm above the heated substrate, which was maintained at 225°C on a hot plate (EQ-HP-1515-LD, MTI Corporation). The precursor solution was sprayed onto the preheated FTO substrates at a controlled flow rate of 0.3 $mL \cdot h^{-1}$. A multistage X-Y axis CNC controller (MSK-USP-ST1, MTI Corporation) ensured uniform deposition across the substrate through programmed scanning motion. The spray coating process was repeated twice to achieve a homogeneous, nanostructured $BiVO_4$ film.

Following deposition, the coated substrates were annealed in a muffle furnace at 460°C for 2 hours with a ramp rate of 2°C per minute to crystallise $BiVO_4$ into its monoclinic scheelite phase. The annealed substrates were then cooled to room temperature and air-dried. The resulting films exhibited a uniform yellowish appearance, confirming successful fabrication and crystallization.

To prepare the photoanode for photoelectrochemical experiments, a 10 cm copper wire was attached to the coated side of the photoanode. The wire was placed on the surface, and carbon paste (Dycotec DM-CAP-4701S) was applied to ensure a strong electrical connection. The photoanode was placed on a hot plate, and the carbon paste was allowed to dry at room temperature for 2 hours, ensuring no copper wire was exposed. A polyurethane resin (Electro lube) was mixed and left to thicken for 30 minutes before being applied over the dried carbon paste as a protective insulating layer. The prepared photoanode was then placed in an oven at 60°C for 4 hours to harden the resin and secure the connection. The finalized photoanode was ready for use in photoelectrochemical experiments.

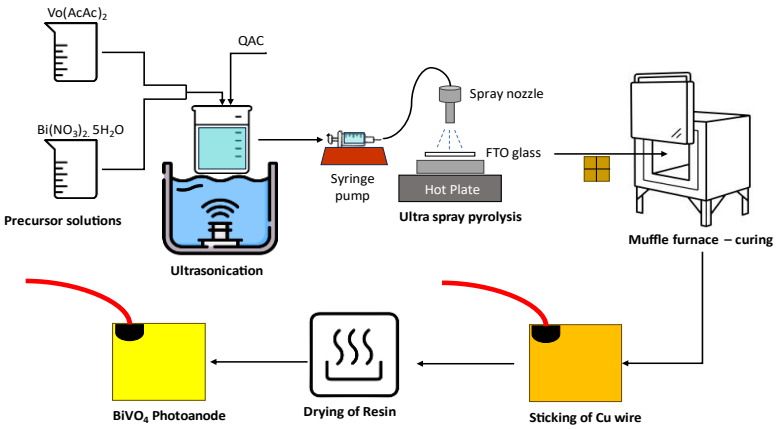

Figure 4. Schematic representation of the $BiVO_4$ photoanode synthesis process

3.3 Optimization of QAC addition to the precursor solution

The optimization of QAC concentrations in the $BiVO_4$ precursor solution was performed using a JAR test. The test started by adding incremental concentrations of QACs—alkyl trimethyl ammonium chloride (ATMAC, C16–C18), benzalkonium chloride (BAC, C16–C18), and Diallyl dimethylammonium Chloride (DADMAC, C16–C18)—to the $BiVO_4$ precursor solution. Initial tests evaluated concentrations between 10 to 100 mg/L, which were followed by larger increments from 100 to 800 mg/L to determine the upper solubility limits.

For ATMAC and BAC, concentrations up to 400 mg/L dissolved easily in the precursor solution using only ultrasonication for 10 minutes, maintaining a transparent state without the need for external heating. However, DADMAC showed limited solubility under the same conditions, as it failed to dissolve completely with ultrasonication alone. To achieve a homogeneous and transparent solution, the DADMAC containing precursor solution required simultaneous heating to 40°C along with ultrasonication for 10 minutes. This combined method effectively integrated DADMAC into the $BiVO_4$ precursor solution, ensuring a uniform mixture ready for the spray pyrolysis process. DADMAC has two allyl groups with double bonds that reduce the polarity and introduce rigidity into the molecule. This contrasts with ATMAC and BAC, in which the long flexible alkyl chains are more hydrophobic but lack the rigidity of allyl groups, so they can interact with water molecules more easily. Thus, DADMAC is less soluble in water at room temperature and must be heated to dissolve properly.

3.4 Experimental Setup for Photoelectrochemical Degradation

The PEC degradation experiments were conducted using a custom-built PEC reactor. The system consisted of a three-electrode configuration: the $BiVO_4$ photoanode with QAC modifications served as the working electrode, a carbon stick as the counter electrode, and a saturated Ag/Ag^+ (KCl) electrode as the reference electrode. The photoelectrochemical (PEC) degradation experiments were conducted using an electrochemical workstation (Autolab B.V., AUT85176, The Netherlands) to control and monitor the system. The degradation reactor consisted of a 175 mL electrode cube quartz cell, where the prepared $BiVO_4$ photoanode served as the working electrode and a carbon stick was used as the counter electrode.

The reactor was placed in a solar simulator (Atlas, SUNTEST XXL+, USA) equipped with three Xenon lamps (1700 W) during the degradation process. The setup provided an irradiance of 60 W/m^2 from directly above to simulate sunlight conditions. The photoanode was immersed in the electrolyte solution, ensuring the non-coated side facing the light source for optimal photoactivation. 0.1 M sodium sulfate (Na_2SO_4) was added to OMP spiked wastewater

The electrolyte solution used in the reactor was a 0.1 M sodium sulfate (Na_2SO_4) solution, prepared using ultrapure water. The reactor was operated under constant stirring to maintain homogeneity during degradation. Effluent samples were collected regularly, filtered through a 0.02 μm membrane filter, and analysed for OMP concentrations and degradation byproducts using high-performance liquid chromatography coupled with tandem mass spectrometry (HPLC-MS/MS).

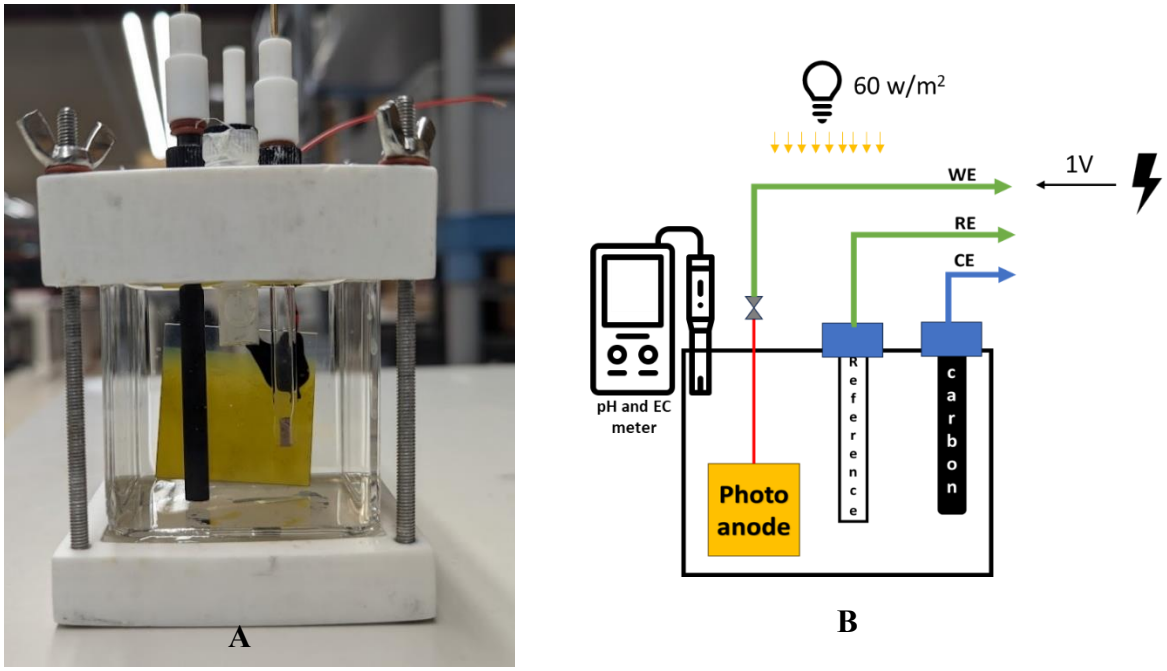

Figure 5. A. PEC Lab Reactor Setup B. Schematic of the setup – WE: working electrode Photoanode RE: Reference electrode CE: Counter electrode

3.5 Analytical Methods

Water Characterization: Physicochemical parameters such as pH, electrical conductivity (EC), and total organic carbon (TOC) were measured to assess matrix effects on PEC degradation. Major anions and cations were quantified by ion chromatography (IC).The Secondary wastewater samples were pre-filtered using 0.45 µm membrane filters before the experiment. The concentration of target OMPs in the samples was measured by high-performance liquid chromatography combined with tandem mass spectrometry (LC-MS). Prior to analysis, all samples were filtered through 0.2 µm glass fibre filters and diluted using ultrapure water. A mixture of 495 µL of this solution and 5 µL of internal standard calibration solution was transferred into LC-MS sample vials. Quantification of the target OMPs was then performed using a Waters Acquity LC-MS system.

After obtaining the contaminant concentrations, the degradation efficiency (%) was calculated to evaluate the photoelectrocatalytic performance of the photoanodes using the following equation:

$$Degradation\ efficacy\ (\%) : \left(1 - \frac{C}{C_0}\right) * 100$$

C_0 : Initial concentration C: Sample concentration ‘

Each experiment was performed in duplicate to ensure reproducibility. The results were averaged, and the standard deviation was calculated to evaluate experimental variability.

Scanning Electron Microscopy (SEM): SEM is a high-resolution imaging technique used to study the surface morphology and microstructure of photocatalyst films. It provides detailed insights into particle size, porosity, and uniformity, which are crucial for optimizing photocatalytic performance. The technique is often paired with energy-dispersive X-ray Spectroscopy (EDX) to analyze the elemental composition and distribution of dopants. The morphology and microstructure of the prepared photoanodes were examined using a FEI Quanta 650 Field Emission Scanning Electron Microscope, coupled with an energy-dispersive X-ray spectrometer (EDS) equipped with an Inca 250 SSD XMax20 detector.

X-ray Diffraction (XRD): XRD is a powerful technique for determining the crystallographic structure, phase purity, and degree of crystallinity of photocatalytic materials. It helps identify the presence of specific crystal phases, such as anatase and rutile in TiO_2-based materials, which influence photocatalytic efficacy. The crystalline structure and phase composition of the photocatalyst films were analysed using a Bruker D8 Advance diffractometer operating at 45 kV and 40 mA with Cu Kα radiation in a Bragg–Brentano configuration.

X-ray Photoelectron Spectroscopy (XPS): XPS is a surface-sensitive technique that provides information on the elemental composition, oxidation states, and chemical bonding of materials. It is essential for understanding surface modifications, dopant incorporation, and charge transfer mechanisms in photocatalytic systems. The chemical states of the elements were analysed using a Thermo Fisher K-Alpha surface analysis system.

UV-Vis (Ultraviolet – Visible) Spectroscopy: UV-Vis spectroscopy is used to evaluate the optical properties and bandgap energy of photocatalysts. It determines the material's ability to absorb light, which directly affects its photocatalytic efficacy. The absorbance spectra also help estimate the bandgap energy through Tauc plot analysis. UV-Vi's absorption spectra were recorded using a LAMBDA 1050+ UV/Vis/NIR spectrophotometer in the wavelength range of 280–800 nm.

Linear Sweep Voltammetry (LSV): LSV is an electrochemical technique used to measure photocurrent response and evaluate the charge transfer properties of PEC electrodes. It helps determine onset potential and overall photoelectrocatalytic efficacy. A higher photocurrent indicates improved charge separation and enhanced PEC activity. LSV was conducted in a three-electrode setup, scanning from -0.2 V to 1.5 V (vs. reference electrode) at a scan rate of 0.1 V/s.

Chapter 4. Results and Discussion

4.1 Characterization studies

4.1.1 X-ray Diffraction (XRD)

The XRD analysis of the synthesized $BiVO_4$ sample provides insights into the material's structural properties and phase composition. Figure 7 shows that the obtained XRD pattern exhibits distinct peaks at 2θ values of 19.55°, 29.40°, 31.00°, 35.67°, 40.04°, 47.98°, 53.37°, and 59.50°. These peaks correspond to the characteristic planes (110), (121), (040), (200), (002), (042), (202), and (161), respectively, of monoclinic scheelite $BiVO_4$. This identification is consistent with the reference JCPDS card no. 14-0688 (Ali, Wu, et al., 2023), which confirms the successful formation of the monoclinic phase.

The X-ray diffraction (XRD) patterns of $BiVO_4$ modified with various quaternary ammonium compounds (QACs)—DADMAC, BAC, and ATMAC—show slight variations compared to the unmodified $BiVO_4$. While the characteristic peaks of the monoclinic scheelite phase (indexed to JCPDS 14-0688) remain consistent in their overall presence, slight shifts and intensity changes are observed, reflecting the influence of QAC adsorption on the $BiVO_4$ surface.

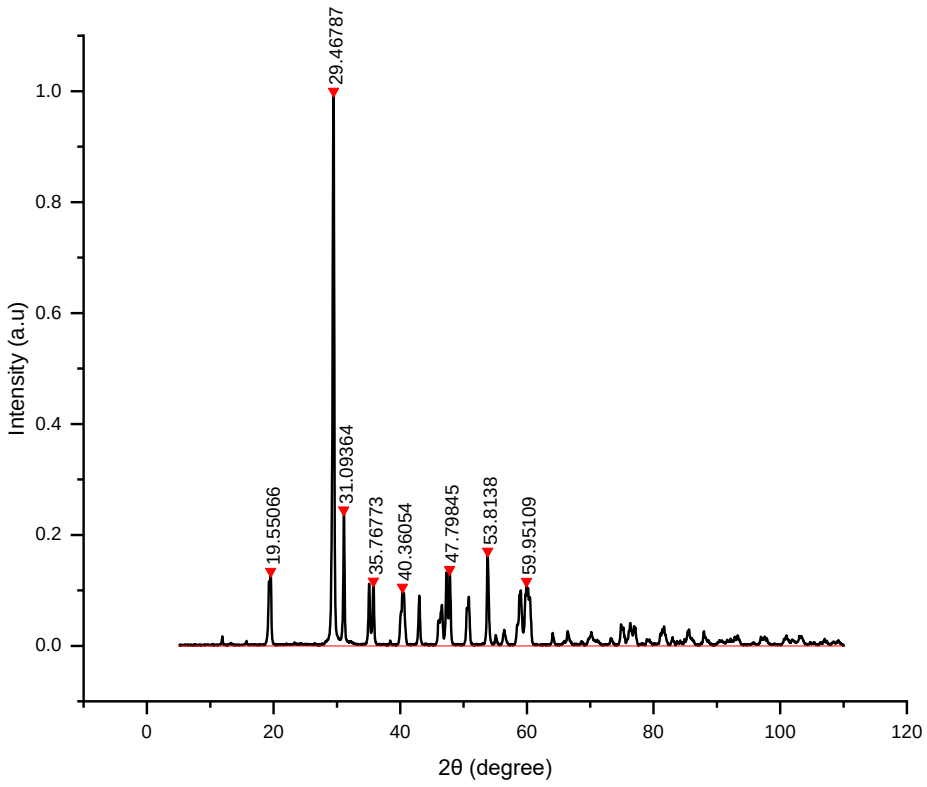

Figure 6. Detailed XRD analysis of the crystalline structure of $BiVO_4$

The 29.40° peak, the strongest reflection for $BiVO_4$, shows a slight shift in some variants, with ATMAC C18 and DADMAC C18 exhibiting a slight reduction in intensity. For the 31.00° peak, ATMAC variants display higher intensity, while BAC variants show moderate intensity compared to pure $BiVO_4$. These suggest some lattice strain which might have been induced by

the interaction of QAC. Apart from these variations, the overall diffraction patterns remain largely similar across all samples. These observed structural changes highlight the significant influence of QAC modifications on the surface properties of $BiVO_4$, while the bulk crystalline structure remains intact, ensuring the material's structural integrity is preserved. This aligns with the findings of (Z. Chen et al., 2022a) Whose studies on CTAB-modified $BiVO_4$ showed that the addition of QAC did not alter the monoclinic phase of $BiVO_4$ much

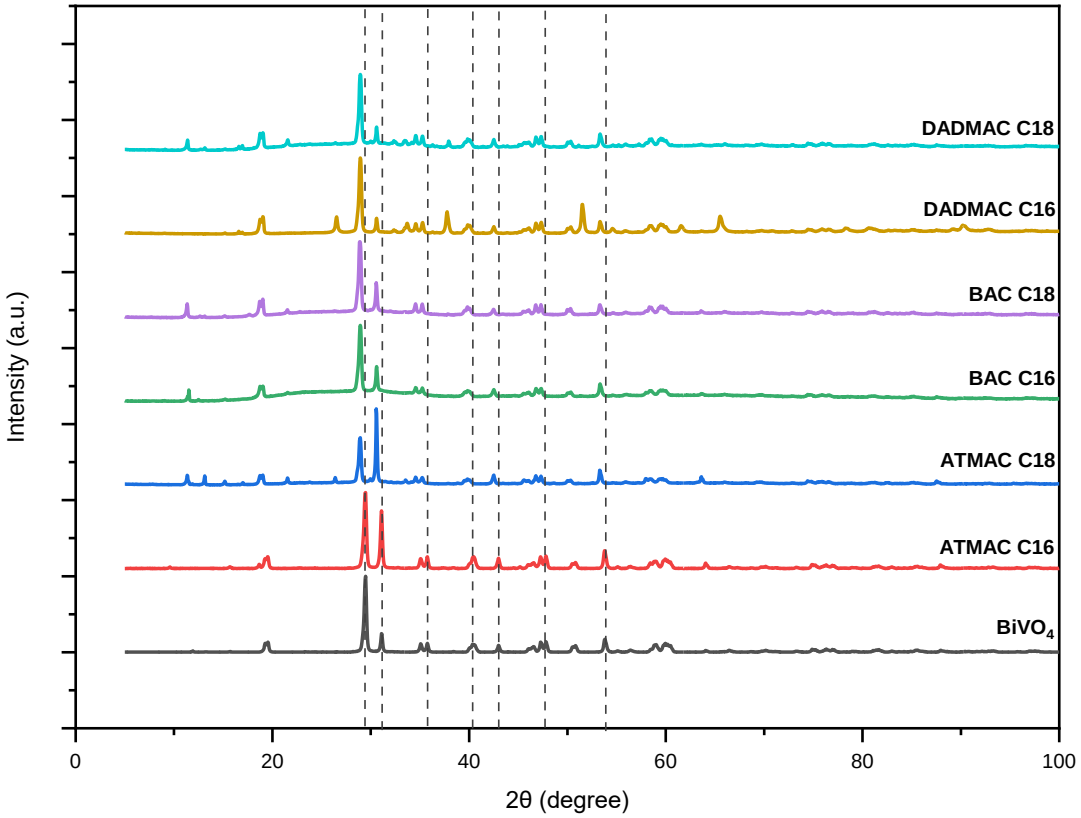

Figure 7. XRD graph of variants as compared the Base $BiVO_4$

4.1.2 Morphology studies

Scanning Electron Microscopy (SEM) was employed to study the morphology of the prepared samples. SEM images were captured for pure $BiVO_4$ and the three QAC-doped variants: ATMAC, BAC, and DADMAC, each with C16 and C18 chain types. A Secondary Electron Detector (SED**)** was used to collect secondary electrons emitted from the sample surface upon electron beam bombardment, enabling high-resolution surface imaging. An accelerating voltage of 5.00 – 10.00 kV was selected for imaging the QAC-based samples, as the lower kV minimises damage to sensitive materials and enhances resolution, providing better insights into surface details. Due to the irregular nature of the sample surfaces, a working distance (WD) of approximately 10 mm was maintained to achieve a balance between depth of field and resolution. The SEM analysis was further complemented using ImageJ software to measure particle sizes and analyze image features. The measurements were guided by the field of view (FOV)**,** magnification, and scale bars provided within the images, ensuring accurate dimensional analysis of the surface morphology. In the main text, SEM images of the unmodified $BiVO_4$ and the best-performing modified photoanode, DADMAC-C18, are presented.

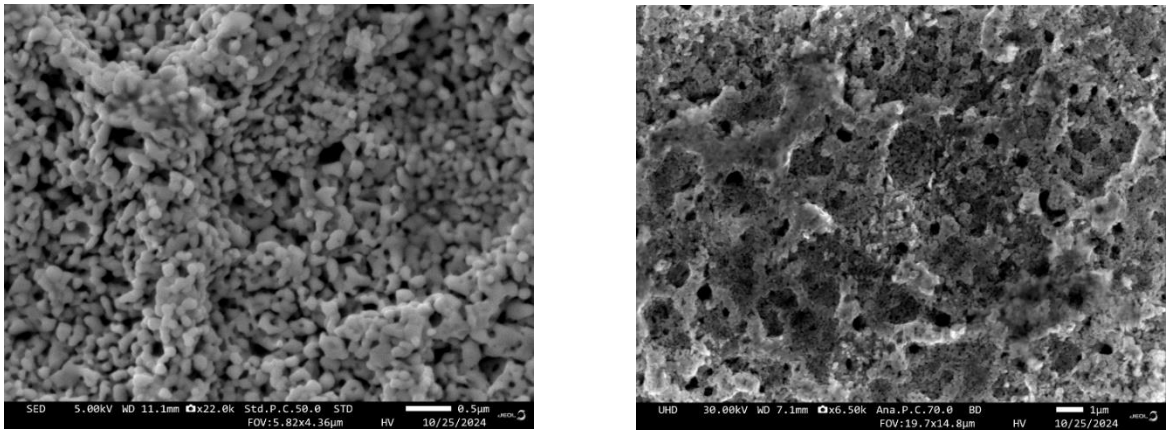

Figure 8. SEM images of Pure BiVO4 photoanodes for magnification 22000X and 65000X

The SEM images of pure $BiVO_4$ show a surface made up of small, granular particles that are distributed on the FTO glass. These granules form a porous structure with spaces and clusters, giving the material a high surface area as seen in Figure 1. The particles are closely packed, creating a compact layer that could help improve electron transfer in photoanodes.

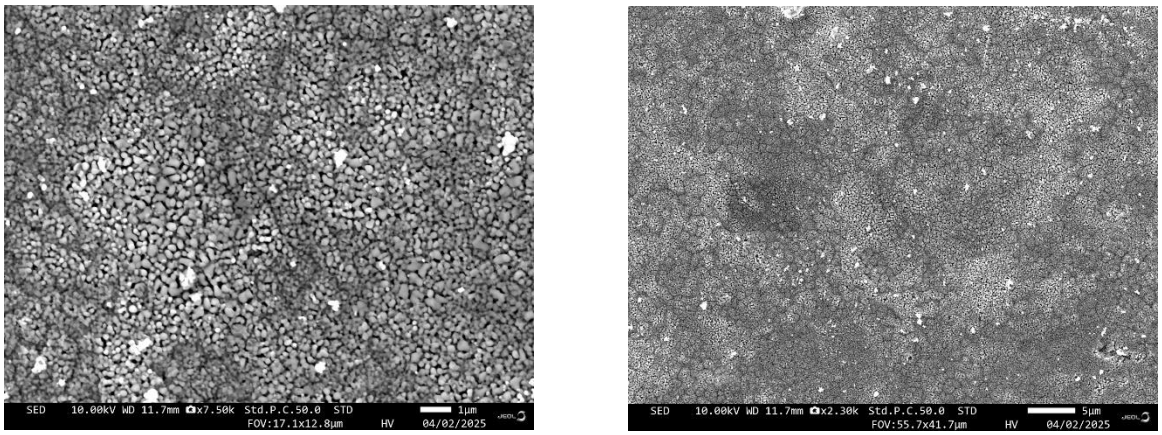

The DADMAC-C18 image revealed a granular morphology like that of pristine $BiVO_4$, indicating that the surface structure was preserved. Moreover, the QAC modifier appeared to be well-dispersed and uniformly integrated into the $BiVO_4$ matrix.

Similar surface characteristics were observed in other QAC-modified variants, confirming consistent mixing and deposition across all samples. Additional SEM images of photoanodes fabricated on a 300 °C hot plate is included in the Appendix for reference.

EDX analysis was conducted to determine the elemental composition of the synthesized photoanodes. For the unmodified $BiVO_4$ sample, the dominant elements detected were carbon (52.6%), oxygen (29.8%), vanadium (3.7%), and bismuth (3.7%). The high carbon content may be attributed to surface contamination or sample cleaning residual. In contrast, the DADMAC C18 exhibited a distinct elemental profile, with carbon at 25.3%, oxygen at 39.1%, vanadium at 22.5%, and bismuth at 11.0%. The increased content of vanadium and bismuth, along with reduced carbon levels, suggests improved exposure of the $BiVO_4$ surface

and successful incorporation of DADMAC-C18 These findings support the SEM observation of uniform QAC dispersion and surface modification.

4.1.3 X-ray Photon Spectrophotometer

X-ray photoelectron spectroscopy (XPS) was employed to investigate the surface chemical composition and oxidation states of the $BiVO_4$ photocatalyst and its modified counterparts. High-resolution spectra were acquired in the Bi 4f, V 2p, C 1s, and O 1s regions to determine the oxidation states of Bi and V, as well as to analyze the presence and chemical state of carbon and oxygen within the samples. The XPS results of the base photoanode and the best-performing photoanode modified with DADMAC C18 are specifically presented for comparative analysis. The XPS data of all photoanode variants prepared previously at 300°C is provided in the Appendix.

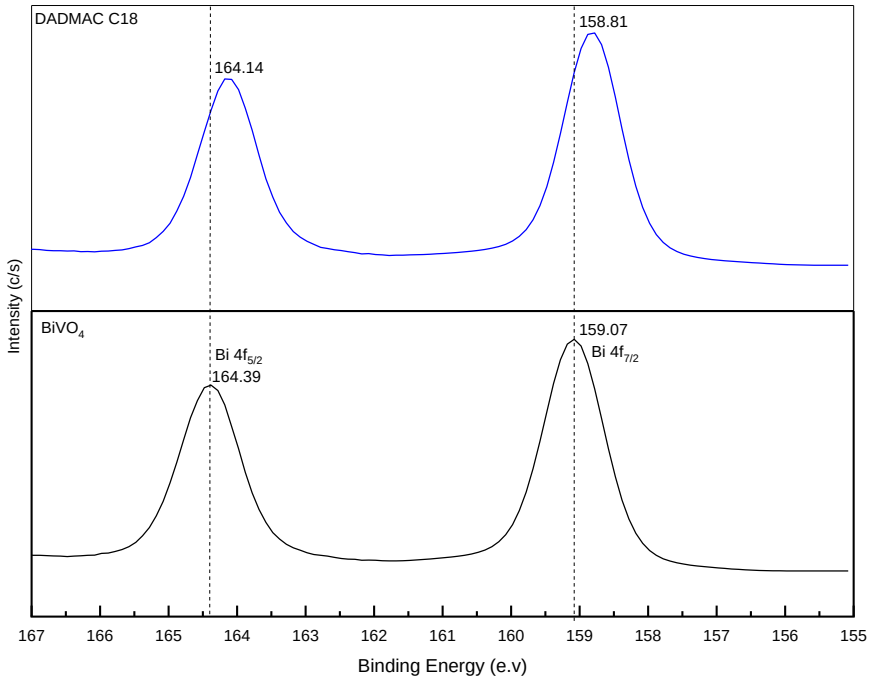

Figure 9. XPS spectra of Bi 4f for $BiVO_4$ and DADMAC C18, highlighting shifts in the $4f_{5/2}$ and $4f_{7/2}$ peak positions across different variants.

Bi4f:

The XPS Bi 4f spectra for the base $BiVO_4$ and DADMAC C18 modified photoanodes show two clear peaks corresponding to Bi $4f_{5/2}$ and Bi $4f_{7/2}$, confirming the Bi^{3+} oxidation state. Compared to the unmodified $BiVO_4$ (peaks at 164.39 eV and 159.07 eV), the DADMAC C18 modified variant exhibits a slight shift towards lower binding energies (164.14 eV and 158.81 eV). This negative shift suggests that the Bi^{3+} in the modified sample experiences a less

electronegative environment, potentially due to interactions with the QAC modifier covering the $BiVO_4$ surface.

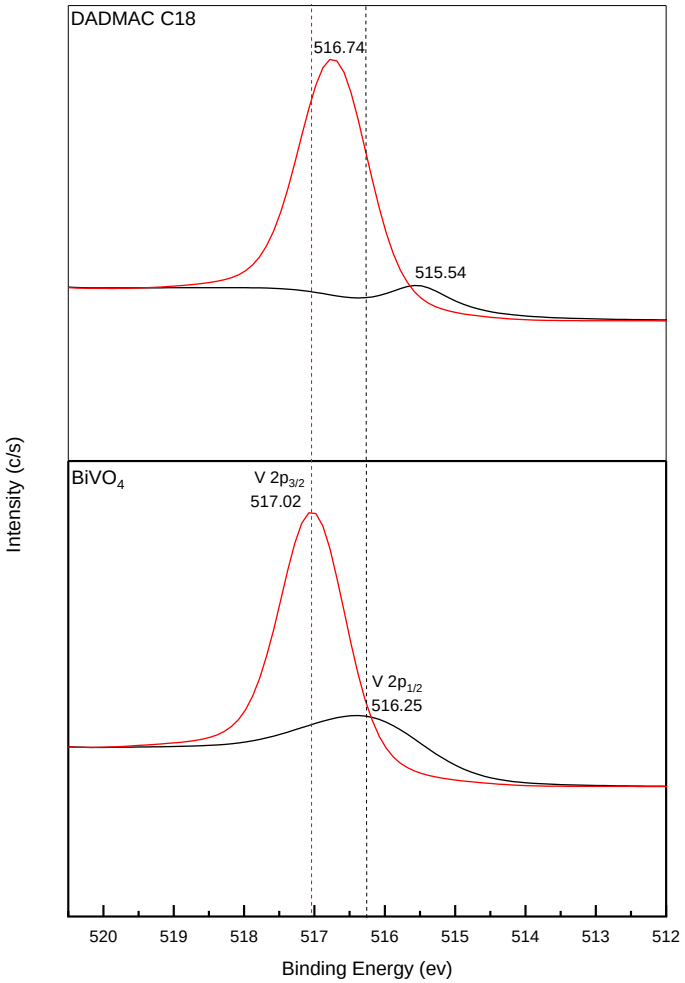

Figure 10. XPS spectra of V 2p for $BiVO_4$ and DADMAC C18, highlighting shifts in the $2p_{1/2}$ and $2p_{3/2}$ peak positions across different variants

V 2p:

XPS analysis in the V 2p region, consisting of V $2p_{1/2}$ and V $2p_{3/2}$ orbitals, confirms the presence of V^{5+} oxidation states in both $BiVO_4$ and its modified counterparts. The base $BiVO_4$ photoanode displays characteristic peaks at 517.02 eV (V $2p_{1/2}$) and 516.25 eV (V $2p_{3/2}$). The DADMAC C18 modified variant shows a slight positive shift with peaks at 516.74 eV (V $2p_{1/2}$) and 515.54 eV (V $2p_{3/2}$). The binding energies around 515.4 eV and 516.5 eV are associated with surface V^{4+} and V^{5+}, respectively, with V^{4+} indicating potential formation of oxygen vacancies (Jiang et al., 2019). The observed shift in DADMAC C18 indicates the likelihood of enhanced oxygen vacancies on the surface compared to pure $BiVO_4$.

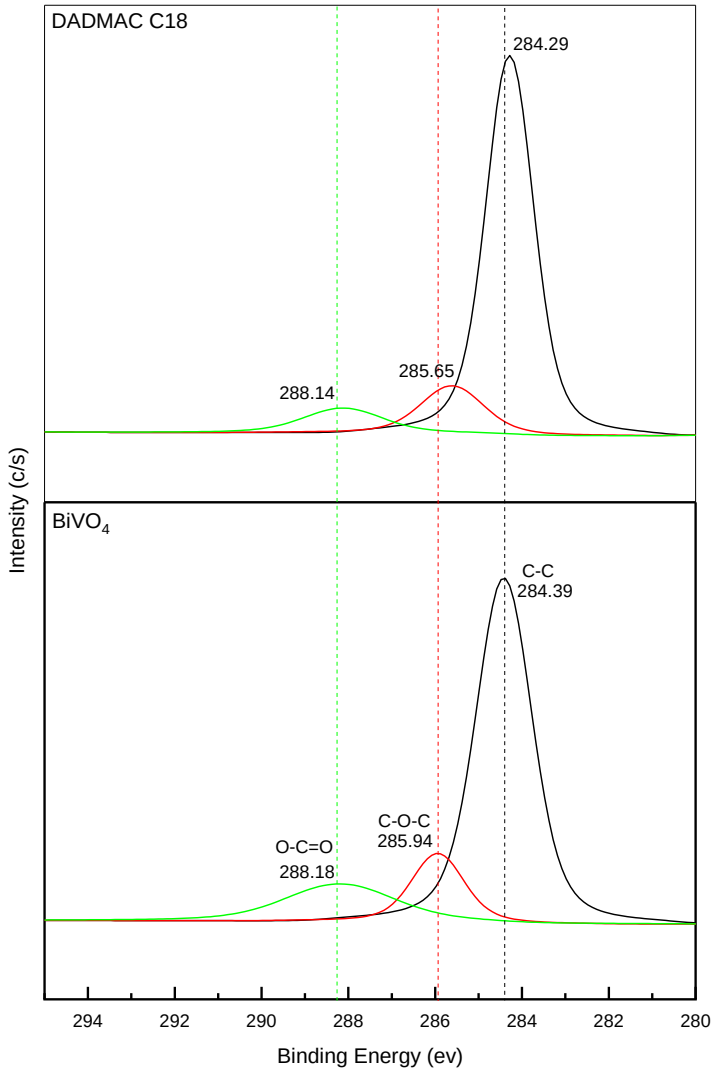

Figure 11. XPS spectra of C 1s for $BiVO_4$ and DADMAC C18, highlighting the C–C, C–O–C, and O–C=O peak variations across different variants

C1 s:

XP S analysis of C1s provides insights into the chemical state of C on the surface. The base $BiVO_4$ displays characteristic peaks at binding energies of approximately 284.39 eV (C–C), 285.94 eV (C–O–C), and 288.18 eV (O–C=O). For the DADMAC C18 modified sample, a slight negative shift in binding energies is observed (C–C at 284.29 eV, C–O–C at 285.65 eV, O–C=O at 288.14 eV), suggesting a change in the chemical environment of carbon due to QAC interaction.

The area under the C1S peaks were also studied, the area under C – O and O – C = O represents the relative abundance of carbon species on the surface. The percentage area was calculated using normalized peak area and the contribution of C – O and O – C = O were expressed in terms of percentage area. Unmodified $BiVO_4$ exhibits a balanced distribution of oxygenated carbon species, with 14.96% of the surface area corresponding to O–C=O (carboxyl/carbonate groups) and 13.14% to C–O–C (hydroxyl/ether groups). This suggests the presence of oxidized carbon functionalities that can contribute to hydrophilicity and interaction with the aqueous environment. DADMAC C18 shows that the C–O–C proportion remains comparable at 12.78%, the O–C=O content drops to 8.35%, suggesting reduced surface oxidation. This may

imply fewer carboxyl functional groups, which typically facilitate electrostatic interactions with the surrounding medium.

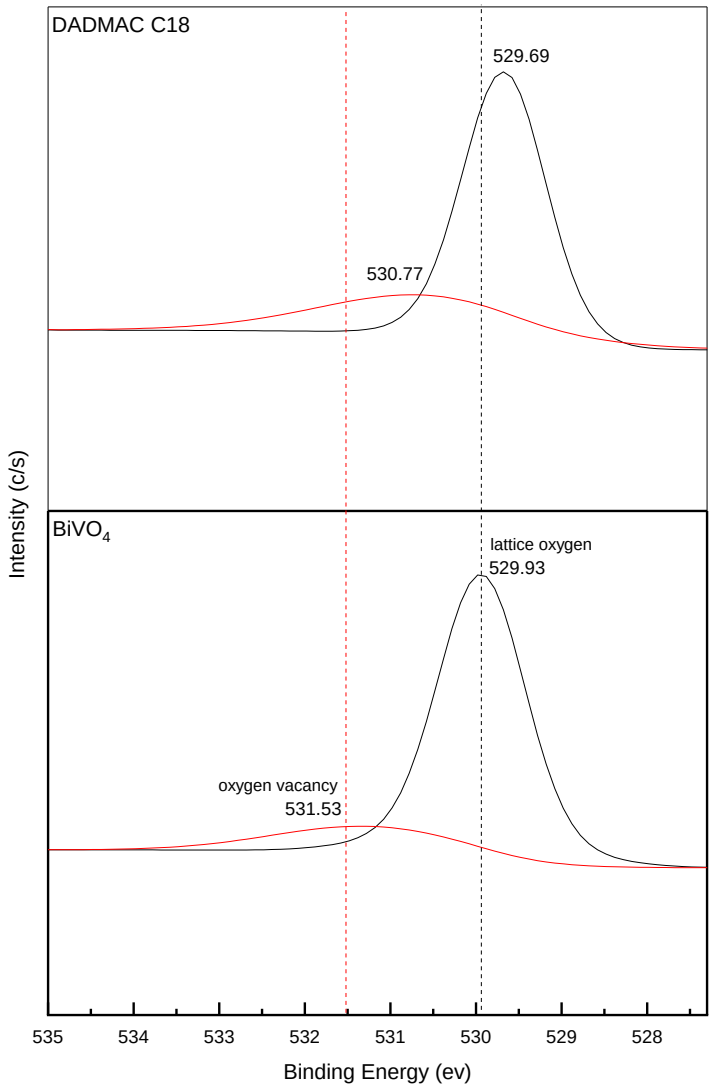

Figure14. XPS analysis of O 1s in $BiVO_4$ and QAC-modified photoanodes, showing differences in peak shifts and intensities for lattice oxygen, oxygen vacancies, and chemisorbed oxygen

O1s :

The XPS O 1s spectra provide insights into the oxygen chemistry on the $BiVO_4$ surface and its DADMAC C18-modified variant. The unmodified $BiVO_4$ shows a lattice oxygen (O_L) peak at 529.93 eV, corresponding to bulk Bi–O–V bonds, and an oxygen vacancy/hydroxyl (-OH) peak at 531.53 eV, indicative of surface defects facilitating charge transfer. Upon modification with DADMAC C18, the lattice oxygen peak slightly shifts to 529.68 eV, and the oxygen vacancy peak moves to 530.77 eV, suggesting an altered defect environment. These shifts and intensity changes point to an increase in oxygen vacancies or surface hydroxyl groups.
The area under the XPS O 1s peaks was analysed, with the lattice oxygen peak representing structural integrity in $BiVO_4$ and the oxygen vacancy peak indicating defect concentration. Unmodified $BiVO_4$ exhibits a high lattice oxygen content (84.84%) and a relatively low oxygen

vacancy proportion (15.16%), suggesting a stable framework with fewer surface defects. In contrast, the DADMAC C18-modified $BiVO_4$ shows a significant increase in oxygen vacancies (26.86%), indicating enhanced surface defects that can potentially improve photocatalytic performance by facilitating better charge separation and transport. Correspondingly, its reduced lattice oxygen percentage (73.14%) implies more structural modifications and a slightly less stable $BiVO_4$ framework.

4.1.4 UV-Visible absorbance spectrophotometry

Ultraviolet-visible (UV-Vis) absorption spectroscopy was used to assess the optical properties of the photoanode materials over a wavelength range of 200–800 nm. Absorbance spectra were plotted to evaluate their light absorption behaviour. The displayed graph represents UV-Vis absorbance data for all QAC-modified variants prepared with a lower concentration of 100 mg/L, in contrast to the 400 mg/L concentration used in the final experimental photoanodes.

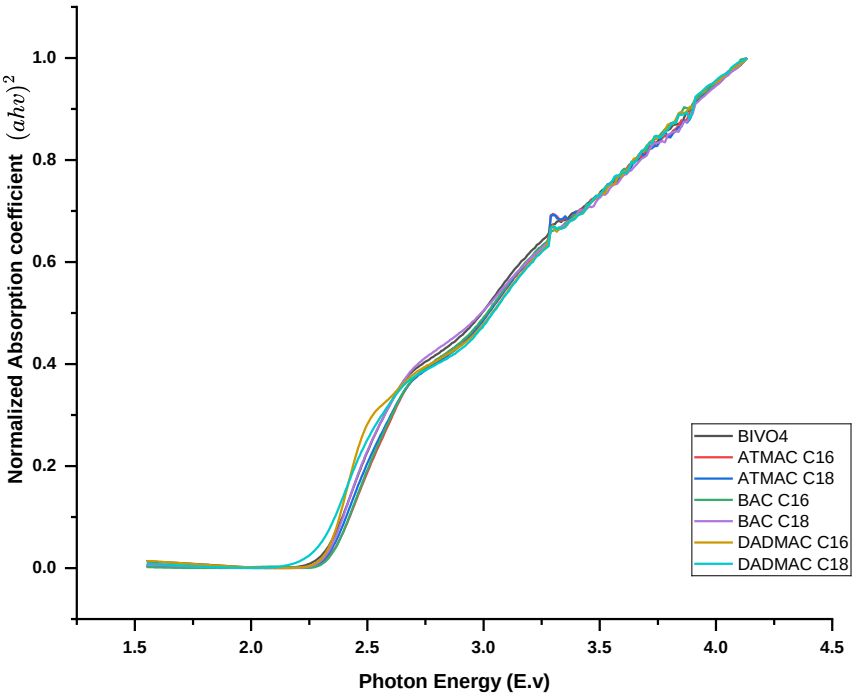

Figure 15. UV-visible absorbance spectra of Photoanode variants with Normalized Absorption coefficient plotted against Photon Energy

To estimate the optical band gap energy (E_g)of $BiVO_4$, the Tauc equation was applied, which is expressed as: $(\alpha hv)^n = A(hv - E_g)$

Where α is the absorption coefficient, calculated as $\alpha = \frac{2.303A}{L}$; A is the absorbance and L is the path length 1 cm. hν represents the photon energy, determined using $hv = 1240/\lambda$ which is derived from Planck's equation where λ is the wavelength nm. E_g is the optical band gap energy and n depends on the nature of the electronic transition. Since $BiVO_4$ exhibits an indirect

band gap n = 2 was used for the analysis. Tauc plot was plotted with $(\alpha hv)^2$. Against photon energy (hv) and the band gap energy was determined by extrapolating the linear region to the x-axis as shown in Figure 15

Table 7. Bandgap Energy of QAC modified $BiVO_4$ Photoanodes

Photoanode Variant	Ev
$BiVO_4$	2.22
ATMAC C16	2.45
ATMAC C18	2.23
BAC C16	2.23
BAC C18	2.24
DADMAC C16	2.25
DADMAC C18	2.16

The Bandgap energy of $BiVO_4$ was estimated at around 2.22 eV, and the average band gap energy of other Photoanode variant was around that as seen in Table 9. ATMAC C16 variant showed a higher band gap energy of 2.45 eV, While DADMAC C18 showed the lowest with 2.16 eV. The Bandgap energy of the Photoanode is in the working energy of visible range and it is a known a narrower band gap energy and broader visible light absorption typically correspond to enhanced photocatalytic performance of a photocatalyst (Ali, Wu, et al., 2023)

4.1.5 Linear sweep Voltammetry

To assess the photoelectrochemical performance of the fabricated photoanodes, linear sweep voltammetry (LSV) measurements were conducted. These measurements were performed in a 0.1 M Na_2SO_4 electrolyte solution at a scan rate of 0.1 V/s. Both dark and illuminated conditions were evaluated, with illumination provided from the backside of the photoanode during testing.

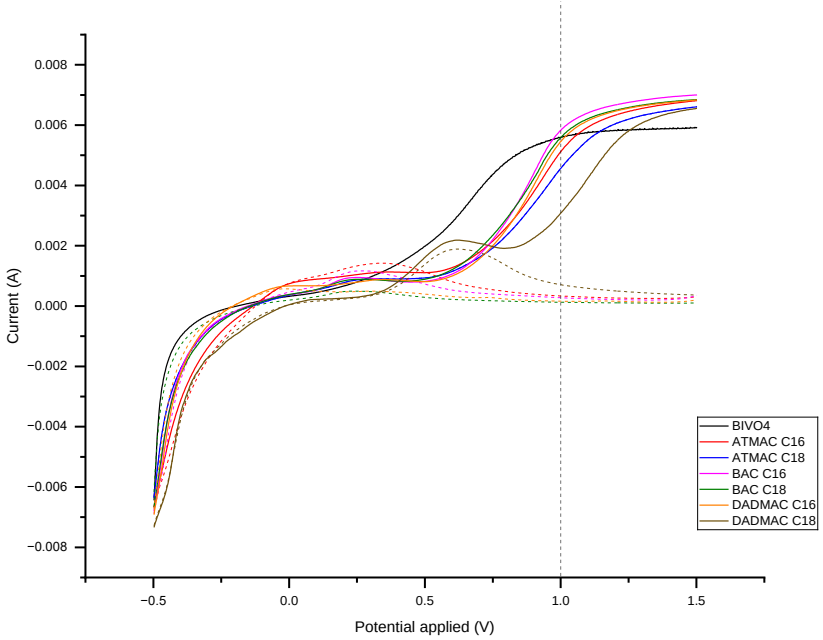

Figure 12. LSV curves of $BiVO_4$ and QAC-modified photoanodes under dark and light conditions, (with solid and dashed lines representing light and dark conditions respectively) A reference line at Potential voltage 1V indicates the photocurrent value (mA) for each variant.

The LSV curves in dark and light conditions are shown in Figure 19. In the dark conditions, the output current of all the Photoanode turned flat nearing 0 mA. This suggests the photoanode was working only under light conditions. The unmodified $BiVO_4$ shows a steady increase with the applied current. When the applied voltage is slightly above 0 (~ 0.2 V) the current begins to rise gradually marking the onset potential where the photoanode starts facilitating the oxidation reaction in the setup, after which there is a steep increase in the output photocurrent indication charge separation and water oxidation activity. This current output stabilizes after the potential voltage reaches around 1.2V which might suggest some charge transport limitations. The other QAC-modified photoanode follows a similar pattern except with the onset potential being around ~ 0.2V but we observe a small plateau till 0.5V and onset starts after that with a steep increase until 1.2V. Due to the surface modification and some resistance, the modified photoanodes might need more voltage to reach the onset potential.

Table 9 shows output photocurrent in terms of mA and mA/cm^2 (Photocurrent density was obtained by dividing the output current by the area of the Photoanode 16 cm^2). The photocurrent output was in the range from 3.078 – 5.58 mA, showing optimum current for pharmaceutical degradation while the unmodified $BiVO_4$ showed a current output of 5.59 mA i.e., ~ 0.35 mA/cm^2 which is in line with the report literature value of the output photocurrent which should be in between 0.1 – 1 mA/cm^2 (Ali, Jagannathan, et al., 2023a) serving as a baseline for other evaluating other modification. When the Photoanode was illuminated, BAC C16 showed the highest current output at 1V at 5.83 mA while DADMAC C18 showed the lowest current output at 3.08 mA. In the case of the variants C18 chain showed less current output as compared to their respective C16 chain. A higher photocurrent is ideal as it indicates more electron-hole pairs being separated and driven into the circuit. Overall, it shows the photoanodes have a good light response.

Table 8. Photocurrent density of QAC modified BiVO4 Photoanode at 1V applied voltage

Photoanode Variant	mA	mA/cm^2
$BiVO_4$	5.596	0.349
ATMAC C16	5.117	0.319
ATMAC C18	4.561	0.285
BAC C16	5.828	0.364
BAC C18	5.588	0.349
DADMAC C16	5.458	0.341
DADMAC C18	3.078	0.192

The characterization studies provide insights into the structural, morphological, elemental, and electrochemical properties of the synthesized $BiVO_4$ and its QAC-modified variants. The XRD results confirm that QAC modification induces minor shifts and intensity variations but does not alter the fundamental monoclinic structure of $BiVO_4$. LSV analysis further supports the photoactivity of all samples, demonstrating good photocurrent density, with the BAC-modified variants and pure $BiVO_4$ exhibiting the highest performance.

The SEM images clearly show the deposition of QACs as a surface layer on $BiVO_4$, While the EDX confirmed that the petal structure on top is QAC due to its carbon content. EDX analysis highlights differences in oxygen and bismuth distribution, with DADMAC-modified variants exhibiting the highest O content, while BAC C18 shows the highest bismuth (Bi) content. The higher Bi content in BAC C18 aligns with XPS findings, which indicate that it retains the most lattice oxygen, suggesting a more stable $BiVO_4$ framework with fewer defects. BAC C16 exhibits the highest C–O content and records the highest photocurrent output

On the fact that DADMAC variants have high O, DADMAC C16 and C18 also exhibit a strong potential for oxygen vacancy formation and a high presence of C–O functional groups, indicating an increased concentration of hydroxyl (-OH) groups. Additionally, DADMAC shows the lowest Bi intensity in XPS, suggesting significant surface coverage by QACs

4.2 Degradation studies

4.2.1 Experimental Condition

To evaluate the degradation capabilities of various $BiVO_4$-based photoanodes, experiments were conducted on 20 pharmaceutical compounds spiked to ~10 µg/L in the secondary effluent wastewater. The PEC degradation process was performed under a bias potential of 1 V, with 0.1 M Na_2SO_4 as the supporting electrolyte and an irradiance intensity of 60 W/m² to simulate natural solar radiation for 120 minutes.

Five $BiVO_4$ photoanode variants modified with QACs—ATMAC C16, ATMAC C18, BAC C18, DADMAC C16, and DADMAC C18—were tested to assess how structural modifications influence PEC performance. Duplicate experiments were conducted for each variant, and degradation was monitored over 120 minutes to evaluate both removal efficacy and reaction kinetics. This study aims to identify the most effective photoanode variant for pharmaceutical removal in wastewater treatment.

During the degradation experiment, Current (I), Temperature (C), Electric conductivity (EC), and pH were measured. The current varied for each of the photoanodes as observed in Figure (13), but the Temperature, EC, and pH followed a similar pattern among the variants except for some variance as observed in Figure (14).

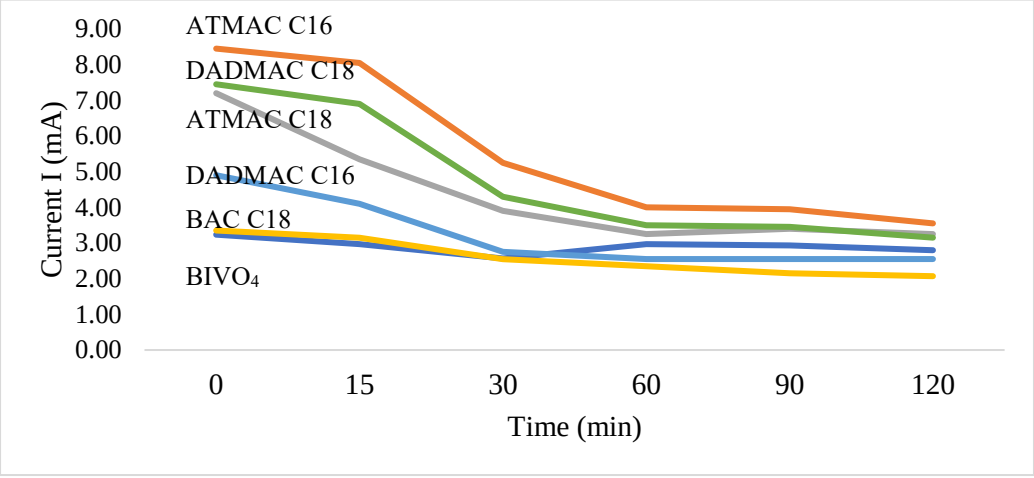

Figure 13 Photocurrent (mA) response of $BiVO_4$ and QAC modified variants over the experiment duration

At the beginning of the experiment, current values varied considerably across the photoanodes, indicating differences in charge transfer efficacy and photoelectrocatalytic activity, as shown

in Figure (20). The base variant $BiVO_4$ had the lowest initial current at 3.2 mA. The ATMAC C16 variant initially had the highest current output at 8.45 mA, followed by DADMAC C18 (7.45 mA) and ATMAC C18 (7.2 mA). A gradual decline in current was observed for all photoanode variants, but from 60 minutes, most photoanodes reached a steady state with minimal current reduction. The initial decline in the photocurrent until it reached a steady state might be since as the reaction proceeds the concentration of reactants decreases in the solution as they get formed into by-products

As discussed later, ATMAC C16 and DADMAC C18 initially showed a high current density, which is in agreement with their strong degrading performance. BAC C18 had the least degradation, which is again in direct agreement with its current output.

The temperature, EC and pH showed similar trends in all the variants with slight variability (Figure 2). The temperature increased over time from ~ 15 °C to 50 °C for the reaction with a deviation of ± 19% initially, which was reduced to ± 1% in the end. The increased temperature is due to the prolonged solar irradiation and heating from the applied potential. The EC starts at ~ 14.5 mS/cm and peaks at ~16 mS/cm at the 0^{th} minute when the solar illumination is started. This spike at the 0^{th} minute is when the reaction starts due to the start of the mixing in the reaction. After which, the EC remains constant throughout the reaction period with a deviation of ± 4.05%. This implies a steady reaction and stability of the electrolyte medium. The initial pH starts at around 7, which is the pH of the secondary wastewater effluent. At the 0^{th} minute, it increases to ~ 7.5, which decreases and stabilizes at 60 minutes to ~ 7.1 over the remaining time of the reaction.

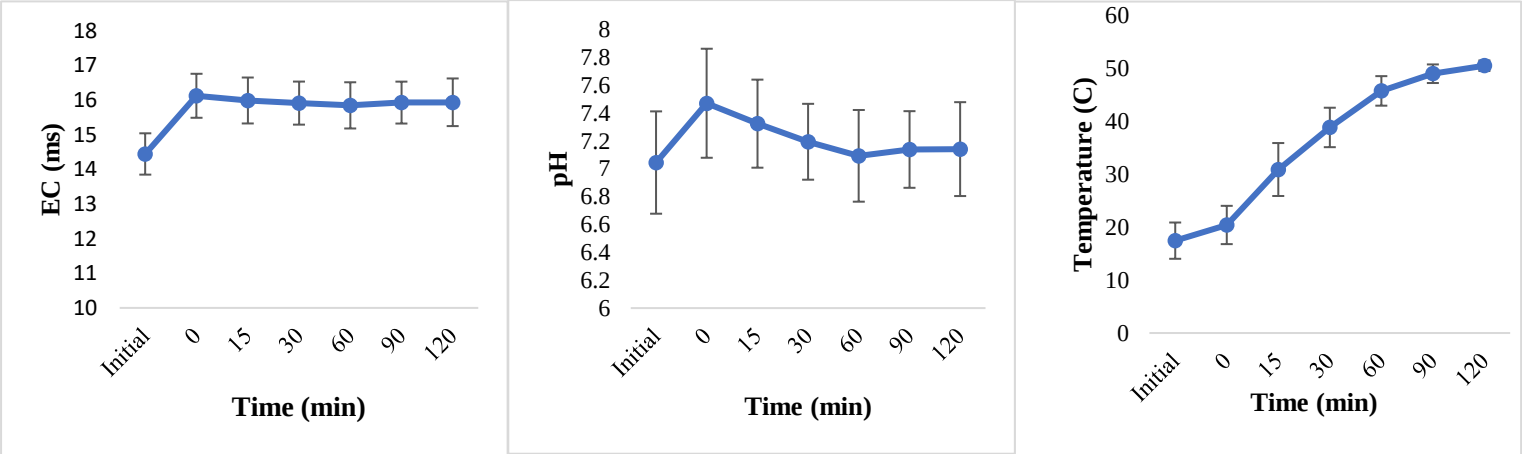

Figure 14. Average measurements of key parameters (A. EC, B. pH, C. Temperature) across all photoanodes throughout the experiment period

4.2.2 Degradation study

Degradation experiments were conducted to test the overall degradation of pharmaceutical compounds over a reaction time of 120 min with the various photoanodes. Samples from the reactor were collected at – 30 which is also referred to as the initial value before we dip the Photoanode, 0, 15, 30, 60, 90 and 120 minutes. The concentrations of pharmaceuticals were determined using either IS calibration curve. An external calibration curve was established for each pharmaceutical where the IS curve cannot be used. The data were normalized, and mean concentrations and actual standard deviations were calculated to ensure consistency and reliability.

Table 9. Degradation efficacy (%) of different $BiVO_4$ variants for various pharmaceutical compounds over a period of 120 minute (Green represents higher efficacy and Red represents lower efficacy among the variants)

Compound	$BiVO_4$	ATMAC C16	ATMAC C18	BAC C18	DADMAC C16	DADMAC C18
Metoprolol	59.9	42.4	33.3	23.3	33.0	40.6
Propranolol	63.1	63.1	59.9	55.1	65.9	68.2
Sotalol	50.2	50.2	41.3	22.8	38.4	51.6
Trimethoprim	19.4	3.6	25.0	10.0	20.1	20.3
Clarithromycin	21.5	26.5	11.0	87.1	61.5	39.6
Caffeine	28.9	27.4	22.1	25.9	26.6	34.5
Theophylline	26.4	25.9	27.8	13.2	38.0	38.9
Metformin	20.6	24.1	13.4	17.4	25.0	22.1
Gabapentin	21.9	20.9	7.4	1.5	21.5	5.2
Acetaminophen	45.6	35.1	41.9	41.5	43.1	57.3

After analyzing the results, the DADMAC C18 variant exhibited a high removal for most of the pharmaceuticals. This was particularly evident in the removal of metoprolol (40.59%), propranolol (68.15%), sotalol (51.59%), and acetaminophen (57.28%), where it consistently outperformed other variants. This was then followed by $BiVO_4$ alone (unmodified) ranked second in overall degradation performance, demonstrating comparable removal efficiencies for several compounds, particularly propranolol (63.13%), sotalol (50.16%), and acetaminophen (45.55%). DADMAC C16 showed consistent removal, next to $BiVO_4$ and its other DADMAC variant C18. While ATMAC C16 performed well for propranolol (63.13%) and sotalol (50.16%), its performance on other compounds was less consistent. BAC C18 showed the lowest overall degradation efficacy, particularly in the removal of trimethoprim (10%), gabapentin (1.49%), and metformin (17.44%)

Among the compounds, propranolol exhibited the highest removal efficacy across all variants, with a peak removal of 68.15% (DADMAC C18) and an average removal of 62.5% with a deviation of only ± 7.3%. This suggests that propranolol is more susceptible to PEC degradation. Trimethoprim and gabapentin were most resistant to degradation with very little degradation efficacy.

Beta-blockers - Metoprolol, Propranolol and Sotalol have had high degradation efficacy in this study among other Pharmaceuticals. Before this no study has been conducted to show the degradation of beta blockers –in a $BiVO_4$-based system yet advanced sulfate radical-based oxidation methods are used to degrade beta blockers from water (Tay & Ismail, 2016). Phan et al., 2022 obtained 71% degradation of Propranolol with the help of visible light-assisted PMS-mediated degradation over a period of 2 hours which is like our studies. This suggests addition of PMS will enhance the degradation of these particles. There is a lot of research available on the degradation of Caffeine by $BiVO_4$ in a PEC setting with some reaching 100% degradation of Caffeine (Prado et al., 2022). Yet when it was tested in a setting with various

pharmaceuticals present Caffeine showed less degradation due to its slow removal kinetics under solar stimulated light. This is the result of a deficiency of the electron-donating group in Caffeine(Ali et al., 2025). Our studies have performed marginally better with a degradation reaching ~ 35% (DADMAC C18). Chinnaiyan et al., 2019 studied the degradation of Metformin in synthetic hospital wastewater using TiO_2 Photocatalysis and achieved 98% degradation in 150 minutes. This is contrary to what results this study obtained where metformin was one of the more resistive compounds. The degradation of Acetaminophen has been studied using $BiVO_4$ for PEC setting, (Ali, Wu, et al., 2023) achieved a removal of 87% with modified $BiVO_4$ under stimulated sunlight in 120 minutes. Our research also achieved a degradation of 57% which is not as high but one of the better degrading compounds. Some pharmaceutical compounds in this study exhibited similar degradation trends to previous research; however, the overall degradation efficacy was lower. This discrepancy is likely due to the higher number of pharmaceutical compounds present simultaneously, leading to increased competition for active sites on the photocatalyst. In contrast, most previous studies focused on the degradation of a single pharmaceutical compound, which does not fully reflect real wastewater conditions. Also, since we used actual wastewater in our studies, the presence of common water anions has an inhibitory role in photocatalytic processes due to the competition between target pollutant and anion to the active sites and the ability of anions to act as hole scavengers (Tavakoli Joorabi et al., 2022)

4.2.3 Degradation efficacy over time

Apart from studying overall degradation efficacy, it is also important to analyze degradation kinetics progress over time to determine how long it takes for pharmaceutical compounds to break down. This will help optimize the retention time required for effective wastewater treatmentThis was done for selected pharmaceutical data, which were consistent and had less standard deviation among the duplicates.

Considering the time-based performance, $BiVO_4$ exhibited the fasted degradation kinetics within the first 30 minutes. Particularly for the compound Metoprolol and propranolol, more than 70% of its removal is done in the first 15 minutes. ATMAC C16 also has high kinetics when it comes to removal. Propranolol and Caffeine achieved 70% removal in the first 15 minutes. At the same time, metoprolol and sotalol achieved 50%. It is also observed that the compounds metoprolol and propranolol have some of the best degradation within 15 minutes across the variants.

DADMAC C18 demonstrated a consistent degradation profile, ensuring uniform breakdown of pharmaceutical compounds over the entire 120-minute reaction period. Unlike other variants that exhibit sharp initial removal, DADMAC C18 maintains steady degradation, particularly for sotalol, propranolol, and acetaminophen, suggesting sustained catalytic activity. After this, even ATMAC C18 showed consistent degradation for these compounds, but the degradation efficacy was not very high. Among the compounds, acetaminophen and sotalol showed consistent removal time across the variants, followed by caffeine, which had lesser degradation but was uniform across the variants.

DADMAC C16 and BAC C18 slowed degradation, with major degradation starting after a 60-minute reaction time. Across the variants, gabapentin showed the least degradation, followed by trimethoprim and caffeine. The unmodified $BiVO_4$ variant and C16 variants – ATMAC C16 and DADMAC C16 showed ~ 20% overall removal of gabapentin, the C18 variants showed a removal of below 10% for gabapentin.

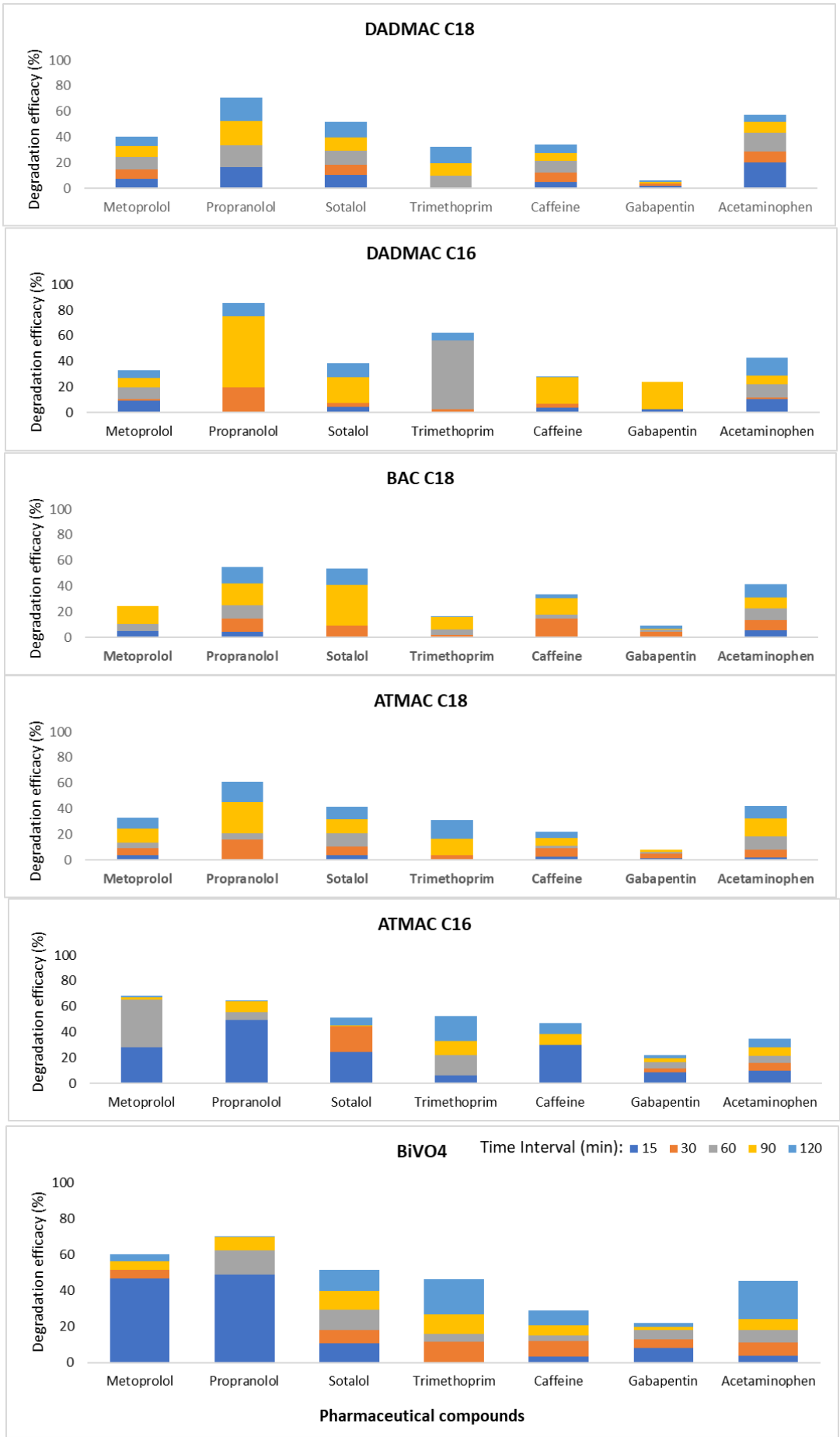

Figure 15. Degradation progression of pharmaceuticals using $BiVO_4$ and QAC-modified photoanodes, showing percentage removal at 15, 30, 60, 90, and 120 minutes for each variant

4.2.4 Kinetic studies

To better understand the degradation behaviour of pharmaceuticals, a kinetic study was conducted using the best-performing photoanode variant (DADMAC C18). The degradation data were plotted to zero-order, first-order, and second-order kinetic models, and the best model was selected based on the highest R^2 value. The rate coefficient (K) for each compound was determined, and the half-life ($t_{1/2}$) was calculated accordingly to quantify the extent of degradation (Table 11). This approach provides insights into the reaction mechanisms governing PEC degradation and helps identify compounds that degrade rapidly versus those that exhibit persistence in the system.

Table 10. Reaction order details of all compounds for DADMAC C18

Reaction order	**Pharmaceuticals**	**Rate constant (k)**	**Half-life (min)**	**R^2**
2^{nd} order	Metoprolol	0.2577 L μg^{-1} min^{-1}	3.53	0.8765
	Propranolol	0.4312 L μg^{-1} min^{-1}	2.19	0.9389
	Sotalol	0.1889 L μg^{-1} min^{-1}	5.17	0.8866
	Gabapentin	0.0511 L μg^{-1} min^{-1}	19.34	0.9794
1^{st} order	Theophylline	0.0833 min^{-1}	8.19	0.9669
	Sulfamethoxazole	0.0245 min^{-1}	28.17	0.9501
	Sulfadimethoxine	0.4328 min^{-1}	1.36	0.9786
0^{th} order	Caffeine	0.0475 μg L^{-1} min^{-1}	10.32	0.9516
	Acetaminophen	0.0663 μg L^{-1} min^{-1}	7.32	0.8648
	Metformin	0.0409 μg L^{-1} min^{-1}	12.13	0.9862

Among the compounds following 1^{st} order kinetics, sulfadimethoxine exhibited the fastest degradation rate with a half-life of 1.60 minutes, followed by theophylline. Sulfamethoxazole has a half-life of 28.29 minutes, which is the slowest degradation among all compounds. Then, we have the compounds that followed the 0^{th}-order kinetics during the experimental period. Among them, acetaminophen exhibited a steady degradation rate, yet it was faster than compounds following the 0^{th} order, such as caffeine and metformin. However, when the half-lives of all 10 compounds were compared, Sulfadimethoxine was found to degrade faster, followed by propanol and metoprolol. We need to study the kinetic studies as it can provide insights on critical pharmaceutical and the retention time in the reactor should be based on that. Here it is understood sulfamethoxazole is the critical compound with slow rate

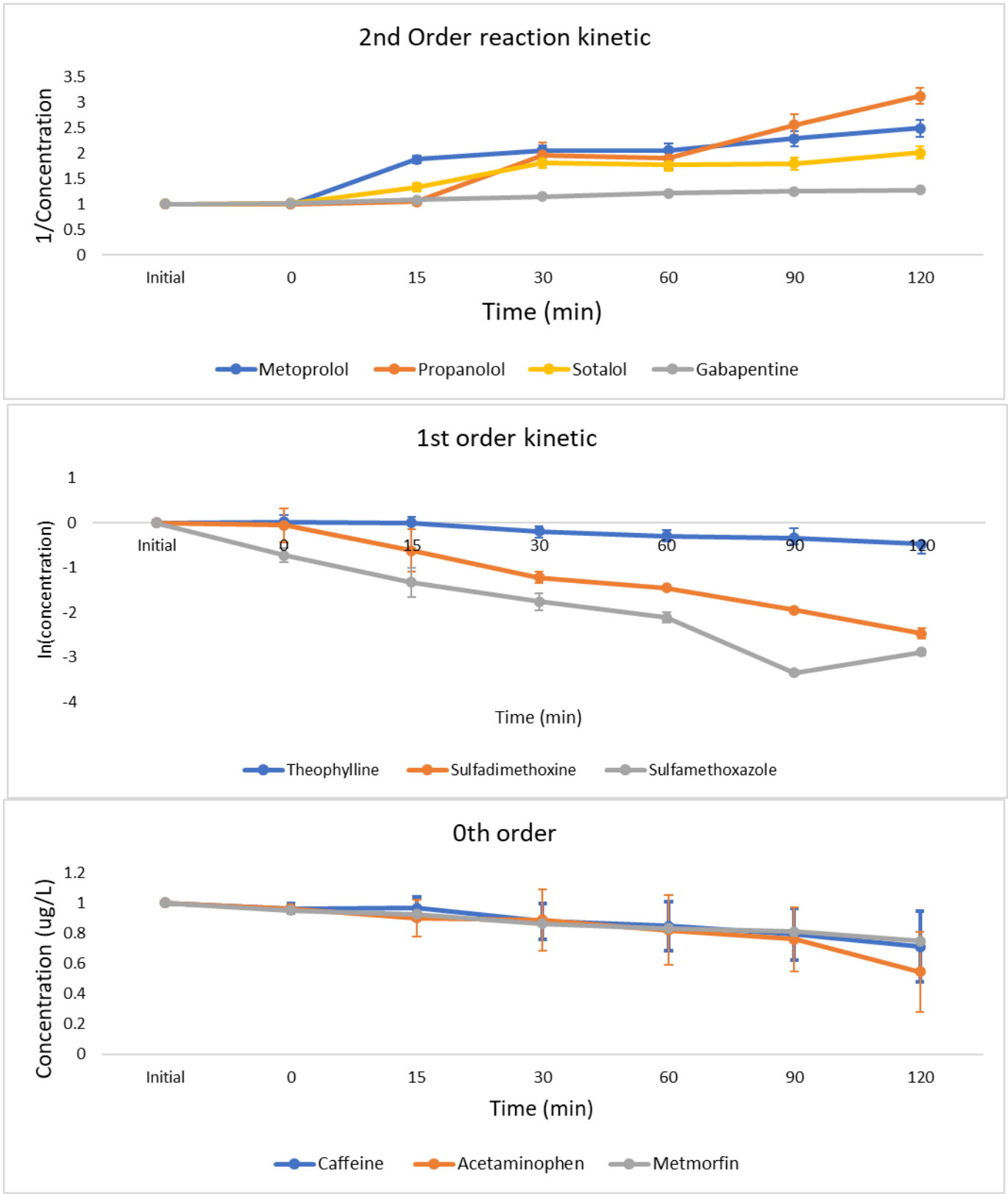

Figure 17. 0th, 1st and 2nd order kinetic graphs of the pharmaceutical compounds for DADMAC C18 for each compound in the respective kinetic models

Chapter 5. Full-scale implementation of Photoelectrocatalysis

Several studies have explored PEC systems beyond laboratory settings, with notable progress in pilot-scale applications. Reactor designs such as parabolic trough reactors (PTR) and compound parabolic collectors (CPC) have demonstrated efficient sunlight utilization in environmental remediation. Similarly, slurry and panel reactors have been tested for both wastewater treatment and hydrogen generation, each presenting unique advantages in scalability and efficacy. Despite these advancements, the transition from lab-scale experiments to industrial-scale PEC systems faces challenges related to catalyst durability, energy costs, and reactor optimization. These hurdles underscore the need for innovative designs and material improvements to fully realize the potential of PEC in real-world applications.

There are several considerations which need to be taken in regard when scaling up a Photocatalytic rector. The Photoanode material quality is an important factor to be considered for full-scale development. It is important to use the right balance of material concerning performance and cost. Increasing photon conversion efficacy from 1% to 5% reduces production costs by up to 75% (Toe et al., 2022). The mechanical stability of the photoanode and its material is crucial for large-scale water treatment applications. Thin films are susceptible to abrasions and may scrap off from the surface. Only those with high mechanical resistance are suitable for repeated use under high-flow conditions. It has been observed that over time mechanical degradation rather than chemical deactivation is the primary cause of performance decline (Ramos et al., 2021) The Photoanode also must have high reusability and durability to be cost-efficient. Simple washing with water can partially restore activity, but more aggressive treatments (e.g., with acetone and UV irradiation) are more effective (Ramos et al., 2021). When it comes to the solar application of the PEC, it is also important, there is the availability of large areas and high solar exposure. The use of solar active cloths – textile-based materials that incorporate Photocatalytic coating to harness maximum solar energy. Pilot tests indicated promising results under varying sunlight intensities, though efficacy dropped under cloudy conditions Installing solar concentrators can also increase photon inputs improving efficacy, these solar concentrators can be connected to optical fibres to utilize maximum visible light (Toe et al., 2022)

There are various reaction configurations which can be considered while installing a full-scale development. Photocatalytic reactors are mainly divided into 2 systems – immobilized and slurry-based. Slurry-based PEC reactors suspend photocatalyst particles directly in wastewater, providing maximum surface area exposure and effective light absorption. However, they require an additional separation step to recover the catalyst after treatment, increasing operational costs.

In contrast, immobilized PEC reactors fix the photocatalyst onto solid supports such as conductive glass or metal meshes, offering several advantages:

- Lower Separation Costs: No need for catalyst recovery, reducing operational expenses.
- Better Light Reachability: Photons reach the catalyst surface directly, enhancing efficacy.
- Portability: Catalysts can be placed flexibly within the reactor, allowing easy system adjustments.
- Improved Photon Penetration: Thin-film designs offer greater surface area and light absorption.

Limitations include challenges with uniform light distribution, dependency on support materials, and higher initial costs for catalyst immobilization. Despite these, immobilized systems are more suitable for large-scale wastewater treatment due to their long-term efficacy and lower maintenance (Thaha et al., 2024).

As of now large-scale implementation of PEC would be a costly affair. An estimated 65% of the total cost is under CAPEX where photoreactor construction accounts for 33.7% for panel systems and 30.8% for slurry-based. The remaining 35% is OPEX cost which is also relatively high due to high material and maintenance costs (Toe et al., 2022). When it comes to using photocatalysis for large-scale purposes, there has already been advancement made in the use of Photocatalysis for Hydrogen generation purposes. Many recent studies have tried to scale it for pilot studies (Jing et al., 2009). While the energy conversion mechanisms of photocatalysis and electrocatalysis differ, both processes rely on mass transfer and surface-dependent catalysis. This commonality enables shared design strategies for catalysts, such as morphology optimization and heterostructure development, allowing photocatalytic reactor configurations to be effectively adapted for Photoelectrocatalysis (J. Li et al., 2024). There are various reactor types which can be adopted for the full-scale system (Ramos et al., 2021)

5.1.1 Full Scale Reactor Types

Single-chamber reactor with a flat plate photoanode is a simple configuration in Photoelectrocatalysis (PEC), initially developed for water splitting and subsequently for use in environment-related processes. It is simple, planar configuration provides one-sided light exposure, making it an optimum choice for lab-scale studies and a stepping stone to larger systems. The reactor's transparent design maximizes light penetration, while its flat photoanode ensures a large reactive surface area on one side. This type of reactor comes with a large disadvantage when it comes to the potential fouling of the photoanode and less bed contact between the catalyst surface and water. There are also issues with sunlight not being able to penetrate entirely due to its shape, all these factors make this type of reactor undesirable for full-scale (J. Li et al., 2024; Meng et al., 2015). To address these limitations of a single-chamber reactor, slant-placed electrodes PEC system was introduced. The electrodes are positioned at an angle to maximize light exposure and fluid flow across the active surfaces. This geometry improves photocatalytic efficacy by reducing light shading and ensuring uniform illumination of the Photoanode materials. The slant orientation also promotes better mass transfer and reduces bubble accumulation during reactions. This design came with the disadvantage of a higher chance of Photoanode degradability and issues with increased design complexities (Meng et al., 2015). Unlike flat plate photoanodes, which suffer from high degradation rates and limited contact with light and water, the cylindrical PEC model with annular electrodes offers a significant advantage. Its concentric geometry enhances light distribution and surface interaction, while the annular electrode arrangement maximizes the active catalytic surface area, ensuring more uniform illumination compared to flat plate designs. This design also promotes efficient fluid dynamics, reducing stagnant zones and improving the contact between pollutants and the reactive surface. Such reactors are particularly effective for removing pharmaceuticals such as antibiotics and hormones from wastewater, as the cylindrical configuration allows continuous operation with improved mass transfer and reduced electron-hole recombination. The reactor's enclosed design also makes it suitable for solar and artificial light sources, enhancing its scalability, The design allows for enhanced light distribution and minimal catalyst wear (Ramos et al., 2021). Circular Reactor PEC design can be further optimized for better mass and light transfer to attain better contact between the pollutants and the photocatalysts. The rotating disk photoelectrochemical (PEC)

reactor is an innovative design aimed at enhancing reaction efficacy and light utilization by integrating mechanical rotational motion. It is an improved version of the circular PEC system where the photocatalytic electrode is mounted on a rotating disk that moves continuously through the reaction medium, ensuring uniform light exposure and efficient contact with reactants. The rotation reduces the boundary layer thickness and it prevents the accumulation of reaction by-products on the electrode surface, extending the catalyst's lifespan. However, the complexity of the design, along with the need for precise engineering and regular maintenance, poses challenges for large-scale implementation. Additionally, the energy demands of the rotating mechanism can reduce overall system efficacy (Braham & Harris, 2009). A vortex PEC reactor is one of the more advanced reactors, in this system, a vortex flow is induced within the reactor chamber, generating high turbulence that promotes effective mixing of reactants and uniform distribution of light across the photocatalytic electrode surface. This swirling motion minimizes the diffusion boundary layer, facilitating improved interaction between the reactants and the photocatalytic materials. Despite its advantages, implementing vortex PEC reactors presents challenges such as precise fluid dynamic control and high energy demands for maintaining vortex flow. Scaling up for industrial use also requires addressing design constraints, energy efficacy, and structural integrity. However, vortex PEC reactors remain a promising innovation, driving advancements in sustainable photoelectrochemical technologies (Meng et al., 2015).

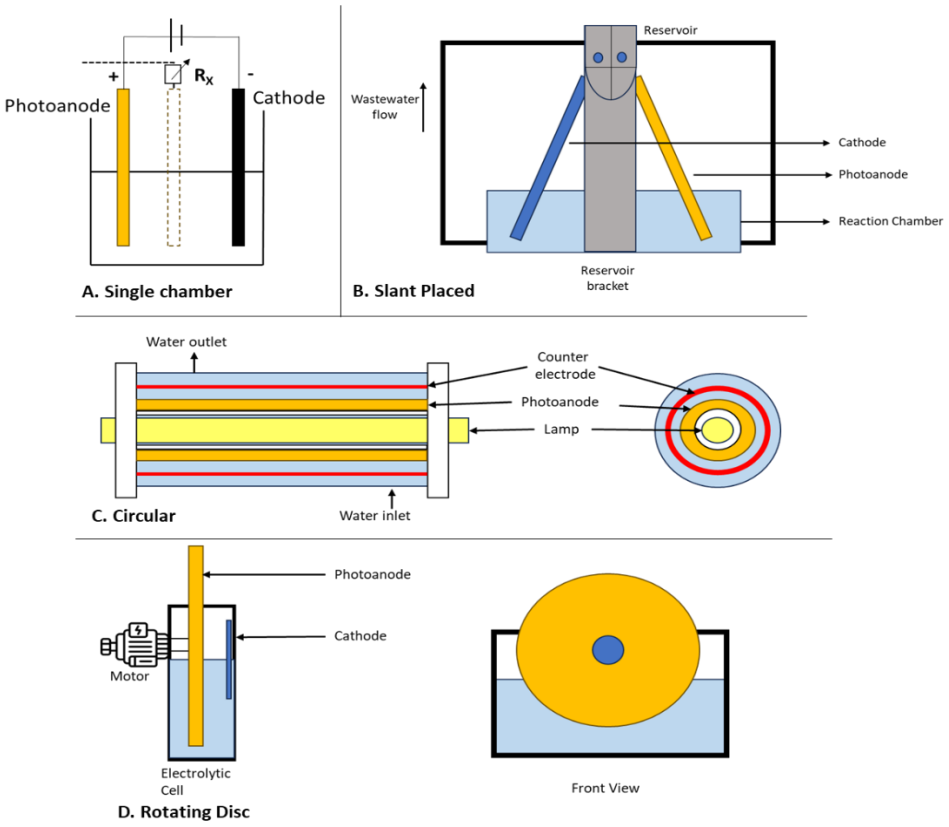

Figure 18. Schematics of full-scale PEC reactors A. Single Chamber three electrode flat plate photoanode B. Slant placed Photoanode (Xu et al., 2013) C. Circular reactor with annular rods (Marugán et al., 2013) D. Rotating disk PEC (Zhang et al., 2011)

5.1.2 Best Suited Technology

Each of the discussed models have some features, however to determine the most suitable full – scale PEC system, a performance evaluation was done based on some Key parameter index (KPI) to evaluate reactors based on performance and operational complexities

Table 11. Performance evaluation of PEC reactor models based on KPI parameters. The colour code indicates performance levels: red for low suitability, yellow for moderate, and green for high preference.

KPI Category	Single Compartment Flat Plate	Slant-Placed Thin Film	Cylindrical PEC	Rotating Disc PEC	Vortex PEC
Scalability	Low – Limited light penetration	Medium – Needs further scaling	High – Adaptable to continuous flow	Medium – Complex moving parts	High – Efficient mass transfer
Ease of Maintenance	Low – Prone to fouling	Medium – Requires careful cleaning	High – Reduced fouling	Low – Frequent maintenance needed	Medium – Some wear concerns
Energy Efficiency	Medium – Light loss issues	Medium – Lower energy input needed	High – Optimized energy use	Medium – Energy for rotation	Medium – Energy for vortex flow
Reactor Complexity	Low – Simple design	Medium – Precise fabrication needed	Medium – Moderate complexity	High – Requires precise engineering	High – Complex flow control
Durability of Materials	Medium – Degrades over time	High– enhanced longevity	High – Protected structure	Medium – Wear from moving parts	High – Stable with mixing
Cost of Implementation	Low – Cost-effective	Medium – Higher fabrication costs	Medium – Balanced costs	High – Expensive mechanical parts	High – Advanced control systems

From the performance index table 12, it can be concluded that the cylindrical design form of PEC is ideal due to its high scalability, efficient light absorption, and reduced maintenance needs. Unlike the Chamber flat reactor, there are minimal dead zones and improved mass transfer. The reactor takes up a lesser volume, offers higher efficacy and can accommodate continuous flow systems. Rotating discs can also be installed in a circular reactor however that makes the reactor more expensive and increases the maintenance. Vortex design PEC comes with a high price and complexity. Even though Circular PEC might be costlier than its flat plate counterparts it provides a balance of durability, benefits, and performance efficacy with less complexity as it does not use rotating motors.

5.2 Design Adoption for the Treatment Plant

5.2.1 RWZI (WWTP) Horstermeer

Over the course of the report, RWZI Horstermeer will be referred to as WWTP Horstermeer. The WWTP Horstermeer, constructed in 1985, is a vital facility managed by the Amstel, Gooi, and Vecht Water Board, with a hydraulic capacity of 120 MLD. The plant employs a multi-stage treatment process, including bar screening, primary and secondary sedimentation (integrated with Enhanced Biological Phosphorus Removal, EBPR), and advanced purification technology to treat emerging contaminants.

This plant has implemented an innovative two-step purification process combining ozone treatment with activated carbon filtration, completed in 2024 in concern with the growing pharmaceutical waste. In the UV oxidation stage, wastewater is treated with high-intensity ultraviolet (UV) light, which helps break down complex organic pollutants, including pharmaceutical residues and harmful microorganisms. This process not only disinfects the water but also makes persistent contaminants easier to degrade. After UV treatment, the water flows through an activated carbon filtration system, where the carbon material captures and adsorbs any remaining pollutants. This combined approach ensures that even hard-to-remove substances are effectively filtered out, resulting in cleaner, safer water.

This advanced system effectively removes up to 80% of pharmaceutical residues, such as painkillers, contraceptives, and psychiatric drugs, which previously posed a significant threat to aquatic ecosystems in the Vecht River.

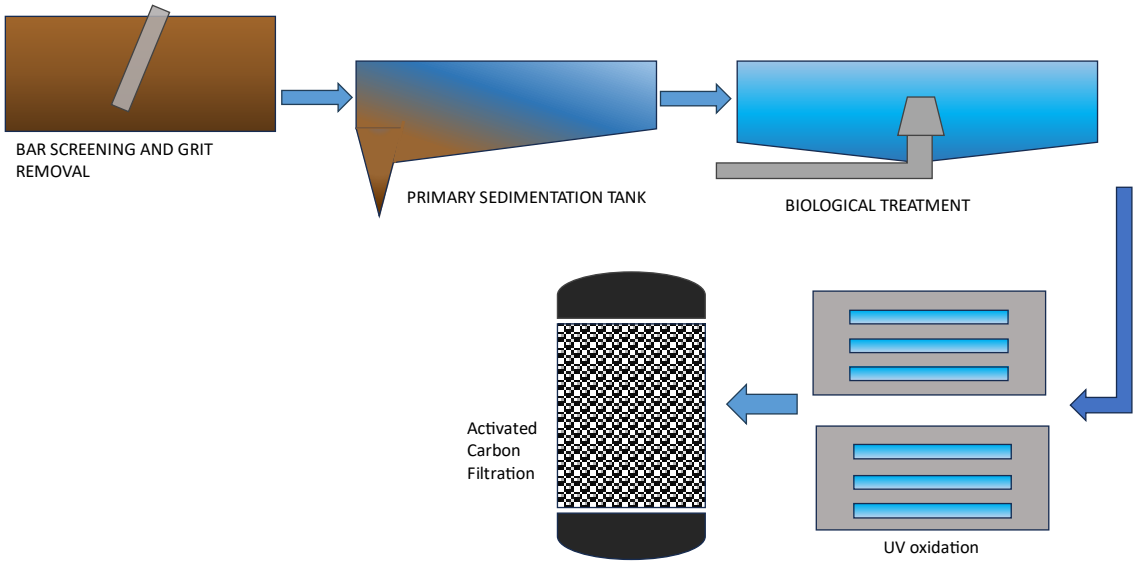

Figure 19 Wastewater Treatment train of RWZI Hoerstmeer

The Horstermeer WWTP is an ideal example for studying the implementation of a large-scale PEC system because it focuses on pharmaceutical removal. With existing advanced treatments such as ozone and activated carbon filtration, the plant offers a strong base to see how PEC can improve the removal of pharmaceutical compounds

5.2.2 Design consideration and specification

As reported a cylindrical PEC reactor features an annular arrangement of parallel electrodes, where the photoanode (e.g., $BiVO_4$-coated substrates) is placed on the inner cylinder, and the cathode is positioned on the outer wall. This design allows for uniform light distribution from the centre outward, maximizing the active catalytic surface. The large-scale advantage of such a reactor is it allows for full irradiation from all directions enhancing photocatalytic reaction. It is also very horizontal and vertical installations depending on space constraints. To sustain a large amount of flow, advised we install parallel or series configurations of the reactor (Meng et al., 2015b). Even for a cylindrical PEC reactor, it is important same light intensity passes through the reactor to make sure there is a steady reaction throughout the reactor. Minimal distance between light sources such as solar concentrator and the photoanode, Proper reflective inner surface can enhance reactivity. Turbulence and stirring also need to be maintained using mechanical stirring and hydraulic design adjustment (J. Li et al., 2024)

Overall Scaling up a PEC reactor involves a lot of computation and mathematical modelling. Kinetic modelling is calculated to understand the reaction rate prediction which will help provide us with a rough idea of the required time of degradation and reactor volume. Pseudo-first-order reaction is generally used to represent pharmaceutical degradation (Binjhade et al., 2022).

The critical compound while calculating the retention time of the would-be sulfamethoxazole with the slowest half time ($t_{1/2}$) of 28.17 min. Sulfamethoxazole first order reaction rate, with a rate kinetic k = 0.0245 min^{-1} . Applying this rate in hydraulic model of plug flow reactor and continuos mixed stir tank reactor

$$Plug\ flow: C = C_O e^{-kt} \qquad Continuos\ stirred\ tank\ reactor\ \ C = \frac{C_0}{1 + kt}$$

Plugging in the kinetic rate of sulfamethoxazole, assuming we want a removal of 75% in the same conditions of the lab experiment, The required HRT for Plug flow reactor would be 39 min and for continuous stirred tank reactor it would be 122 min

Mass transfer analysis should be done to optimize mass transfer efficacy providing us with information for the optimum flow and mixing for the reaction to occur. Optical stimulation within the reactor must be studied using Beer-Lambert Law to optimize the reactor for maximum light efficacy (Meng et al., 2015b). Computational modelling with the help of Computational fluid dynamics must be done for the setup to help analyze the flow distribution, mass transport effect and electrode spacing for efficient charge transfer. Furthermore, Kinetic Monte Carlo (KMC) simulations predict electron-hole recombination rates, while Artificial Neural Networks (ANN) are increasingly applied to optimize operational parameters such as applied bias potential (Alalm et al., 2021)

5.2.3 Techno – Economical Assessment

To understand the large-scale modelling of a PEC system for pharmaceutical wastewater treatment, a rough case study was conducted to examine its functionality and potential benefits. The full-scale design was studied considering it to be a replacement for the UV oxidation reactor present. The Electrode material considered for the development of such a reactor would be $BiVO_4$ supported on a stable conductive substrate FTO. Cathode rods and reference would

be the ones which we used in the lab scale experiment. For the full-scale model to start with, we shall test the model for 25 MLD (Million Liters per Day) which is equivalent to 25000 m^3/day.

Based on experimental observations, most pharmaceutical compounds showed substantial degradation within the first 90 min of photoelectrocatalytic treatment. Among these, sulfamethoxazole was identified as the most persistent, with calculations indicating that a 75% removal would require approximately 122 minutes in an ideal completely mixed system. However, other compounds showed major degradation, particularly within the first 15–20 minutes of treatment. To strike a practical balance between treatment efficiency and reactor volume, a hydraulic retention time of 20 minutes is selected. This decision prioritizes the effective removal of fast-reacting compounds while keeping the system design compact and operationally feasible. To manage the high influent volume of 25,000 m^3/day, the entire water flow will be divided into multiple treatment modules. This modular approach ensures scalability and facilitates operational flexibility under high-load conditions. Each module of the PEC would be designed for a volume of 1000 L (1 m^3). Considering these 350 individual modules of the PEC reactor would be needed to treat the water.

An idea of a full – scale model of a PEC was envisioned based on the information.

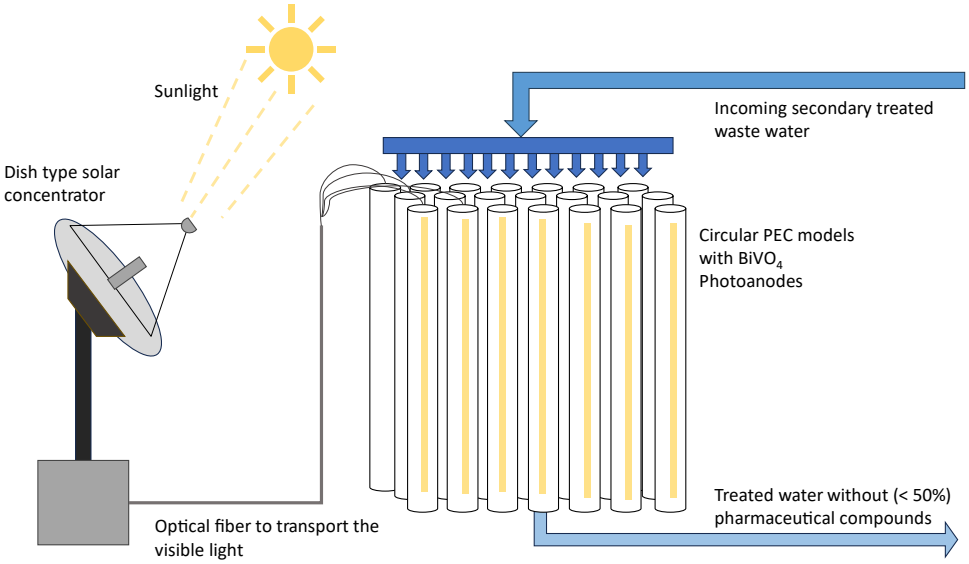

Figure 20. Schematics of an Idea of a full-scale PEC system

The application of Bismuth–based Photoelectrocatalysis for treating pharmaceuticals from wastewater was assessed.

Capital Cost (CAPEX):

The initial investment considered represents the capital cost of the reactor itself, machinery, pipes, and instruments.

Table 12. CAPEX of a PEC system

Component	Description	Value
Photocatalytic Reactor	Cost per module = 11780 € (calculation in the appendix includes the price of the quartz reactor system, the total price of raw materials used for fabrication and the electrodes)	4324250 €
Solar Concentrator system	Solar dish concentrator and fibre optic system (Calculations in appendix)	30000 €
Electrical and PEC Hardware	Power supply units, electrical control panel,	100000 €
Pump, Piping and Installation	Pipes, valves, and feed pumps	100000 €
Miscellaneous	Includes service buildings and installation – 10% of CAPEX	227712 €
Engineering and construction cost	10% of total cost	478196 €

From Table 12, summing up the rough estimates: Photoanodes (€ 4.3 M) + Solar concentrator system (€ 30 K) + Electrical and PEC hardware system (€ 100 K) + Pump and piping (€ 100 K) + Miscellaneous (€ 230K) + Engineering and Construction cost (€ 480K) yields a total investment of € 5.3 M. This figure is a rough approximation as the cost of making photocatalytic reactor will considerably reduce when manufacturing is done at large scale. The land cost also is not considered as it is going to replace an existing setting in our scenario; however, it is safe to assume due to the high HRT and volume requirement, the land footprint required for the process will be very high. If we consider a lifespan of 10 years for the Photocatalytic reactor, the treatment cost per m^3 is € 0.07/m^3

Operational Cost (OPEX)

OPEX includes all ongoing costs to run the PEC system, typically electricity, electrode replacement, labour/maintenance, and consumables

Table 13. OPEX of PEC system

Component	Description	Value/year
Energy Cost	Annual Energy consumed 31 kWh per year (calculation in Appendix)	10000 €
Electrode replacement and investment cost	Every 10-year replacement – 10 % of the Reactor cost for the previous investment and replacement	860000 €

Maintenance	2% of CAPEX	100000 €
Engineer and worker	High-skilled engineers and labourers	300000 €
Chemicals	Electrolyte Na_2SO_4 and other	10000 €

From Table 13, we get a rough estimate of the total annual operational cost. The energy cost (€ 10K) + Electrode replacement cost (€ 860K) + Maintenance cost (€ 100K) + Salary remuneration (€ 300K) + Other chemicals and consumables (€ 10K) yield a total of € 1.27 M annually for the smooth operation of the system. The unit treatment cost of PEC can be estimated as € 0.17/m^3 considering the OPEX price.

Including the CAPEX and OPEX the total treatment cost of using a PEC system would come up to € 0.24/m^3 The PEC system has high potential savings in consumables and energy as it utilizes almost no consumables and most of the energy can be obtained from solar. There is no established cost review available, however there are few other emerging companies working on electrochemical oxidation method to remove persistent chemicals from wastewater. SUKI is working on electrochemical oxidation with special electrode able to treat wastewater for persistent compound at € 2 -3 /m^3 (SUIKI by TDK) It is important to understand this is the pilot scale rough estimation of cost, this cost would be further reduced when such methods are implemented on a full-scale phase

When compared to the likes of UV, Capital cost-wise, the cost of treatment of is ~ € 20/m^3 (Mahamuni & Adewuyi, 2010). This amount is much higher than that of the oxidation method but UV is much more well-established. UV process as such has a much smaller footprint and this point provides a big advantage. When it comes to the operational cost aspect UV processes will be much higher than the PEC as it requires high energy inputs for the UV lamp and ozone generation The PEC system, by contrast, has minimal chemical input and could largely run on solar energy. In Treating efficacy UV is a very well-established technology degrading a broad spectrum of pharmaceuticals but on the other hand, PEC is still in the research phase.

5.3 Business Implementation of Large-Scale Photoelectrocatalysis

As industries transition toward sustainable solutions, PEC emerges as a promising technology for wastewater treatment and green hydrogen production. However, its large-scale implementation requires navigating regulatory frameworks, business overview, and ethical considerations.

Over the years the regulations for pharmaceutical discharge have been getting more stringent. The new EU Wastewater directive requires WWTPs around to expand their treatment to 4^{th} stage purification and the cost must be shared by individual pharmaceutical companies. In principle, all producers of medicinal products for human use or cosmetics will be required to bear the costs. This is to all the EU member states. The amended directive also stipulates that 50% of the WWTP with a municipal population must be upgraded to the 4^{th} treatment stage by 2030. Due to such policy initiatives, the requirement for a cost-effective pharmaceutical treatment method will increase

PEC also has many other market advantages, which will further increase its market share due to its various functionalities beyond water treatment. PEC manufacturers are not restricted to Pollutant destruction from water but also expand their applications to other uses, such as

removal of other contaminants, air purification, hydrogen generation, and CO_2 reduction (Spasiano et al., 2015). This serves as a motivation for companies to pivot towards PEC-based treatment.

The market for pharmaceutical removal from wastewater is highly competitive, with an increasing requirement for a 4th treatment stage in water purification targeting key OMPs. Activated carbon and ozonation are two of the main technologies, holding major share of the market. Among these, UV-based ozonation is a major competitor, as both are advanced oxidation process (AOP)-based technologies. Some of the main suppliers of activated carbon and UV-based ozonation systems include Veolia, Pinnacle Ozone Solutions, Calgon Carbon, Chemviron, and Desotec.

More incentives should be provided to these companies to encourage a shift towards PEC-based pharmaceutical degradation. However, with the emerging trend favouring photocatalysis (PC), several startups and companies are now working on air and water purification using visible-light-driven photocatalysis.

- NanoPtek (USA) is working on a pilot-scale project using visible-light-activated TiO_2 for water and air purification (*Visible Light Photocatalysts | NANOPTEK*).
- Puralytics (USA) is developing UV-activated nanotechnology systems, such as the SolarBag and Shield, for water purification using light-driven oxidation (Puralytics).
- Brochier Technologies (France) is leading the AQUAPHOTEX project, which is developing photocatalytic textiles coated with TiO_2 for organic micropollutant (OMP) degradation in water (Indermühle et al., 2016).

All these projects are still at the pilot demonstration scale, and a full-scale commercial project is yet to be implemented. In terms of cost competitiveness, UV-based treatment currently has an advantage due to its smaller space requirement. However, with advancements in PEC and its ability to utilize visible-light-driven solar energy, operational costs will significantly decrease due to its reliance on a renewable energy source. Despite its potential, PEC still requires significant investment and stronger public-private partnerships. Additionally, there are still hurdles that must be overcome for widespread adoption.

For large-scale adoption, it is important to consider human and ethical values when employing such emerging technology. Access to clean water is a fundamental human right, and it must be ensured that this remains affordable for all communities. The cost of water should not increase significantly due to the integration of such high-end technology.

The introduction of PEC should be accompanied by comprehensive long-term testing to assess whether the byproducts have harmful effects at the usage level. Since PEC is still a developing technology, we are uncertain about the byproducts that might emerge over time, or whether photocatalyst materials degrade, potentially releasing small particles into the environment, and causing unintended harm. Therefore, proper lifecycle assessments and socio-economic evaluations must be conducted for PEC.

A well-structured stakeholder engagement is crucial, involving:

- Water treatment plants
- Government bodies
- State/regional environmental authorities

- Material manufacturers
- Local communities and awareness programs

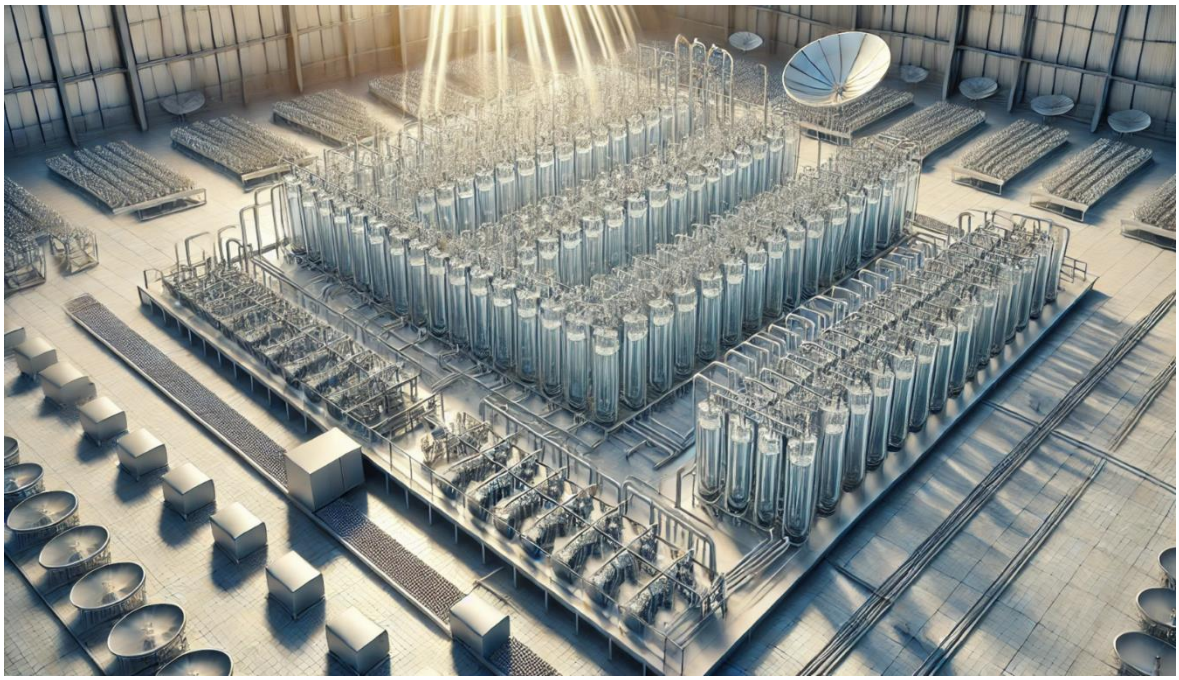

Figure 21. A model representation of a full – scale PEC system with solar concentrators generated with the help of AI

Chapter 6. Conclusion

This study focussed on the effectiveness of QAC-modified $BiVO_4$ photoanodes for the PEC degradation of pharmaceutical contaminants in real wastewater. Through a combination of structural, morphological, electrochemical, and degradation studies, the research provides insights into how surface modifications impact $BiVO_4$ performance and its potential for large-scale wastewater treatment. The findings are discussed with the three key research questions.

Main objective:

To evaluate the effectiveness of $BiVO_4$ photoanodes modified with Quaternary Ammonium Compounds (QACs) in the photoelectrocatalytic degradation of pharmaceutical compounds present in real wastewater treatment plant (WWTP) effluent

Characterization confirmed the deposition of QAC on the photoanode surface, with variations in properties among the different modifications. Degradation studies indicated that while DADMAC C18 performed slightly better than $BiVO_4$ in pharmaceutical removal, other QAC variants showed no significant improvement.

Answers to the research questions were:

1. **Fabrication and Characterization**

   What are the structural, optical, and electrochemical properties of $BiVO_4$ photoanodes modified with various QACs?

   The structural, optical, and electrochemical properties of the Photoanodes were studied using characterization studies – XRD, SEM, EDX, XPS, UV and LSV. From this we could conclude that the optimization of BiVO4 with QAC did not have much change in its crystalline phase with BiVO4 maintaining its monolithic crystalline form. The SEM and EDX analyses confirmed that the QAC was successfully incorporated into the photoanode and was uniformly distributed across its surface.The XPS confirmed the elemental state of the elements present. It showed the difference in the oxygen vacancies in the QAC modified photoanodes with the DADMAC variant showing higher oxygen vacancies percentage. The LSV results showed that all the Photoanode variants are light responsive and BAC C18 showed the highest output Photocurrent density from the variants

2. **Performance Evaluation**

   What is the removal efficacy of the individual pharmaceuticals in the mixture of the target pharmaceuticals using QAC-modified $BiVO_4$ photoanodes?
   The Degradation studies showed the individual removal efficacy of Pharmaceuticals for each variant of QAC modified BiVO4 photoanodes. From the results we concluded that overall DADMAC C18 variant performed good. It showed the best removal (%) for 5 pharmaceutical compounds – Propranolol (68.2%), Sotalol (51.6%), Caffeine (34.5%), Theophylline (38.9%) and Acetaminophen (57.3%). This was followed by the performance of BiVO4 where it showed the best removal for the pharmaceutical compound Metoprolol (59.9%). BAC C18 showed the worst removal efficacy for most of the pharmaceutical compounds. Considering the time, it takes for the Pharmaceutical to breakdown for the variants. ATMAC C16 variant removed many Pharmaceutical

(>50%) in less than 15 minutes. DADMAC C18 showed a more consistent breakdown of pharmaceutical compounds over time. Time-based kinetic analysis showed that some pharmaceuticals, such as metoprolol and propranolol, were degraded rapidly, while others, like gabapentin, were more resistant. The kinetics of pharmaceutical compounds was studied for DADMAC C18 variant and it was concluded that sulfamethoxazole was one of the more critical compounds due to its high half life time

3. **Scaling UP PEC for Real-World Applications**

What are the key challenges and potential solutions for scaling up the PEC process for the removal of pharmaceuticals in wastewater treatment?

The full-scale implication of PEC was studied using BiVO4 Photoanode. The model was implemented for WWTP Hoestmeer , where it would serve as a replacement for the UV oxidation which is working right now. Some key challenges when scaling up the PEC full – scale model was found to optimize use of the solar visible light which could be solved by using solar concentrators , High volume and reactor space which could be combated by using reactor with less HRT by increasing the time it takes to remove the pharmaceutical, this can be done by adding PMS to further optimize the reaction rates. The technoeconomic analysis was done to conclude that it would take 0.17 Euro/m^3 which should be reduced for it be really implemented in a real-life setting

6.1 Challenges throughout the experiment

This research involved many multidisciplinary activities and presented multiple challenges in various stages of the experiment. Systematic troubleshooting and optimization were done to ensure this do not affect the overall studies and ensure consistent and reliable results. Difficulty in Dissolving Quaternary Ammonium Compounds

One of the initial challenges was the poor solubility of QACs in the $BiVO_4$ precursor solution. Following the literature, nitric acid (HNO_3) was first used, but it failed to dissolve the QACs. Gentle heating at 45°C was attempted, but this also proved ineffective. Further increasing the temperature led to the formation of suspended $BiVO_4$ nanoparticles in water, interfering with the synthesis. The issue was resolved by switching from demineralized water to Milli-Q deionized water, which successfully dissolved the QACs. Once solubility was achieved, the concentration was gradually increased to determine the maximum dissolvable amount, ensuring effective QAC incorporation into the $BiVO_4$ matrix.

1. Poor Adhesion of Copper wire to the Photoanode

Securing the copper wire to the photoanode was another challenge, as it did not stick well and could be easily detached, affecting electrical connectivity. Several adhesives, including marine adhesive tape, nail polish, and conductive tape, were tested but failed to provide a strong connection. Through systematic trials, it was determined that pre-heating the carbon black material to 70–80°C before mixing it with resin improved adhesion. Allowing the mixture to thicken for 30 minutes or pre-curing it in an oven at 50–60°C for 10 minutes ensured a stable consistency. Applying the resin at this stage prevented exposure to carbon black, which could cause current leakage. Final curing at 60°C for 4 hours or 45°C overnight provided strong adhesion and long-term stability.

2. Inconsistent Spray deposition

Fabrication inconsistencies were frequently observed during ultrasonic spray deposition, resulting in droplet formation and uneven coatings. Clogging of the spray nozzle was identified as a major issue. To address this, the nozzle was regularly flushed with ethanol and a low-concentration NaOH solution to remove residues, soaked overnight in ethanol, and the spray pipe was replaced every two weeks. Additionally, airflow stability was essential for uniform film deposition. Fixing the air pressure at an optimal point and installing a shut-off valve near the setup ensured steady spray performance while adjusting the spray height based on airflow maintained uniform coatings. These optimizations significantly improved the quality and reproducibility of $BiVO_4$ thin films.

3. Leakage issue in the PEC system

During PEC system assembly, leakage was observed, leading to water dripping into the solar simulator. This was critical as if the water level dropped below the photoanode, the photocurrent would suddenly fall to 0 mA, invalidating the experiment. To prevent this**,** all screws were tightened properly, ensuring a sealed reaction chamber. Additionally, pH and electrical conductivity (EC) were adjusted carefully to minimize leakage risks. The complexity of the design, involving multiple screws and sealing components, made this setup particularly challenging to maintain.

4. Optimization of Temperature in the Hot Plate

Previous studies suggested heating the hot plate to 300°C for photoanode fabrication (Ali et al., 2025). However, this temperature resulted in incorrect photoanode colouration, producing a dark yellow film instead of the expected brighter yellow. Additionally, linear sweep voltammetry (LSV) measurements showed significantly lower photocurrent densities, around 0.1 mA/cm^2, indicating poor photoelectrochemical performance. After troubleshooting, it was determined that reducing the temperature to 225°C produced photoanodes with the correct colour and improved LSV performance, confirming it as the optimal synthesis temperature.

5. Recommendation for a better model

Based on these issues particularly concerning the design of the PEC reactor, some design changes are recommended to make the research smoother, avoid leakage issues, and reduce the time the pH and EC meters were removed for collecting the samples. Researchers have used different kinds of models to perform such studies with immobilized photoanodes in a cube quartz reactor (Man et al., 2025). The suggestions recommended have taken some inspiration from their models

- Replace the screw with clip type nail mechanism and use rubber-sealed caps to prevent leakage. This ensures faster assembly and consistent pressure application.
- The use of modular caps with threaded screw systems will help eliminate the use of screws. Rubber-sealed caps can be placed to ensure no leakage. The combination provides for better sealing and quicker insertion. The modular caps can be installed with slot based Photoanode holders which eliminates the need for manual adjustment of the photoanode and the level of photoanode is the same in all experiments preventing misalignments
- To address leakage issues due to the electrode ports, rubber O ring or gaskets with the same size as the Ph/EC meter to ensure a tight seal. A dedicated sample collection port with a small cap will be added, allowing for easy sample extraction without removing

the pH and EC meter each time. This prevents disturbance to the experimental setup and improves consistency in measurements.

6.2 Future Recommendations

Further work is proposed to further enhance the understanding and applicability of the research work

Integrations of Peroxymonosulfate (PMS) to Enhance kinetics

Future experiments should investigate the synergistic effect of PMS addition on PEC degradation performance. PMS acts as a strong oxidant and electron acceptor, enhancing charge separation and reactive oxygen species (ROS) generation. The carbon-rich structure of QACs may further assist in activating PMS, potentially increasing the formation of sulfate and hydroxyl radicals, and accelerating pharmaceutical breakdown.

Radical Mechanism and Degradation pathway studies

A deeper understanding of the degradation mechanism is essential. Radical scavenging experiments and analytical techniques should be employed to quantify ROS (e.g., •OH, $SO_4^{\bullet -}$) and to identify degradation intermediates. This will clarify the dominant pathways and assess any risks associated with transformation by-products.

Photoanode Longevity and Reusability

The operational stability of QAC-modified $BiVO_4$ photoanodes should be assessed over multiple degradation cycles. Studies focusing on corrosion, surface fouling, and reusability will help determine the long-term feasibility of implementing these photoanodes in real-world treatment systems.

Reference

Alalm, M. G., Djellabi, R., Meroni, D., Pirola, C., Bianchi, C. L., & Boffito, D. C. (2021). Toward scaling-up photocatalytic process for multiphase environmental applications. In *Catalysts* (Vol. 11, Issue 5). MDPI. https://doi.org/10.3390/catal11050562

Ali, A. Z., Jagannathan, S., Bennani, Y. D., van der Hoek, J. P., & Spanjers, H. (2023a). Photoelectrocatalytic based simultaneous removal of multiple organic micro-pollutants by using a visible light driven BiVO4 photoanode. *Journal of Water Process Engineering*, *56*, 104471. https://doi.org/10.1016/J.JWPE.2023.104471

Ali, A. Z., Jagannathan, S., Bennani, Y. D., van der Hoek, J. P., & Spanjers, H. (2023b). Photoelectrocatalytic based simultaneous removal of multiple organic micro-pollutants by using a visible light driven BiVO4 photoanode. *Journal of Water Process Engineering*, *56*, 104471. https://doi.org/10.1016/J.JWPE.2023.104471

Ali, A. Z., Wu, Y., Bennani, Y. D., Spanjers, H., & Hoek, J. P. van der. (2023). Photo-electrocatalytic based removal of acetaminophen: Application of visible light driven heterojunction based BiVO4/BiOI photoanode. *Chemosphere*, *324*, 138322. https://doi.org/10.1016/J.CHEMOSPHERE.2023.138322

Ali, A. Z., Wu, Y., Wols, B., Zeidan, M., Spanjers, H., & van der Hoek, J. P. (2025). Simultaneous removal of multiple organic OMPs via UV-visible light driven BiVO4/TiO2-GO photoanode: Experimental and CFD study. *Chemical Engineering Journal Advances*, *22*, 100721. https://doi.org/10.1016/j.ceja.2025.100721

Alulema-Pullupaxi, P., Espinoza-Montero, P. J., Sigcha-Pallo, C., Vargas, R., Fernández, L., Peralta-Hernández, J. M., & Paz, J. L. (2021). Fundamentals and applications of photoelectrocatalysis as an efficient process to remove pollutants from water: A review. *Chemosphere*, *281*, 130821. https://doi.org/10.1016/J.CHEMOSPHERE.2021.130821

Amanlou, Y., Hashjin, T. T., Ghobadian, B., Najafi, G., & Mamat, R. (2016). A comprehensive review of Uniform Solar Illumination at Low Concentration Photovoltaic (LCPV) Systems. In *Renewable and Sustainable Energy Reviews* (Vol. 60, pp. 1430–1441). Elsevier Ltd. https://doi.org/10.1016/j.rser.2016.03.032

Arunachalam, P., Shaddad, M. N., Amer, M. S., & AL-Qadi, A. (2024). Enhanced photoelectrochemical water splitting coupled with pharmaceutical pollutants degradation on Zr:BiVO4 photoanodes by synergetic catalytic activity of NiFeOOH nanostructures. *Alexandria Engineering Journal*, *99*, 64–75. https://doi.org/10.1016/j.aej.2024.05.012

Arunachalam, P., Shaddad, M. N., Amer, M. S., Alsalman, A. M., & Madhavan, J. (2024). Cooperative catalytic behavior of CoS and Bi2S3 nanoparticles on Zr:BiVO4 photoanodes for enhanced photoelectrochemical sulfite oxidation coupled with pharmaceutical pollution degradation. *Environmental Science: Nano*, *11*(6), 2668–2682. https://doi.org/10.1039/d4en00018h

Bessegato, G. G., Guaraldo, T. T., de Brito, J. F., Brugnera, M. F., & Zanoni, M. V. B. (2015). Achievements and Trends in Photoelectrocatalysis: from Environmental to Energy Applications. *Electrocatalysis 2015 6:5*, *6*(5), 415–441. https://doi.org/10.1007/S12678-015-0259-9

Binjhade, R., Mondal, R., & Mondal, S. (2022). Continuous photocatalytic reactor: Critical review on the design and performance. In *Journal of Environmental Chemical Engineering* (Vol. 10, Issue 3). Elsevier Ltd. https://doi.org/10.1016/j.jece.2022.107746

Braham, R. J., & Harris, A. T. (2009). Review of major design and scale-up considerations for solar photocatalytic reactors. In *Industrial and Engineering Chemistry Research* (Vol. 48, Issue 19, pp. 8890–8905). https://doi.org/10.1021/ie900859z

Bureš, F. (2019). Quaternary Ammonium Compounds: Simple in Structure, Complex in Application. In *Topics in Current Chemistry* (Vol. 377, Issue 3). Springer International Publishing. https://doi.org/10.1007/s41061-019-0239-2

Chen, S., Huang, D., Du, L., Lei, L., Chen, Y., Wang, G., Wang, Z., Zhou, W., Tao, J., Li, R., & Zhou, C. (2022). Peroxymonosulfate activation by surface-modified bismuth vanadate for ciprofloxacin abatement under visible light: Insights into the generation of singlet oxygen. *Chemical Engineering Journal*, *444*, 136373. https://doi.org/10.1016/J.CEJ.2022.136373

Chen, Z., Mi, N., Huang, L., Wang, W., Li, C., Teng, Y., & Gu, C. (2022a). Snow-like BiVO4 with rich oxygen defects for efficient visible light photocatalytic degradation of ciprofloxacin. *Science of The Total Environment*, *808*, 152083. https://doi.org/10.1016/J.SCITOTENV.2021.152083

Chen, Z., Mi, N., Huang, L., Wang, W., Li, C., Teng, Y., & Gu, C. (2022b). Snow-like BiVO4 with rich oxygen defects for efficient visible light photocatalytic degradation of ciprofloxacin. *Science of The Total Environment*, *808*, 152083. https://doi.org/10.1016/J.SCITOTENV.2021.152083

Chinnaiyan, P., Thampi, S. G., Kumar, M., & Balachandran, M. (2019). Photocatalytic degradation of metformin and amoxicillin in synthetic hospital wastewater: effect of classical parameters. *International Journal of Environmental Science and Technology*, *16*(10), 5463–5474. https://doi.org/10.1007/s13762-018-1935-0

Davies, K. R., Allan, M. G., Nagarajan, S., Townsend, R., Asokan, V., Watson, T., Godfrey, A. R., Maroto-Valer, M. M., Kuehnel, M. F., & Pitchaimuthu, S. (2023). Photoelectrocatalytic Surfactant Pollutant Degradation and Simultaneous Green Hydrogen Generation. *Industrial and Engineering Chemistry Research*. https://doi.org/10.1021/acs.iecr.3c00840

Eliminate PFAS in effluent water - SUIKI by TDK. (n.d.). Retrieved March 12, 2025, from https://suiki.earth/

Fiaz, A., Zhu, D., & Sun, J. (2021). Environmental fate of tetracycline antibiotics: degradation pathway mechanisms, challenges, and perspectives. In *Environmental Sciences Europe* (Vol. 33, Issue 1). Springer Science and Business Media Deutschland GmbH. https://doi.org/10.1186/s12302-021-00505-y

Fu, L., Li, Z., & Shang, X. (2024). Recent surficial modification strategies on BiVO4 based photoanodes for photoelectrochemical water splitting enhancement. In *International Journal of Hydrogen Energy* (Vol. 55, pp. 611–624). Elsevier Ltd. https://doi.org/10.1016/j.ijhydene.2023.11.253

Fuentes-Camargo, I., Carrera-Crespo, J. E., Vazquez-Arenas, J., Romero-Ibarra, I., Rodríguez, J. L., Lartundo-Rojas, L., & Cardoso-Martínez, J. (2020). Pulse-Plating Electrodeposition of Metallic Bi in an Organic-Free Aqueous Electrolyte and Its Conversion into BiVO<inf>4</inf> to Improve Photoelectrochemical Activity toward Pollutant Degradation under Visible Light. *Journal of Physical Chemistry C*, *124*(2), 1421–1428. https://doi.org/10.1021/acs.jpcc.9b09898

Ganapathi, G. (2012). *Low-Cost, Lightweight Solar Concentrator*. www.solar.energy.gov/sunshot/csp.html

Ghosh, S., Pourebrahimi, S., Malloum, A., Ajala, O. J., AlKafaas, S. S., Onyeaka, H., Nnaji, N. D., Oroke, A., Bornman, C., Christian, O., Ahmadi, S., & Wani, M. Y. (2023). A review on ciprofloxacin removal from wastewater as a pharmaceutical contaminant: Covering adsorption to advanced oxidation processes to computational studies. *Materials Today Communications*, *37*, 107500. https://doi.org/10.1016/J.MTCOMM.2023.107500

Goodarzi, N., Ashrafi-Peyman, Z., Khani, E., & Moshfegh, A. Z. (2023). Recent Progress on Semiconductor Heterogeneous Photocatalysts in Clean Energy Production and Environmental Remediation. In *Catalysts* (Vol. 13, Issue 7). Multidisciplinary Digital Publishing Institute (MDPI). https://doi.org/10.3390/catal13071102

Guan, B., Chen, J., Li, Z., Zhuang, Z., Chen, Y., Ma, Z., Guo, J., Zhu, C., Hu, X., Zhao, S., Dang, H., Chen, L., Shu, K., Guo, Z., Shi, K., Li, Y., Yi, C., Hu, J., & Huang, Z. (2024). Review on Synthesis, Modification, Morphology, and Combination of BiVO4-based Catalysts for Photochemistry: Status, Advances, and Perspectives. In *Energy and Fuels* (Vol. 38, Issue 2, pp. 806–853). American Chemical Society. https://doi.org/10.1021/acs.energyfuels.3c03932

Indermühle, C., Puzenat, E., Simonet, F., Peruchon, L., Brochier, C., & Guillard, C. (2016). Modelling of UV optical ageing of optical fibre fabric coated with TiO2. *Applied Catalysis B: Environmental*, *182*, 229–235. https://doi.org/10.1016/j.apcatb.2015.09.037

Jiang, L., Chen, D., Qin, L., Liang, J., Sun, X., & Huang, Y. (2019). Enhanced photocatalytic activity of hydrogenated BiVO4 with rich surface-oxygen-vacancies for remarkable degradation of tetracycline hydrochloride. *Journal of Alloys and Compounds*, *783*, 10–18. https://doi.org/10.1016/j.jallcom.2018.12.290

Jing, D., Liu, H., Zhang, X., Zhao, L., & Guo, L. (2009). Photocatalytic hydrogen production under direct solar light in a CPC based solar reactor: Reactor design and preliminary results. *Energy Conversion and Management*, *50*(12), 2919–2926. https://doi.org/10.1016/j.enconman.2009.07.012

Kanaujiya, D. K., Paul, T., Sinharoy, A., & Pakshirajan, K. (2019). Biological Treatment Processes for the Removal of Organic Micropollutants from Wastewater: a Review. In *Current Pollution Reports* (Vol. 5, Issue 3, pp. 112–128). Springer. https://doi.org/10.1007/s40726-019-00110-x

Kang, J., Tang, Y., Wang, M., Jin, C., Liu, J., Li, S., Li, Z., & Zhu, J. (2021a). The enhanced peroxymonosulfate-assisted photocatalytic degradation of tetracycline under visible light by g-C3N4/Na-BiVO4 heterojunction catalyst and its mechanism. *Journal of Environmental Chemical Engineering*, *9*(4), 105524. https://doi.org/10.1016/J.JECE.2021.105524

Kang, J., Tang, Y., Wang, M., Jin, C., Liu, J., Li, S., Li, Z., & Zhu, J. (2021b). The enhanced peroxymonosulfate-assisted photocatalytic degradation of tetracycline under visible light by g-C3N4/Na-BiVO4 heterojunction catalyst and its mechanism. *Journal of Environmental Chemical Engineering*, *9*(4), 105524. https://doi.org/10.1016/J.JECE.2021.105524

Kulišťáková, A. (2023). Removal of pharmaceutical micropollutants from real wastewater matrices by means of photochemical advanced oxidation processes – A review. In *Journal of Water Process Engineering* (Vol. 53). Elsevier Ltd. https://doi.org/10.1016/j.jwpe.2023.103727

Łęcki, T., Hamad, H., Zarębska, K., Wierzyńska, E., & Skompska, M. (2022). Mechanistic insight into photochemical and photoelectrochemical degradation of organic pollutants with the use of BiVO4 and BiVO4/Co-Pi. *Electrochimica Acta*, *434*, 141292. https://doi.org/10.1016/J.ELECTACTA.2022.141292

Li, J., Ren, J., Li, S., Li, G., Li, M. M. J., Li, R., Kang, Y. S., Zou, X., Luo, Y., Liu, B., & Zhao, Y. (2024). Potential industrial applications of photo/electrocatalysis: Recent progress and future challenges. In *Green Energy and Environment* (Vol. 9, Issue 5, pp. 859–876). KeAi Publishing Communications Ltd. https://doi.org/10.1016/j.gee.2023.05.003

Li, Y., Bai, B., Zhu, M., Li, J., Mei, Q., & Wang, Q. (2024a). BiVO4 photoanode modified with FeOOH cocatalyst for visible-light-driven photoelectrocatalytic degradation of organic pollutants. *Journal of Environmental Chemical Engineering*, *12*(4). https://doi.org/10.1016/j.jece.2024.113079

Li, Y., Bai, B., Zhu, M., Li, J., Mei, Q., & Wang, Q. (2024b). BiVO4 photoanode modified with FeOOH cocatalyst for visible-light-driven photoelectrocatalytic degradation of organic pollutants. *Journal of Environmental Chemical Engineering*, *12*(4), 113079. https://doi.org/10.1016/J.JECE.2024.113079

Li, Y., Sun, X., Tang, Y., Ng, Y. H., Li, L., Jiang, F., Wang, J., Chen, W., & Li, L. (2021a). Understanding photoelectrocatalytic degradation of tetracycline over three-dimensional coral-like ZnO/BiVO4 nanocomposite. *Materials Chemistry and Physics*, *271*, 124871. https://doi.org/10.1016/J.MATCHEMPHYS.2021.124871

Li, Y., Sun, X., Tang, Y., Ng, Y. H., Li, L., Jiang, F., Wang, J., Chen, W., & Li, L. (2021b). Understanding photoelectrocatalytic degradation of tetracycline over three-dimensional coral-like ZnO/BiVO4 nanocomposite. *Materials Chemistry and Physics*, *271*, 124871. https://doi.org/10.1016/J.MATCHEMPHYS.2021.124871

Liu, C., Ding, Z., Shi, M., Wang, D., Chen, Q., Xia, M., & Wang, F. (2024). Dependence of superoxide radical generation on peroxymonosulfate under visible light: Enrofloxacin degradation and mechanism insight. *Chemical Engineering Journal*, *485*. https://doi.org/10.1016/j.cej.2024.149721

Liu, J., Li, B., Kong, L., Xiao, Q., & Huang, S. (2023). Surfactants-assisted morphological regulation of BiVO4 nanostructures for photocatalytic degradation of organic pollutants in wastewater. *Journal of Physics and Chemistry of Solids*, *172*. https://doi.org/10.1016/j.jpcs.2022.111079

Liu, J., Li, J., Li, Y., Guo, J., Xu, S. M., Zhang, R., & Shao, M. (2020). Photoelectrochemical water splitting coupled with degradation of organic pollutants enhanced by surface and interface engineering of BiVO4 photoanode. *Applied Catalysis B: Environmental*, *278*. https://doi.org/10.1016/j.apcatb.2020.119268

Liu, Y., Yu, Y., Xu, L., Hao, R., Yang, T., Huang, H., & Hu, J. (2024). Rod-like BiVO4 with two-phase structure to boost photoelectrocatalytic degradation activity for tetracycline via the p-n junction. *Applied Surface Science*, *656*. https://doi.org/10.1016/j.apsusc.2024.159719

Loganathan, P., Vigneswaran, S., Kandasamy, J., Cuprys, A. K., Maletskyi, Z., & Ratnaweera, H. (2023). Treatment Trends and Combined Methods in Removing Pharmaceuticals and Personal Care Products from Wastewater—A Review. *Membranes*, *13*(2). https://doi.org/10.3390/membranes13020158

Long, Z., Li, Q., Wei, T., Zhang, G., & Ren, Z. (2020). Historical development and prospects of photocatalysts for pollutant removal in water. *Journal of Hazardous Materials*, *395*, 122599. https://doi.org/10.1016/J.JHAZMAT.2020.122599

Ma, D., Yi, H., Lai, C., Liu, X., Huo, X., An, Z., Li, L., Fu, Y., Li, B., Zhang, M., Qin, L., Liu, S., & Yang, L. (2021). Critical review of advanced oxidation processes in organic wastewater treatment. In *Chemosphere* (Vol. 275). Elsevier Ltd. https://doi.org/10.1016/j.chemosphere.2021.130104

Mahamuni, N. N., & Adewuyi, Y. G. (2010). Advanced oxidation processes (AOPs) involving ultrasound for waste water treatment: A review with emphasis on cost estimation. *Ultrasonics Sonochemistry*, *17*(6), 990–1003. https://doi.org/10.1016/j.ultsonch.2009.09.005

Malathi, A., Madhavan, J., Ashokkumar, M., & Arunachalam, P. (2018). A review on BiVO4 photocatalyst: Activity enhancement methods for solar photocatalytic applications. *Applied Catalysis A: General*, *555*, 47–74. https://doi.org/10.1016/J.APCATA.2018.02.010

Man, J. H. K., Zheng, Z., Dong, T., Lung, C. W., Cheung, H. Y. M., Wang, X., Dong, H., Guan, X., & Lo, I. M. C. (2025). Photoelectrochemical activation of free chlorine utilizing vacancies-engineered BiVO4 photoanode for simultaneous pharmaceuticals and personal care products (PPCPs) degradation and bacterial inactivation: An integrative batch and continuous flow reactor study. *Separation and Purification Technology*, *360*. https://doi.org/10.1016/j.seppur.2024.130959

Marugán, J., Van Grieken, R., Pablos, C., Adán, C., & Timmers, R. (2013). Determination of photochemical, electrochemical and photoelectrochemical efficiencies in a photoelectrocatalytic reactor. *International Journal of Chemical Reactor Engineering*, *11*(2), 787–797. https://doi.org/10.1515/ijcre-2012-0014

Meng, X., Zhang, Z., & Li, X. (2015a). Synergetic photoelectrocatalytic reactors for environmental remediation: A review. *Journal of Photochemistry and Photobiology C: Photochemistry Reviews*, *24*, 83–101. https://doi.org/10.1016/J.JPHOTOCHEMREV.2015.07.003

Meng, X., Zhang, Z., & Li, X. (2015b). Synergetic photoelectrocatalytic reactors for environmental remediation: A review. In *Journal of Photochemistry and Photobiology C: Photochemistry Reviews* (Vol. 24, pp. 83–101). Elsevier. https://doi.org/10.1016/j.jphotochemrev.2015.07.003

Mohapatra, S., Yutao, L., Goh, S. G., Ng, C., Luhua, Y., Tran, N. H., & Gin, K. Y. H. (2023). Quaternary ammonium compounds of emerging concern: Classification, occurrence, fate, toxicity and antimicrobial resistance. In *Journal of Hazardous Materials* (Vol. 445). Elsevier B.V. https://doi.org/10.1016/j.jhazmat.2022.130393

Monfort, O., & Plesch, G. (2018). Bismuth vanadate-based semiconductor photocatalysts: a short critical review on the efficacy and the mechanism of photodegradation of organic pollutants. *Environmental Science and Pollution Research 2018 25:20*, *25*(20), 19362–19379. https://doi.org/10.1007/S11356-018-2437-9

Nguyen, L. M., Nguyen, N. T. T., Nguyen, T. T. T., Nguyen, T. T., Nguyen, D. T. C., & Tran, T. Van. (2022). Occurrence, toxicity and adsorptive removal of the chloramphenicol antibiotic in water: a review. In *Environmental Chemistry Letters* (Vol. 20, Issue 3, pp. 1929–1963). Springer Science and Business Media Deutschland GmbH. https://doi.org/10.1007/s10311-022-01416-x

Nguyen, T. D., Nguyen, V. H., Nanda, S., Vo, D. V. N., Nguyen, V. H., Van Tran, T., Nong, L. X., Nguyen, T. T., Bach, L. G., Abdullah, B., Hong, S. S., & Van Nguyen, T. (2020). BiVO4 photocatalysis design and applications to oxygen production and degradation of organic compounds: a review. In *Environmental Chemistry Letters* (Vol. 18, Issue 6, pp. 1779–1801). Springer Science and Business Media Deutschland GmbH. https://doi.org/10.1007/s10311-020-01039-0

Orimolade, B. O., & Arotiba, O. A. (2020a). Bismuth vanadate in photoelectrocatalytic water treatment systems for the degradation of organics: A review on recent trends. *Journal of Electroanalytical Chemistry*, *878*. https://doi.org/10.1016/j.jelechem.2020.114724

Orimolade, B. O., & Arotiba, O. A. (2020b). Towards visible light driven photoelectrocatalysis for water treatment: Application of a FTO/BiVO4/Ag2S heterojunction anode for the removal of emerging pharmaceutical pollutants. *Scientific Reports*, *10*(1). https://doi.org/10.1038/s41598-020-62425-w

Orimolade, B. O., & Arotiba, O. A. (2022). Enhanced photoelectrocatalytic degradation of diclofenac sodium using a system of Ag-BiVO4/BiOI anode and Ag-BiOI cathode. *Scientific Reports*, *12*(1). https://doi.org/10.1038/s41598-022-08213-0

Orimolade, B. O., Koiki, B. A., Peleyeju, G. M., & Arotiba, O. A. (2019). Visible light driven photoelectrocatalysis on a FTO/BiVO4/BiOI anode for water treatment involving emerging pharmaceutical pollutants. *Electrochimica Acta*, *307*, 285–292. https://doi.org/10.1016/J.ELECTACTA.2019.03.217

Orimolade, B. O., Zwane, B. N., Koiki, B. A., Tshwenya, L., Peleyeju, G. M., Mabuba, N., Zhou, M., & Arotiba, O. A. (2020). Solar photoelectrocatalytic degradation of ciprofloxacin at a FTO/BiVO4/MnO2 anode: Kinetics, intermediate products and degradation pathway studies. *Journal of Environmental Chemical Engineering*, *8*(1), 103607. https://doi.org/10.1016/J.JECE.2019.103607

Pan, T., Tang, Y., Liao, Y., Chen, J., Li, Y., Wang, J., Li, L., & Li, X. (2023). BiVO4 modifying with cobalt-phosphate cluster cocatalyst for persulfate assisted photoelectrocatalytic degradation of tetracycline. *Molecular Catalysis*, *549*, 113527. https://doi.org/10.1016/J.MCAT.2023.113527

Phan, H. T. B., Nguyen, A. Q. K., Ahn, Y. Y., Kim, K., Kim, S., & Kim, J. (2022). Visible light-induced degradation of propranolol with peroxymonosulfate as an oxidant and a radical precursor. *Separation and Purification Technology*, *289*. https://doi.org/10.1016/j.seppur.2022.120764

Prado, T. M., Silva, F. L., Carrico, A., Lanza, M. R. D. V., Fatibello-Filho, O., & Moraes, F. C. (2022). Photoelectrocatalytic degradation of caffeine using bismuth vanadate modified with reduced graphene oxide. *Materials Research Bulletin*, *145*. https://doi.org/10.1016/j.materresbull.2021.111539

Puralytics. (n.d.). *Puralytics*. Retrieved February 25, 2025, from https://puralytics.com/

Qiao, S., Di, M., Jiang, J. X., & Han, B. H. (2022). Conjugated porous polymers for photocatalysis: The road from catalytic mechanism, molecular structure to advanced applications. *EnergyChem*, *4*(6), 100094. https://doi.org/10.1016/J.ENCHEM.2022.100094

Ramos, D. R., Iazykov, M., Fernandez, M. I., Santaballa, J. A., & Canle, M. (2021). Mechanical Stability Is Key for Large-Scale Implementation of Photocatalytic Surface-Attached Film

Technologies in Water Treatment. *Frontiers in Chemical Engineering*, *3*. https://doi.org/10.3389/fceng.2021.688498

Singla, S., Devi, P., & Basu, S. (2023). Revolutionizing the Role of Solar Light Responsive BiVO4/BiOBr Heterojunction Photocatalyst for the Photocatalytic Deterioration of Tetracycline and Photoelectrocatalytic Water Splitting. *Materials*, *16*(16). https://doi.org/10.3390/ma16165661

Spasiano, D., Marotta, R., Malato, S., Fernandez-Ibañez, P., & Di Somma, I. (2015). Solar photocatalysis: Materials, reactors, some commercial, and pre-industrialized applications. A comprehensive approach. In *Applied Catalysis B: Environmental* (Vols. 170–171, pp. 90–123). Elsevier. https://doi.org/10.1016/j.apcatb.2014.12.050

Su, W., Lu, Z., Shi, Q., Cheng, C., Liu, C., Lu, C., Xie, H., Lu, B., Huang, K., Xu, M., Xu, C., Pan, H., & Zhao, C. (2024). Surface States of Mo-Doped BiVO4 Nanoparticle-Based Photoanodes for Photoelectrochemical Degradation of Chloramphenicol. *ACS Applied Nano Materials*. https://doi.org/10.1021/acsanm.4c01743

Tavakoli Joorabi, F., Kamali, M., & Sheibani, S. (2022). Effect of aqueous inorganic anions on the photocatalytic activity of CuO–Cu2O nanocomposite on MB and MO dyes degradation. *Materials Science in Semiconductor Processing*, *139*. https://doi.org/10.1016/j.mssp.2021.106335

Tay, K. S., & Ismail, N. S. B. (2016). Degradation of β-blockers in water by sulfate radical-based oxidation: kinetics, mechanism and ecotoxicity assessment. *International Journal of Environmental Science and Technology*, *13*(10), 2495–2504. https://doi.org/10.1007/s13762-016-1083-3

Thaha, S. K. S. M., Nalandhiran, P., Kaliyamoorthy, S., Mizota, I., Mangalaraja, R. V., & Sathishkumar, P. (2024). Critical Review of Photocatalytic Reactor Designs for Environmental Applications. *Green Energy and Technology*, *Part F2928*, 1–50. https://doi.org/10.1007/978-981-97-1939-6_1/TABLES/9

Toe, C. Y., Pan, J., Scott, J., & Amal, R. (2022). Identifying Key Design Criteria for Large-Scale Photocatalytic Hydrogen Generation from Engineering and Economic Perspectives. In *ACS ES and T Engineering* (Vol. 2, Issue 6, pp. 1130–1143). American Chemical Society. https://doi.org/10.1021/acsestengg.2c00030

Visible Light Photocatalysts | NANOPTEK and LIGHTFUEL. (n.d.). Retrieved February 25, 2025, from https://nanoptek.com/pilot-production/products-2/

Wang, J., Tian, Z., Huo, Y., Yang, M., Zheng, X., & Zhang, Y. (2018). Monitoring of 943 organic micropollutants in wastewater from municipal wastewater treatment plants with secondary and advanced treatment processes. *Journal of Environmental Sciences (China)*, *67*, 309–317. https://doi.org/10.1016/j.jes.2017.09.014

Wang, K., Liang, G., Waqas, M., Yang, B., Xiao, K., Zhu, C., & Zhang, J. (2020a). Peroxymonosulfate enhanced photoelectrocatalytic degradation of ofloxacin using an easily coated cathode. *Separation and Purification Technology*, *236*. https://doi.org/10.1016/j.seppur.2019.116301

Wang, K., Liang, G., Waqas, M., Yang, B., Xiao, K., Zhu, C., & Zhang, J. (2020b). Peroxymonosulfate enhanced photoelectrocatalytic degradation of ofloxacin using an easily coated cathode. *Separation and Purification Technology*, *236*. https://doi.org/10.1016/j.seppur.2019.116301

Wang, W., Liu, X., Jing, J., Mu, J., Wang, R., Du, C., & Su, Y. (2023). Photoelectrocatalytic peroxymonosulfate activation over CoFe2O4-BiVO4 photoanode for environmental purification: Unveiling of multi-active sites, interfacial engineering and degradation pathways. *Journal of Colloid and Interface Science*, *644*, 519–532. https://doi.org/10.1016/J.JCIS.2023.03.202

Wu, S., & Hu, Y. H. (2021). A comprehensive review on catalysts for electrocatalytic and photoelectrocatalytic degradation of antibiotics. In *Chemical Engineering Journal* (Vol. 409). Elsevier B.V. https://doi.org/10.1016/j.cej.2020.127739

Xing, Y., Yi, J., Zhang, X., Jin, X., Peng, Y., Ni, G., Yong, X., & Wang, X. (2024). Fabrication of BiVO4 photoanode loaded with Zn-doped Co9S8 for enhanced photoelectrochemical performance. *Journal of Photochemistry and Photobiology A: Chemistry*, *448*. https://doi.org/10.1016/j.jphotochem.2023.115322

Xu, Y., Zhong, D., Jia, J., Li, K., Li, J., & Quan, X. (2013). Dual slant-placed electrodes thin-film photocatalytic reactor: Enhanced dye degradation efficacy by self-generated electric field. *Chemical Engineering Journal*, *225*, 138–143. https://doi.org/10.1016/j.cej.2013.03.085

Yin, W., Wang, W., Zhou, L., Sun, S., & Zhang, L. (2010). CTAB-assisted synthesis of monoclinic BiVO4 photocatalyst and its highly efficient degradation of organic dye under visible-light irradiation. *Journal of Hazardous Materials*, *173*(1–3), 194–199. https://doi.org/10.1016/j.jhazmat.2009.08.068

Yu, M., Tang, Y., Liao, Y., He, W., Lu, X. xin, & Li, X. (2023). Defect-designed Mo-doped BiVO4 photoanode for efficient photoelectrochemical degradation of phenol. *Journal of Materials Science and Technology*, *165*, 225–234. https://doi.org/10.1016/j.jmst.2023.06.002

Yusuf, T. L., Ogundare, S. A., Opoku, F., Arotiba, O. A., & Mabuba, N. (2023a). Theoretical and experimental insight into the construction of FTO/NiSe<inf>2</inf>/BiVO<inf>4</inf> photoanode towards an efficient charge separation for the degradation of pharmaceuticals in water. *Journal of Environmental Chemical Engineering*, *11*(5). https://doi.org/10.1016/j.jece.2023.110711

Yusuf, T. L., Ogundare, S. A., Opoku, F., Arotiba, O. A., & Mabuba, N. (2023b). Theoretical and experimental insight into the construction of FTO/NiSe2/BiVO4 photoanode towards an efficient charge separation for the degradation of pharmaceuticals in water. *Journal of Environmental Chemical Engineering*, *11*(5), 110711. https://doi.org/10.1016/J.JECE.2023.110711

Zarei, E., & Ojani, R. (2017). Fundamentals and some applications of photoelectrocatalysis and effective factors on its efficacy: a review. In *Journal of Solid State Electrochemistry* (Vol. 21, Issue 2, pp. 305–336). Springer New York LLC. https://doi.org/10.1007/s10008-016-3385-2

Zeng, Q., Li, J., Li, L., Bai, J., Xia, L., & Zhou, B. (2017). Synthesis of WO3/BiVO4 photoanode using a reaction of bismuth nitrate with peroxovanadate on WO3 film for efficient photoelectrocatalytic water splitting and organic pollutant degradation. *Applied Catalysis B: Environmental*, *217*, 21–29. https://doi.org/10.1016/j.apcatb.2017.05.072

Zhang, A., Zhou, M., Han, L., & Zhou, Q. (2011). The combination of rotating disk photocatalytic reactor and TiO2 nanotube arrays for environmental pollutants removal. *Journal of Hazardous Materials*, *186*(2–3), 1374–1383. https://doi.org/10.1016/j.jhazmat.2010.12.022

Zhong, X., Li, Y., Wu, H., & Xie, R. (2023). Recent progress in BiVO4-based heterojunction nanomaterials for photocatalytic applications. *Materials Science and Engineering: B*, *289*, 116278. https://doi.org/10.1016/J.MSEB.2023.116278

Zhu, M., Yang, S., Wang, D., Hogan, J., & Sadrzadeh, M. (2024). CTAC-assisted monoclinic BiVO4 with oxygen defects for efficient photocatalytic performances: A combined experimental and DFT study. *Journal of Alloys and Compounds*, *990*. https://doi.org/10.1016/j.jallcom.2024.174404

Alalm, M. G., Djellabi, R., Meroni, D., Pirola, C., Bianchi, C. L., & Boffito, D. C. (2021). Toward scaling-up photocatalytic process for multiphase environmental applications. In *Catalysts* (Vol. 11, Issue 5). MDPI. https://doi.org/10.3390/catal11050562

Ali, A. Z., Jagannathan, S., Bennani, Y. D., van der Hoek, J. P., & Spanjers, H. (2023a). Photoelectrocatalytic based simultaneous removal of multiple organic micro-pollutants by using a visible light driven BiVO4 photoanode. *Journal of Water Process Engineering*, *56*, 104471. https://doi.org/10.1016/J.JWPE.2023.104471

Ali, A. Z., Jagannathan, S., Bennani, Y. D., van der Hoek, J. P., & Spanjers, H. (2023b). Photoelectrocatalytic based simultaneous removal of multiple organic micro-pollutants by using a visible light driven BiVO4 photoanode. *Journal of Water Process Engineering*, *56*, 104471. https://doi.org/10.1016/J.JWPE.2023.104471

Ali, A. Z., Wu, Y., Bennani, Y. D., Spanjers, H., & Hoek, J. P. van der. (2023). Photo-electrocatalytic based removal of acetaminophen: Application of visible light driven heterojunction based BiVO4/BiOI photoanode. *Chemosphere*, *324*, 138322. https://doi.org/10.1016/J.CHEMOSPHERE.2023.138322

Ali, A. Z., Wu, Y., Wols, B., Zeidan, M., Spanjers, H., & van der Hoek, J. P. (2025). Simultaneous removal of multiple organic micropollutants via UV-visible light driven BiVO4/TiO2-GO photoanode: Experimental and CFD study. *Chemical Engineering Journal Advances*, *22*, 100721. https://doi.org/10.1016/j.ceja.2025.100721

Alulema-Pullupaxi, P., Espinoza-Montero, P. J., Sigcha-Pallo, C., Vargas, R., Fernández, L., Peralta-Hernández, J. M., & Paz, J. L. (2021). Fundamentals and applications of photoelectrocatalysis as an efficient process to remove pollutants from water: A review. *Chemosphere*, *281*, 130821. https://doi.org/10.1016/J.CHEMOSPHERE.2021.130821

Amanlou, Y., Hashjin, T. T., Ghobadian, B., Najafi, G., & Mamat, R. (2016). A comprehensive review of Uniform Solar Illumination at Low Concentration Photovoltaic (LCPV) Systems. In *Renewable and Sustainable Energy Reviews* (Vol. 60, pp. 1430–1441). Elsevier Ltd. https://doi.org/10.1016/j.rser.2016.03.032

Arunachalam, P., Shaddad, M. N., Amer, M. S., & AL-Qadi, A. (2024). Enhanced photoelectrochemical water splitting coupled with pharmaceutical pollutants degradation on Zr:BiVO4 photoanodes by synergetic catalytic activity of NiFeOOH nanostructures. *Alexandria Engineering Journal*, *99*, 64–75. https://doi.org/10.1016/j.aej.2024.05.012

Arunachalam, P., Shaddad, M. N., Amer, M. S., Alsalman, A. M., & Madhavan, J. (2024). Cooperative catalytic behavior of CoS and Bi2S3 nanoparticles on Zr:BiVO4 photoanodes for enhanced photoelectrochemical sulfite oxidation coupled with pharmaceutical pollution degradation. *Environmental Science: Nano*, *11*(6), 2668–2682. https://doi.org/10.1039/d4en00018h

Bessegato, G. G., Guaraldo, T. T., de Brito, J. F., Brugnera, M. F., & Zanoni, M. V. B. (2015). Achievements and Trends in Photoelectrocatalysis: from Environmental to Energy Applications. *Electrocatalysis 2015 6:5*, *6*(5), 415–441. https://doi.org/10.1007/S12678-015-0259-9

Binjhade, R., Mondal, R., & Mondal, S. (2022). Continuous photocatalytic reactor: Critical review on the design and performance. In *Journal of Environmental Chemical Engineering* (Vol. 10, Issue 3). Elsevier Ltd. https://doi.org/10.1016/j.jece.2022.107746

Braham, R. J., & Harris, A. T. (2009). Review of major design and scale-up considerations for solar photocatalytic reactors. In *Industrial and Engineering Chemistry Research* (Vol. 48, Issue 19, pp. 8890–8905). https://doi.org/10.1021/ie900859z

Bureš, F. (2019). Quaternary Ammonium Compounds: Simple in Structure, Complex in Application. In *Topics in Current Chemistry* (Vol. 377, Issue 3). Springer International Publishing. https://doi.org/10.1007/s41061-019-0239-2

Chen, S., Huang, D., Du, L., Lei, L., Chen, Y., Wang, G., Wang, Z., Zhou, W., Tao, J., Li, R., & Zhou, C. (2022). Peroxymonosulfate activation by surface-modified bismuth vanadate for ciprofloxacin abatement under visible light: Insights into the generation of singlet oxygen. *Chemical Engineering Journal*, *444*, 136373. https://doi.org/10.1016/J.CEJ.2022.136373

Chen, Z., Mi, N., Huang, L., Wang, W., Li, C., Teng, Y., & Gu, C. (2022a). Snow-like BiVO4 with rich oxygen defects for efficient visible light photocatalytic degradation of ciprofloxacin. *Science of The Total Environment*, *808*, 152083. https://doi.org/10.1016/J.SCITOTENV.2021.152083

Chen, Z., Mi, N., Huang, L., Wang, W., Li, C., Teng, Y., & Gu, C. (2022b). Snow-like BiVO4 with rich oxygen defects for efficient visible light photocatalytic degradation of ciprofloxacin. *Science of The Total Environment*, *808*, 152083. https://doi.org/10.1016/J.SCITOTENV.2021.152083

Chinnaiyan, P., Thampi, S. G., Kumar, M., & Balachandran, M. (2019). Photocatalytic degradation of metformin and amoxicillin in synthetic hospital wastewater: effect of classical parameters. *International Journal of Environmental Science and Technology*, *16*(10), 5463–5474. https://doi.org/10.1007/s13762-018-1935-0

Davies, K. R., Allan, M. G., Nagarajan, S., Townsend, R., Asokan, V., Watson, T., Godfrey, A. R., Maroto-Valer, M. M., Kuehnel, M. F., & Pitchaimuthu, S. (2023). Photoelectrocatalytic Surfactant Pollutant Degradation and Simultaneous Green Hydrogen Generation. *Industrial and Engineering Chemistry Research*. https://doi.org/10.1021/acs.iecr.3c00840

Eliminate PFAS in effluent water - SUIKI by TDK. (n.d.). Retrieved March 12, 2025, from https://suiki.earth/

Fiaz, A., Zhu, D., & Sun, J. (2021). Environmental fate of tetracycline antibiotics: degradation pathway mechanisms, challenges, and perspectives. In *Environmental Sciences Europe* (Vol. 33, Issue 1). Springer Science and Business Media Deutschland GmbH. https://doi.org/10.1186/s12302-021-00505-y

Fu, L., Li, Z., & Shang, X. (2024). Recent surficial modification strategies on BiVO4 based photoanodes for photoelectrochemical water splitting enhancement. In *International Journal of Hydrogen Energy* (Vol. 55, pp. 611–624). Elsevier Ltd. https://doi.org/10.1016/j.ijhydene.2023.11.253

Fuentes-Camargo, I., Carrera-Crespo, J. E., Vazquez-Arenas, J., Romero-Ibarra, I., Rodríguez, J. L., Lartundo-Rojas, L., & Cardoso-Martínez, J. (2020). Pulse-Plating Electrodeposition of Metallic Bi in an Organic-Free Aqueous Electrolyte and Its Conversion into BiVO<inf>4</inf> to Improve Photoelectrochemical Activity toward Pollutant Degradation under Visible Light. *Journal of Physical Chemistry C*, *124*(2), 1421–1428. https://doi.org/10.1021/acs.jpcc.9b09898

Ganapathi, G. (2012). *Low-Cost, Lightweight Solar Concentrator*. www.solar.energy.gov/sunshot/csp.html

Ghosh, S., Pourebrahimi, S., Malloum, A., Ajala, O. J., AlKafaas, S. S., Onyeaka, H., Nnaji, N. D., Oroke, A., Bornman, C., Christian, O., Ahmadi, S., & Wani, M. Y. (2023). A review on ciprofloxacin removal from wastewater as a pharmaceutical contaminant: Covering adsorption to advanced oxidation processes to computational studies. *Materials Today Communications*, *37*, 107500. https://doi.org/10.1016/J.MTCOMM.2023.107500

Goodarzi, N., Ashrafi-Peyman, Z., Khani, E., & Moshfegh, A. Z. (2023). Recent Progress on Semiconductor Heterogeneous Photocatalysts in Clean Energy Production and Environmental Remediation. In *Catalysts* (Vol. 13, Issue 7). Multidisciplinary Digital Publishing Institute (MDPI). https://doi.org/10.3390/catal13071102

Guan, B., Chen, J., Li, Z., Zhuang, Z., Chen, Y., Ma, Z., Guo, J., Zhu, C., Hu, X., Zhao, S., Dang, H., Chen, L., Shu, K., Guo, Z., Shi, K., Li, Y., Yi, C., Hu, J., & Huang, Z. (2024). Review on Synthesis, Modification, Morphology, and Combination of BiVO4-based Catalysts for Photochemistry: Status, Advances, and Perspectives. In *Energy and Fuels* (Vol. 38, Issue 2, pp. 806–853). American Chemical Society. https://doi.org/10.1021/acs.energyfuels.3c03932

Indermühle, C., Puzenat, E., Simonet, F., Peruchon, L., Brochier, C., & Guillard, C. (2016). Modelling of UV optical ageing of optical fibre fabric coated with TiO2. *Applied Catalysis B: Environmental*, *182*, 229–235. https://doi.org/10.1016/j.apcatb.2015.09.037

Jiang, L., Chen, D., Qin, L., Liang, J., Sun, X., & Huang, Y. (2019). Enhanced photocatalytic activity of hydrogenated BiVO4 with rich surface-oxygen-vacancies for remarkable degradation of tetracycline hydrochloride. *Journal of Alloys and Compounds*, *783*, 10–18. https://doi.org/10.1016/j.jallcom.2018.12.290

Jing, D., Liu, H., Zhang, X., Zhao, L., & Guo, L. (2009). Photocatalytic hydrogen production under direct solar light in a CPC based solar reactor: Reactor design and preliminary results. *Energy Conversion and Management*, *50*(12), 2919–2926. https://doi.org/10.1016/j.enconman.2009.07.012

Kanaujiya, D. K., Paul, T., Sinharoy, A., & Pakshirajan, K. (2019). Biological Treatment Processes for the Removal of Organic Micropollutants from Wastewater: a Review. In *Current Pollution Reports* (Vol. 5, Issue 3, pp. 112–128). Springer. https://doi.org/10.1007/s40726-019-00110-x

Kang, J., Tang, Y., Wang, M., Jin, C., Liu, J., Li, S., Li, Z., & Zhu, J. (2021a). The enhanced peroxymonosulfate-assisted photocatalytic degradation of tetracycline under visible light by g-C3N4/Na-BiVO4 heterojunction catalyst and its mechanism. *Journal of Environmental Chemical Engineering*, *9*(4), 105524. https://doi.org/10.1016/J.JECE.2021.105524

Kang, J., Tang, Y., Wang, M., Jin, C., Liu, J., Li, S., Li, Z., & Zhu, J. (2021b). The enhanced peroxymonosulfate-assisted photocatalytic degradation of tetracycline under visible light by g-C3N4/Na-BiVO4 heterojunction catalyst and its mechanism. *Journal of*

Environmental Chemical Engineering, *9*(4), 105524. https://doi.org/10.1016/J.JECE.2021.105524

Kulišťáková, A. (2023). Removal of pharmaceutical micropollutants from real wastewater matrices by means of photochemical advanced oxidation processes – A review. In *Journal of Water Process Engineering* (Vol. 53). Elsevier Ltd. https://doi.org/10.1016/j.jwpe.2023.103727

Łęcki, T., Hamad, H., Zarębska, K., Wierzyńska, E., & Skompska, M. (2022). Mechanistic insight into photochemical and photoelectrochemical degradation of organic pollutants with the use of BiVO4 and BiVO4/Co-Pi. *Electrochimica Acta*, *434*, 141292. https://doi.org/10.1016/J.ELECTACTA.2022.141292

Li, J., Ren, J., Li, S., Li, G., Li, M. M. J., Li, R., Kang, Y. S., Zou, X., Luo, Y., Liu, B., & Zhao, Y. (2024). Potential industrial applications of photo/electrocatalysis: Recent progress and future challenges. In *Green Energy and Environment* (Vol. 9, Issue 5, pp. 859–876). KeAi Publishing Communications Ltd. https://doi.org/10.1016/j.gee.2023.05.003

Li, Y., Bai, B., Zhu, M., Li, J., Mei, Q., & Wang, Q. (2024a). BiVO4 photoanode modified with FeOOH cocatalyst for visible-light-driven photoelectrocatalytic degradation of organic pollutants. *Journal of Environmental Chemical Engineering*, *12*(4). https://doi.org/10.1016/j.jece.2024.113079

Li, Y., Bai, B., Zhu, M., Li, J., Mei, Q., & Wang, Q. (2024b). BiVO4 photoanode modified with FeOOH cocatalyst for visible-light-driven photoelectrocatalytic degradation of organic pollutants. *Journal of Environmental Chemical Engineering*, *12*(4), 113079. https://doi.org/10.1016/J.JECE.2024.113079

Li, Y., Sun, X., Tang, Y., Ng, Y. H., Li, L., Jiang, F., Wang, J., Chen, W., & Li, L. (2021a). Understanding photoelectrocatalytic degradation of tetracycline over three-dimensional coral-like ZnO/BiVO4 nanocomposite. *Materials Chemistry and Physics*, *271*, 124871. https://doi.org/10.1016/J.MATCHEMPHYS.2021.124871

Li, Y., Sun, X., Tang, Y., Ng, Y. H., Li, L., Jiang, F., Wang, J., Chen, W., & Li, L. (2021b). Understanding photoelectrocatalytic degradation of tetracycline over three-dimensional coral-like ZnO/BiVO4 nanocomposite. *Materials Chemistry and Physics*, *271*, 124871. https://doi.org/10.1016/J.MATCHEMPHYS.2021.124871

Liu, C., Ding, Z., Shi, M., Wang, D., Chen, Q., Xia, M., & Wang, F. (2024). Dependence of superoxide radical generation on peroxymonosulfate under visible light: Enrofloxacin degradation and mechanism insight. *Chemical Engineering Journal*, *485*. https://doi.org/10.1016/j.cej.2024.149721

Liu, J., Li, B., Kong, L., Xiao, Q., & Huang, S. (2023). Surfactants-assisted morphological regulation of BiVO4 nanostructures for photocatalytic degradation of organic pollutants in wastewater. *Journal of Physics and Chemistry of Solids*, *172*. https://doi.org/10.1016/j.jpcs.2022.111079

Liu, J., Li, J., Li, Y., Guo, J., Xu, S. M., Zhang, R., & Shao, M. (2020). Photoelectrochemical water splitting coupled with degradation of organic pollutants enhanced by surface and interface engineering of BiVO4 photoanode. *Applied Catalysis B: Environmental*, *278*. https://doi.org/10.1016/j.apcatb.2020.119268

Liu, Y., Yu, Y., Xu, L., Hao, R., Yang, T., Huang, H., & Hu, J. (2024). Rod-like BiVO4 with two-phase structure to boost photoelectrocatalytic degradation activity for tetracycline via

the p-n junction. *Applied Surface Science*, *656*. https://doi.org/10.1016/j.apsusc.2024.159719

Loganathan, P., Vigneswaran, S., Kandasamy, J., Cuprys, A. K., Maletskyi, Z., & Ratnaweera, H. (2023). Treatment Trends and Combined Methods in Removing Pharmaceuticals and Personal Care Products from Wastewater—A Review. *Membranes*, *13*(2). https://doi.org/10.3390/membranes13020158

Long, Z., Li, Q., Wei, T., Zhang, G., & Ren, Z. (2020). Historical development and prospects of photocatalysts for pollutant removal in water. *Journal of Hazardous Materials*, *395*, 122599. https://doi.org/10.1016/J.JHAZMAT.2020.122599

Ma, D., Yi, H., Lai, C., Liu, X., Huo, X., An, Z., Li, L., Fu, Y., Li, B., Zhang, M., Qin, L., Liu, S., & Yang, L. (2021). Critical review of advanced oxidation processes in organic wastewater treatment. In *Chemosphere* (Vol. 275). Elsevier Ltd. https://doi.org/10.1016/j.chemosphere.2021.130104

Mahamuni, N. N., & Adewuyi, Y. G. (2010). Advanced oxidation processes (AOPs) involving ultrasound for waste water treatment: A review with emphasis on cost estimation. *Ultrasonics Sonochemistry*, *17*(6), 990–1003. https://doi.org/10.1016/j.ultsonch.2009.09.005

Malathi, A., Madhavan, J., Ashokkumar, M., & Arunachalam, P. (2018). A review on BiVO4 photocatalyst: Activity enhancement methods for solar photocatalytic applications. *Applied Catalysis A: General*, *555*, 47–74. https://doi.org/10.1016/J.APCATA.2018.02.010

Man, J. H. K., Zheng, Z., Dong, T., Lung, C. W., Cheung, H. Y. M., Wang, X., Dong, H., Guan, X., & Lo, I. M. C. (2025). Photoelectrochemical activation of free chlorine utilizing vacancies-engineered BiVO4 photoanode for simultaneous pharmaceuticals and personal care products (PPCPs) degradation and bacterial inactivation: An integrative batch and continuous flow reactor study. *Separation and Purification Technology*, *360*. https://doi.org/10.1016/j.seppur.2024.130959

Marugán, J., Van Grieken, R., Pablos, C., Adán, C., & Timmers, R. (2013). Determination of photochemical, electrochemical and photoelectrochemical efficiencies in a photoelectrocatalytic reactor. *International Journal of Chemical Reactor Engineering*, *11*(2), 787–797. https://doi.org/10.1515/ijcre-2012-0014

Meng, X., Zhang, Z., & Li, X. (2015a). Synergetic photoelectrocatalytic reactors for environmental remediation: A review. *Journal of Photochemistry and Photobiology C: Photochemistry Reviews*, *24*, 83–101. https://doi.org/10.1016/J.JPHOTOCHEMREV.2015.07.003

Meng, X., Zhang, Z., & Li, X. (2015b). Synergetic photoelectrocatalytic reactors for environmental remediation: A review. In *Journal of Photochemistry and Photobiology C: Photochemistry Reviews* (Vol. 24, pp. 83–101). Elsevier. https://doi.org/10.1016/j.jphotochemrev.2015.07.003

Mohapatra, S., Yutao, L., Goh, S. G., Ng, C., Luhua, Y., Tran, N. H., & Gin, K. Y. H. (2023). Quaternary ammonium compounds of emerging concern: Classification, occurrence, fate, toxicity and antimicrobial resistance. In *Journal of Hazardous Materials* (Vol. 445). Elsevier B.V. https://doi.org/10.1016/j.jhazmat.2022.130393

Monfort, O., & Plesch, G. (2018). Bismuth vanadate-based semiconductor photocatalysts: a short critical review on the efficacy and the mechanism of photodegradation of organic

pollutants. *Environmental Science and Pollution Research 2018 25:20*, *25*(20), 19362–19379. https://doi.org/10.1007/S11356-018-2437-9

Nguyen, L. M., Nguyen, N. T. T., Nguyen, T. T. T., Nguyen, T. T., Nguyen, D. T. C., & Tran, T. Van. (2022). Occurrence, toxicity and adsorptive removal of the chloramphenicol antibiotic in water: a review. In *Environmental Chemistry Letters* (Vol. 20, Issue 3, pp. 1929–1963). Springer Science and Business Media Deutschland GmbH. https://doi.org/10.1007/s10311-022-01416-x

Nguyen, T. D., Nguyen, V. H., Nanda, S., Vo, D. V. N., Nguyen, V. H., Van Tran, T., Nong, L. X., Nguyen, T. T., Bach, L. G., Abdullah, B., Hong, S. S., & Van Nguyen, T. (2020). BiVO4 photocatalysis design and applications to oxygen production and degradation of organic compounds: a review. In *Environmental Chemistry Letters* (Vol. 18, Issue 6, pp. 1779–1801). Springer Science and Business Media Deutschland GmbH. https://doi.org/10.1007/s10311-020-01039-0

Orimolade, B. O., & Arotiba, O. A. (2020a). Bismuth vanadate in photoelectrocatalytic water treatment systems for the degradation of organics: A review on recent trends. *Journal of Electroanalytical Chemistry*, *878*. https://doi.org/10.1016/j.jelechem.2020.114724

Orimolade, B. O., & Arotiba, O. A. (2020b). Towards visible light driven photoelectrocatalysis for water treatment: Application of a FTO/BiVO4/Ag2S heterojunction anode for the removal of emerging pharmaceutical pollutants. *Scientific Reports*, *10*(1). https://doi.org/10.1038/s41598-020-62425-w

Orimolade, B. O., & Arotiba, O. A. (2022). Enhanced photoelectrocatalytic degradation of diclofenac sodium using a system of Ag-BiVO4/BiOI anode and Ag-BiOI cathode. *Scientific Reports*, *12*(1). https://doi.org/10.1038/s41598-022-08213-0

Orimolade, B. O., Koiki, B. A., Peleyeju, G. M., & Arotiba, O. A. (2019). Visible light driven photoelectrocatalysis on a FTO/BiVO4/BiOI anode for water treatment involving emerging pharmaceutical pollutants. *Electrochimica Acta*, *307*, 285–292. https://doi.org/10.1016/J.ELECTACTA.2019.03.217

Orimolade, B. O., Zwane, B. N., Koiki, B. A., Tshwenya, L., Peleyeju, G. M., Mabuba, N., Zhou, M., & Arotiba, O. A. (2020). Solar photoelectrocatalytic degradation of ciprofloxacin at a FTO/BiVO4/MnO2 anode: Kinetics, intermediate products and degradation pathway studies. *Journal of Environmental Chemical Engineering*, *8*(1), 103607. https://doi.org/10.1016/J.JECE.2019.103607

Pan, T., Tang, Y., Liao, Y., Chen, J., Li, Y., Wang, J., Li, L., & Li, X. (2023). BiVO4 modifying with cobalt-phosphate cluster cocatalyst for persulfate assisted photoelectrocatalytic degradation of tetracycline. *Molecular Catalysis*, *549*, 113527. https://doi.org/10.1016/J.MCAT.2023.113527

Phan, H. T. B., Nguyen, A. Q. K., Ahn, Y. Y., Kim, K., Kim, S., & Kim, J. (2022). Visible light-induced degradation of propranolol with peroxymonosulfate as an oxidant and a radical precursor. *Separation and Purification Technology*, *289*. https://doi.org/10.1016/j.seppur.2022.120764

Prado, T. M., Silva, F. L., Carrico, A., Lanza, M. R. D. V., Fatibello-Filho, O., & Moraes, F. C. (2022). Photoelectrocatalytic degradation of caffeine using bismuth vanadate modified with reduced graphene oxide. *Materials Research Bulletin*, *145*. https://doi.org/10.1016/j.materresbull.2021.111539

Puralytics. (n.d.). *Puralytics*. Retrieved February 25, 2025, from https://puralytics.com/

Qiao, S., Di, M., Jiang, J. X., & Han, B. H. (2022). Conjugated porous polymers for photocatalysis: The road from catalytic mechanism, molecular structure to advanced applications. *EnergyChem*, *4*(6), 100094. https://doi.org/10.1016/J.ENCHEM.2022.100094

Ramos, D. R., Iazykov, M., Fernandez, M. I., Santaballa, J. A., & Canle, M. (2021). Mechanical Stability Is Key for Large-Scale Implementation of Photocatalytic Surface-Attached Film Technologies in Water Treatment. *Frontiers in Chemical Engineering*, *3*. https://doi.org/10.3389/fceng.2021.688498

Sathishkumar, P. (n.d.). *Green Energy and Technology Photocatalysis for Energy and Environmental Applications Current Trends and Future Perspectives*.

Singla, S., Devi, P., & Basu, S. (2023). Revolutionizing the Role of Solar Light Responsive BiVO4/BiOBr Heterojunction Photocatalyst for the Photocatalytic Deterioration of Tetracycline and Photoelectrocatalytic Water Splitting. *Materials*, *16*(16). https://doi.org/10.3390/ma16165661

Spasiano, D., Marotta, R., Malato, S., Fernandez-Ibañez, P., & Di Somma, I. (2015). Solar photocatalysis: Materials, reactors, some commercial, and pre-industrialized applications. A comprehensive approach. In *Applied Catalysis B: Environmental* (Vols. 170–171, pp. 90–123). Elsevier. https://doi.org/10.1016/j.apcatb.2014.12.050

Su, W., Lu, Z., Shi, Q., Cheng, C., Liu, C., Lu, C., Xie, H., Lu, B., Huang, K., Xu, M., Xu, C., Pan, H., & Zhao, C. (2024). Surface States of Mo-Doped BiVO4 Nanoparticle-Based Photoanodes for Photoelectrochemical Degradation of Chloramphenicol. *ACS Applied Nano Materials*. https://doi.org/10.1021/acsanm.4c01743

Tavakoli Joorabi, F., Kamali, M., & Sheibani, S. (2022). Effect of aqueous inorganic anions on the photocatalytic activity of CuO–Cu2O nanocomposite on MB and MO dyes degradation. *Materials Science in Semiconductor Processing*, *139*. https://doi.org/10.1016/j.mssp.2021.106335

Tay, K. S., & Ismail, N. S. B. (2016). Degradation of β-blockers in water by sulfate radical-based oxidation: kinetics, mechanism and ecotoxicity assessment. *International Journal of Environmental Science and Technology*, *13*(10), 2495–2504. https://doi.org/10.1007/s13762-016-1083-3

Thaha, S. K. S. M., Nalandhiran, P., Kaliyamoorthy, S., Mizota, I., Mangalaraja, R. V., & Sathishkumar, P. (2024). Critical Review of Photocatalytic Reactor Designs for Environmental Applications. *Green Energy and Technology*, *Part F2928*, 1–50. https://doi.org/10.1007/978-981-97-1939-6_1/TABLES/9

Toe, C. Y., Pan, J., Scott, J., & Amal, R. (2022). Identifying Key Design Criteria for Large-Scale Photocatalytic Hydrogen Generation from Engineering and Economic Perspectives. In *ACS ES and T Engineering* (Vol. 2, Issue 6, pp. 1130–1143). American Chemical Society. https://doi.org/10.1021/acsestengg.2c00030

Visible Light Photocatalysts | NANOPTEK and LIGHTFUEL. (n.d.). Retrieved February 25, 2025, from https://nanoptek.com/pilot-production/products-2/

Wang, J., Tian, Z., Huo, Y., Yang, M., Zheng, X., & Zhang, Y. (2018). Monitoring of 943 organic micropollutants in wastewater from municipal wastewater treatment plants with secondary and advanced treatment processes. *Journal of Environmental Sciences (China)*, *67*, 309–317. https://doi.org/10.1016/j.jes.2017.09.014

Wang, K., Liang, G., Waqas, M., Yang, B., Xiao, K., Zhu, C., & Zhang, J. (2020a). Peroxymonosulfate enhanced photoelectrocatalytic degradation of ofloxacin using an easily coated cathode. *Separation and Purification Technology*, *236*. https://doi.org/10.1016/j.seppur.2019.116301

Wang, K., Liang, G., Waqas, M., Yang, B., Xiao, K., Zhu, C., & Zhang, J. (2020b). Peroxymonosulfate enhanced photoelectrocatalytic degradation of ofloxacin using an easily coated cathode. *Separation and Purification Technology*, *236*. https://doi.org/10.1016/j.seppur.2019.116301

Wang, W., Liu, X., Jing, J., Mu, J., Wang, R., Du, C., & Su, Y. (2023). Photoelectrocatalytic peroxymonosulfate activation over CoFe2O4-BiVO4 photoanode for environmental purification: Unveiling of multi-active sites, interfacial engineering and degradation pathways. *Journal of Colloid and Interface Science*, *644*, 519–532. https://doi.org/10.1016/J.JCIS.2023.03.202

Wu, S., & Hu, Y. H. (2021). A comprehensive review on catalysts for electrocatalytic and photoelectrocatalytic degradation of antibiotics. In *Chemical Engineering Journal* (Vol. 409). Elsevier B.V. https://doi.org/10.1016/j.cej.2020.127739

Xing, Y., Yi, J., Zhang, X., Jin, X., Peng, Y., Ni, G., Yong, X., & Wang, X. (2024). Fabrication of BiVO4 photoanode loaded with Zn-doped Co9S8 for enhanced photoelectrochemical performance. *Journal of Photochemistry and Photobiology A: Chemistry*, *448*. https://doi.org/10.1016/j.jphotochem.2023.115322

Xu, Y., Zhong, D., Jia, J., Li, K., Li, J., & Quan, X. (2013). Dual slant-placed electrodes thin-film photocatalytic reactor: Enhanced dye degradation efficacy by self-generated electric field. *Chemical Engineering Journal*, *225*, 138–143. https://doi.org/10.1016/j.cej.2013.03.085

Yin, W., Wang, W., Zhou, L., Sun, S., & Zhang, L. (2010). CTAB-assisted synthesis of monoclinic BiVO4 photocatalyst and its highly efficient degradation of organic dye under visible-light irradiation. *Journal of Hazardous Materials*, *173*(1–3), 194–199. https://doi.org/10.1016/j.jhazmat.2009.08.068

Yu, M., Tang, Y., Liao, Y., He, W., Lu, X. xin, & Li, X. (2023). Defect-designed Mo-doped BiVO4 photoanode for efficient photoelectrochemical degradation of phenol. *Journal of Materials Science and Technology*, *165*, 225–234. https://doi.org/10.1016/j.jmst.2023.06.002

Yusuf, T. L., Ogundare, S. A., Opoku, F., Arotiba, O. A., & Mabuba, N. (2023a). Theoretical and experimental insight into the construction of FTO/NiSe<inf>2</inf>/BiVO<inf>4</inf> photoanode towards an efficient charge separation for the degradation of pharmaceuticals in water. *Journal of Environmental Chemical Engineering*, *11*(5). https://doi.org/10.1016/j.jece.2023.110711

Yusuf, T. L., Ogundare, S. A., Opoku, F., Arotiba, O. A., & Mabuba, N. (2023b). Theoretical and experimental insight into the construction of FTO/NiSe2/BiVO4 photoanode towards an efficient charge separation for the degradation of pharmaceuticals in water. *Journal of Environmental Chemical Engineering*, *11*(5), 110711. https://doi.org/10.1016/J.JECE.2023.110711

Zarei, E., & Ojani, R. (2017). Fundamentals and some applications of photoelectrocatalysis and effective factors on its efficacy: a review. In *Journal of Solid State Electrochemistry* (Vol. 21, Issue 2, pp. 305–336). Springer New York LLC. https://doi.org/10.1007/s10008-016-3385-2

Zeng, Q., Li, J., Li, L., Bai, J., Xia, L., & Zhou, B. (2017). Synthesis of WO3/BiVO4 photoanode using a reaction of bismuth nitrate with peroxovanadate on WO3 film for efficient photoelectrocatalytic water splitting and organic pollutant degradation. *Applied Catalysis B: Environmental*, *217*, 21–29. https://doi.org/10.1016/j.apcatb.2017.05.072

Zhang, A., Zhou, M., Han, L., & Zhou, Q. (2011). The combination of rotating disk photocatalytic reactor and TiO2 nanotube arrays for environmental pollutants removal. *Journal of Hazardous Materials*, *186*(2–3), 1374–1383. https://doi.org/10.1016/j.jhazmat.2010.12.022

Zhong, X., Li, Y., Wu, H., & Xie, R. (2023). Recent progress in BiVO4-based heterojunction nanomaterials for photocatalytic applications. *Materials Science and Engineering: B*, *289*, 116278. https://doi.org/10.1016/J.MSEB.2023.116278

Zhu, M., Yang, S., Wang, D., Hogan, J., & Sadrzadeh, M. (2024). CTAC-assisted monoclinic BiVO4 with oxygen defects for efficient photocatalytic performances: A combined experimental and DFT study. *Journal of Alloys and Compounds*, *990*. https://doi.org/10.1016/j.jallcom.2024.174404

Appendix:

Pharmaceutical details

OMP	Function/Use	Environmental Effect	Concentration (ug/L)
Benzotriazole	Corrosion inhibitor in industrial and automotive systems.	Persistent and moderately toxic to aquatic organisms.	1.41
4-5-Methyl-Benzotriazole	Methylated derivative of benzotriazole.	Persistent and acutely toxic; highly resistant to degradation.	0.25
Carbamazepine	Anticonvulsant for n€logical disorders.	Endocrine disruptor; persistent in treated wastewater and aquatic systems.	0.06
Diclofenac	Nonsteroidal anti-inflammatory drug (NSAID).	Oxidative stress; reproductive toxicity in fish and invertebrates.	N/A
Ketoprofen	NSAID for pain relief.	Chronic toxicity; contributes to oxidative stress in aquatic organisms.	N/A
Sulfamethoxazole	Antibiotic for bacterial infections.	Promotes antimicrobial resistance; disrupts microbial ecosystems.	0.26
Sulfadimethoxine	Veterinary antibiotic for livestock.	Promotes antimicrobial resistance in aquatic ecosystems.	N/A
Trimethoprim	Antibiotic for bacterial infections.	Persistent and associated with antimicrobial resistance risks.	0.12
Clarithromycin	Macrolide antibiotic for respiratory infections.	Contributes to antimicrobial resistance; toxic to aquatic life.	0.18
Metoprolol	Beta-blocker for cardiovascular conditions.	Cardiovascular disruption in fish; moderately persistent.	1.50
Propranolol	Non-selective beta-blocker for heart conditions.	Endocrine disruption and potential bioaccumulation.	0.064
Sotalol	Beta-blocker and anti-arrhythmic drug.	Persistent in aquatic systems; may disrupt the cardiovascular health of aquatic species.	1.03
Hydrochlorothiazide	Diuretic for hypertension.	Bioaccumulates in aquatic organisms; moderately toxic.	0.084
Metformin	Anti-diabetic medication.	Poses risks of endocrine disruption; bioaccumulation potential in aquatic systems.	0.43
Clofibric Acid	Lipid-regulating drug.	Persistent and bioaccumulative; toxic to aquatic organisms.	N/A
Gabapentin	Anticonvulsant for n€pathic pain.	N€toxicity in aquatic species; persistent in wastewater systems.	0.63
Caffeine	Stimulant found in beverages.	Indicator of human activity; biodegradable under typical treatment.	0.089
Theophylline	Bronchodilator for respiratory conditions.	Persistent and moderately toxic to aquatic ecosystems.	0.25

Acetaminophen	Analgesic and antipyretic.	Generally biodegradable; impacts microbial communities.	N/A

Issues in the experimental process

1. Jar test to determine optimum dosage of QAC

QAC dissolution when HNO3 was used as reagent for dissolving

Bismuth nitrate was dissolved in 10 mL of water using 250 µL of HNO_3. However, after 20 minutes of ultrasonication, complete dissolution was not achieved. An additional 50 µL of HNO_3 was added, followed by another 20 minutes of ultrasonication, , 0.106 g of vanadate acetate was added along with 10 mL of distilled water and ultrasonicated

Quaternary ammonium compounds (QACs) were introduced at concentrations ranging from 40 mg/L to 2000 mg/L, with significant variations in dissolution behaviour. Lower concentrations (40–100 mg/L) resulted in a clear or slightly opaque light blue solution, indicating full dissolution. At 250 mg/L, partial dissolution was observed, with floating particles and an opaque, translucent appearance. Higher concentrations (500 mg/L and above) led to incomplete dissolution, with increasing opacity, thickness, and visible floating particles. At 2000 mg/L, the solution turned turquoise blue, became highly opaque, and exhibited substantial undissolved material, suggesting that excessive QAC concentrations hinder the dissolution process. The final mixtures were ultrasonicated at 40°C for 20 minutes to ensure proper dispersion.

QAC dissolution when Ethanol and Acetic acid was used as reagent for dissolving

Bismuth and vanadate were taken in a 1:1 molar ratio, with 10 mL of acetic acid used to dissolve bismuth nitrate. Separately, 5 mL of ethanol and 15 mL of pure water were added to vanadate acetate, which was then mixed and sonicated to ensure proper dissolution. Quaternary ammonium compounds (QACs) were introduced at concentrations ranging from 100 mg/L to 1000 mg/L, resulting in distinct dissolution behaviour's.

At 100–300 mg/L, the dissolution was quick and complete, with a clear and stable solution. The 400 mg/L concentration was found to be optimal, ensuring good dissolution without noticeable precipitation. However, beyond 500 mg/L, no dissolution was observed, and the solution turned whitish and opaque, with an increasing number of suspended particles as the QAC concentration increased. Since the HNO_3-based method supported higher QAC concentrations, an attempt was made to improve dissolution beyond 400 mg/L by applying heat. However, heating did not enhance dissolution and instead caused the solution to turn greenish, with visible nanoparticle aggregation. Despite this, heating proved effective for DADMAC alone, facilitating its dissolution at higher concentrations.

2. Formation of nanoparticles in precursor solution due to dissolution and heating. The yellow particles which can be seen are the small suspended nanoparticle s

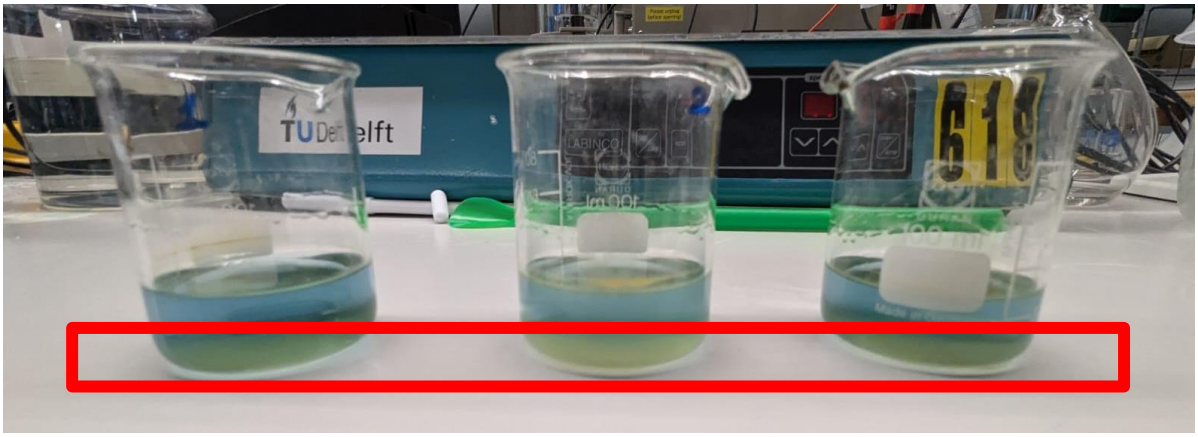

3. Techniques used to fix the Cu wire but failed

Applied carbon layer and stuck Cu to photoanode	Wire did not adhere properly.
Used liquid resin for sticking	Poor Adhesion
Used Underwater Marine Tape	Good Adhesion but invalid LSV result
Replaced Carbon black with conductive tape	Improved adhesion but invalid LSV result
Cured carbon and resin at 60°C for 4 hours in oven	Successfully adhered wire to photoanode.

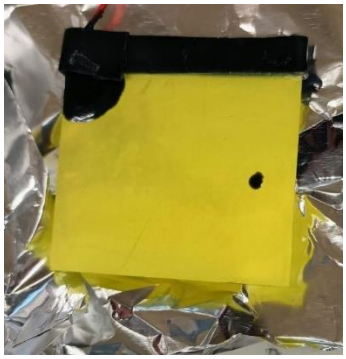

Marine underwater tape

Double side Conductive tape

Cost calculations

PEC module Cost	Quartz reactor cost	2000 € per module	1 module – high quality corrosion resistant	
	Total cost for 350 modules	**700.000 €**		
	Total m^2 of photoanode / module	10 m^2		Based on experiment (2*2 was used for 150ml)
	Total Photoanode required for 350 modules	3500 m^2		
Photoanode Cost	Raw Material cost	828/m^2	All chemical used – bi(no3).5h20 , Vo(AcAc), ethanol and acetic acid	Sigma Aldrich website
	FTO cost	50/m^2	Bulk pricing – prices go to 100 – 150 commercial level	Alibaba
	Fabrication cost	100/m^2	Ultra spray and other processes	
	Total /m^2	978/m^2		
	Total cost for photoanode	**3423000 €**		
Graphite Cathode cost	Total graphite required	50kg/ module		
	Cost for 350 modules	26250	1500 per metric ton	Alibaba
Reference electrode	Cost for 350 modules	175000	500 € per piece	Anodefactory
Total PEC Cost		**4324250 €**	Cost of 1 module 11,780	

Solar Concentrator dish	Cost per unit	100 € /m^2		(Ganapathi, 2012)
	Total area of concentrator	200 m^2		
	Total cost	20000 €		
Fibre optic lighting system	Unit cost per module	100 € / 3m length		Alibaba
	Total length required	300 m	Approx with some extra	
	Total cost	10000 €		
Total cost of solar concentrator system		30000		

Photoanode cost:

Cost of making 4*4 cm2 sample (Experiment)

Bi(NO3)5H20 = 0.0654 € (0.674 €/g)

Vo(AcAc) = 0.3519 € (3.32 €/g)

Acetic acid = 0.548 € (0.054 €/ml)

Ethanol = 0.80 € (0.16 €/ml)

Total cost = 1.765 €

Total cost for 1m2 = 1104

Total cost for bulk production = 828 (reducing 25% as production is in bulk)

Solar concentrator area

Required Irradiance: 60 W/m² (From experiment)

Available Solar Irradiance: 100 W/m² (solar irradiation)

Reactor Exposure Area: 10 m²

Calculation:

CR = 60/100 =0.6 (CR = $I_{desired}$ / I_{solar}) (Amanlou et al., 2016)

Concentrator Area = 100/0.6 = 166.67 m2 ($A_{reactor}$ / CR) ~ 150 m2

Energy Cost			
Current required	10 mA / Module		
Power required per module	0.01 W	P = V*I (1 * 0.01 A)	
Total power required for 350 modules	3.5 W		
Total power required for one year Energy consumption	15.33 kWh/ year	E = power * Time (12h/day 365 days)	
Electricity price	6.82 €	Price in NL, 0.22 per Kwh	

Characterization study data

Characterization data of photoanode prepared at 300

SEM Images

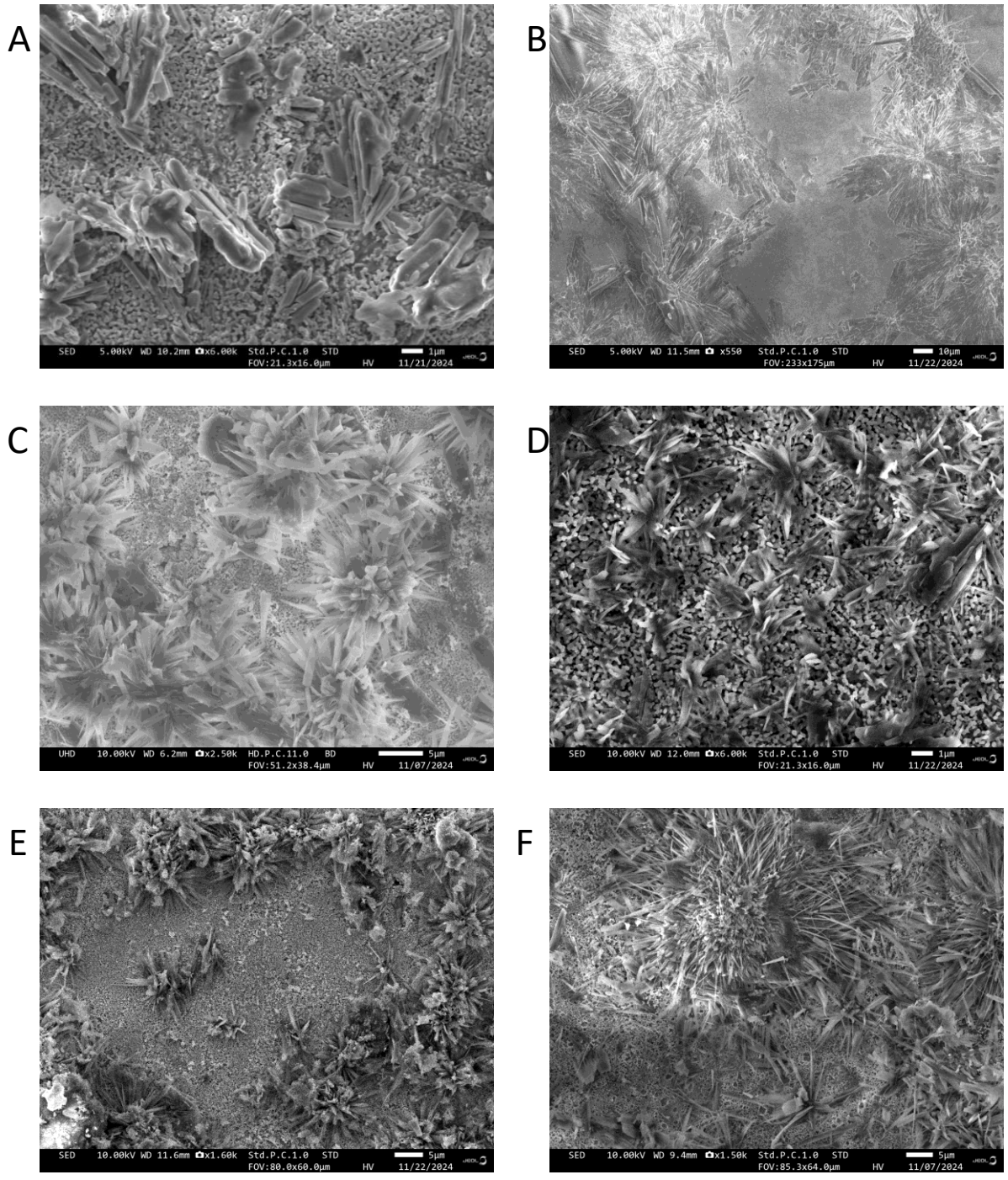

SEM images of (A). ATMAC C16 (B). ATMAC C18 (C). BAC C16 (D). BAC C18 (E). DADMAC C16 (F). DADMAC C18

Petal characteristics

Table. Petal Characteristics in different variants of the modified $BiVO_4$

Sample	**Length (µm)**	**Thickness (µm)**
ATMAC C16	6.077 ± 1.639	0.875 ± 0.076
ATMAC C18	32.756 ± 11.364	0.772 ± 0.340
BAC C16	4.411 ± 0.658	0.892 ± 0.147
BAC C18	2.086 ± 0.374	0.274 ± 0.084
DADMAC C16	4.094 ± 1.450	0.714 ± 0.816
DADMAC C18	10.291 ± 1.570	0.542 ± 0.123